

Unified description of structure and reactions: implementing the Nuclear Field Theory program

R A Broglia^{1,2}, **P F Bortignon**^{1,3}, **F Barranco**⁴, **E Vigezzi**³, **A Idini**⁵ and **G Potel**^{6,7}

¹ Dipartimento di Fisica, Università di Milano, Via Celoria 16, I-20133 Milano, Italy

² The Niels Bohr Institute, University of Copenhagen, DK-2100 Copenhagen, Denmark

³ INFN Sezione di Milano, Via Celoria 16, I-20133 Milano, Italy

⁴ Departamento de Física Aplicada III, Escuela Superior de Ingenieros, Universidad de Sevilla, Camino de los Descubrimientos, Sevilla, Spain

⁵ Department of Physics, University of Jyväskylä, FI-40014 Jyväskylä, Finland

⁶ National Superconducting Cyclotron Laboratory, Michigan State University, East Lansing, Michigan 48824, USA

⁷ Lawrence Livermore National Laboratory L-414, Livermore, CA 94551, USA

Abstract. The modern theory of the atomic nucleus results from the merging of the liquid drop (Niels Bohr and Fritz Kalckar) and of the shell model (Marie Goeppert Meyer and Axel Jensen), which contributed the concepts of collective excitations and of independent-particle motion respectively. The unification of these apparently contradictory views in terms of the particle-vibration (rotation) coupling (Aage Bohr and Ben Mottelson) has allowed for an ever increasingly complete, accurate and detailed description of the nuclear structure, Nuclear Field Theory (NFT, developed by the Copenhagen-Buenos Aires collaboration) providing a powerful quantal embodiment. In keeping with the fact that reactions are not only at the basis of quantum mechanics (statistical interpretation, Max Born), but also the specific tools to probe the atomic nucleus, NFT is being extended to deal with processes which involve the continuum in an intrinsic fashion, so as to be able to treat them on an equal footing with those associated with discrete states (nuclear structure). As a result, spectroscopic studies of transfer to continuum states could eventually use at profit the NFT rules, extended to take care of recoil effects. In the present contribution we review the implementation of the NFT program of structure and reactions, setting special emphasis on open problems and outstanding predictions.

PACS numbers: 21.60.Jz, 23.40.-s, 26.30.-k

1 Foreword

In what follows, one of the authors elaborates on the background which is at the basis of the present article, written to commemorate the 40-year anniversary of the 1975 Nobel Prize in Physics.

Background for subject and title

In the morning of October 4th, 1965, I (RAB) sat in a rather crowded Auditorium A of the Niels Bohr Institute to attend the first of a series of lectures on Nuclear Reactions which were to be delivered by Ben Mottelson. In the following spring term, the Monday lectures were to deal with the subject of Nuclear Structure and the lecturer be Aage Bohr, as it duly happened. After Ben's lecture, an experimental group meeting took place in which experimentalists, as it was the praxis, showed their spectra, likely not yet completely analyzed, while theoreticians attempted at finding confirmation to their predictions in connection with specific peaks of the spectra.

In the afternoon I would continue with the calculation of pairing vibrations I was carrying out in collaboration with Daniel Bès, as well as discuss with Claus Riedel on how to use this information to work out two-nucleon transfer differential cross sections for lead isotopes, quantities newly measured at the Aldermaston facility by Ole Hansen and coworkers. Within this context it did not seem surprising to me, neither to the rest of the attendees of Ben's lecture as far as I recall, that reactions and structure went hand in hand, to the extent that practitioners aimed at checking theory with experiment. Given this background, reinforced through the years by my association with Aage Winther and Daniel Bès, aside from that with Aage Bohr and Ben Mottelson, it is only natural that I view structure and reactions as the two inseparable faces of the same medal.

The pages where I wrote down the notes of Ben's and Aage's lectures have somewhat yellowed in the intervening years. On the other hand, their content, in particular concerning the deep interweaving existing between structure and reactions has not lost a single drop of its depth and simplicity, the mathematics used being elemental, the physics the right one. So even more concerning present day nuclear physics, where the study of halo nuclei has blurred almost completely the distinction between bound and continuum states and forced practitioners to develop inverse kinematics techniques to observe these fragile objects and unveil the new physics hidden in their exotic properties and behaviour. Summing up, structure and reactions are one and the same thing. As a theoretician, I can hardly relate the results of my calculations to experiment in terms of deformation parameters, spectroscopic factors, tunnelling probabilities and the like, but through Coulomb excitation, inelastic scattering, one- and two-particle transfer *absolute* differential cross sections, as well as α - or exotic-decay *absolute* lifetimes, etc., the accent being placed on absolute.

The fact that in Coulomb excitation the kinematic factors associated with the coupling of the relative motion and the intrinsic degrees of freedom can be analytically extracted may induce practitioners to think that one can directly compare counts on a detector with the results of structure models. This is of course not true. Conversely, one cannot compare the lifetimes obtained from tunneling probabilities and barrier attacking

frequencies (reaction) with experiment, without weighting them with the associated formation probabilities of the outgoing particles (structure) (see e.g. Ch. 7 of [1] and refs. therein).

The somewhat worrisome delay with which we, nuclear practitioners, are understanding the nuclear embodiment of a variety of universal phenomena like physical (clothed) single-particle motion, the different mechanisms to break gauge invariance in nuclei (namely bare and induced pairing, this last resulting from the exchange of the variety of collective modes * between nucleons moving in time reversal states close to the Fermi energy), leading to nuclear superfluidity and the like, as compared to other fields of physics, in particular condensed matter, triggered in an important way by a deep understanding of BCS through Cooper pair tunnelling, is, arguably, due to at least two facts†. One, that many nuclear structure practitioners do not deem reactions relevant, let alone those who consider them boring. Another, that reaction experts often combine state of the art reaction theories and their software implementation with less than same level nuclear structure inputs ‡.

2 Introduction

The year 1975 was important for nuclear physics. The second volume of the monograph "Nuclear Structure" written by Aage Bohr and Ben Mottelson was published [19], and the authors shared the Nobel prize in physics [20, 21]. In hindsight, it was important also because of the unexpected contents of Vol. II as compared to those originally planned [22], reflecting the fact that a three volume project had become a two volume one, thus lying a heavy responsibility squarely on the shoulders of the younger collaborators of Aage and Ben.

In particular regarding the implementation of the Nuclear Field Theory (NFT) program. This theory, tailored after Feynman's version of QED [23, 24] and based on the concept of elementary modes of excitation and of their interweaving through the

*Within this context it is of notice the richness of modes which can be used, together with the bare nuclear interaction, to bind Cooper pairs (density, spin, etc. (p-h) collective vibrations, as well as monopole and multipole pairing vibrational states), let alone the fact that one can study the binding of single Cooper pairs in actual nuclear systems, essentially as in the original model [2].

†The BCS papers were published in 1957 [3, 4], Josephson's paper [5, 6] and Anderson's interpretation [7], as the specific probe of gauge phase coherence appeared in 1962 (the same year of Giaever's paper [8, 9]) and 1964 respectively, while the use of the associated Cooper tunneling results by Scalapino to provide a quantitative account of the associated electron-phonon coupling phenomena within a 10% error is of 1968 [10]. Within this context see also the contribution of McMillan and Rowell to [11] as well as [12]. The translation of BCS to atomic nuclei carried out by Bohr, Mottelson and Pines is dated 1958 [13], the recognition of the specificity of two-nucleon transfer differential cross sections to quantitatively probe pairing correlations in nuclei was promptly recognised [14]-[16] (see also [17]), while the implementation as a quantitative tool which can be used within the 10% error level is of only recent date (see [18], in particular Fig. 10, and refs. therein).

‡One is reminded of the fact that your expensive Hi-Fi equipment will sound as good as its cheapest component does.

particle-vibration coupling mechanism [19],[25]-[31] (within this context see footnote number 14 of [21]) was, at the time, essentially developed conceptually, mainly as the result of the Copenhagen-Buenos Aires collaboration [32]-[44] *, (within this context see also [45]-[48]) . On the other hand, its actual workings and its power and limitations had still to be tested and the associated protocols for doing so, worked out.

This fact became particularly poignant during the "Enrico Fermi" International School of Physics on "Elementary modes of excitation in nuclei" which took place in July 1976 at Varenna (Como Lake), under the direction of Aage Bohr and of one of the authors (RAB) [49]. Although a number of applications of NFT were discussed at the School, it was clear that there were ample zones of nuclear structure, let alone nuclear reactions, which had been barely touched upon like: **1)** renormalization and damping of collective modes, including giant resonances (GR) and rotational motion; **2)** the clothing of single-particle motion to make them physical particles, **3)** the role of retardation, state dependent effects, in nuclear pairing correlations, **4)** the calculation of two-nucleon transfer absolute differential cross sections. In the present paper we report on some of the latest developments which testify to the fact that the validity of the implementation of the NFT program has received strong experimental confirmation regarding important predictions for light halo nuclei and has, arguably, reached an important milestone (one would be tempted to say, "been recently completed" †, to the extent that a scientific endeavour can ever be considered completed).

In the process we shall see that subjects 1 (regarding GR) and 3) have become, surprisingly, strongly connected within the scenario of exotic halo nuclei, ‡ in particular in the description of ^{11}Li (Sect. 3), while subjects 1)-4) are found to be strongly linked in the case of the description of the structure of superfluid nuclei, the corresponding results manifesting a deep physical unity which can be represented at profit, in terms of a well funnelled nuclear structure landscape (Sect. 4). Finally in Sect. 5 a number of open problems are discussed §.

*Within this context and regarding dates, one is reminded of the fact that some of the papers referred to had to wait quite long times to clear the peer review and editorial instances, and that ArXiv did not exist at that time.

†This could be closer to becoming "true" if also the optical potential needed to describe direct reactions, in particular one- and two-nucleon transfer processes, had become incorporated among the standard quantities calculated within the NFT framework. Within this context, see the last sentence (in italics) of the caption to Fig. 12 (Sect. 5.2), which vividly summarizes one of the main results of the present contribution.

‡High-lying giant resonances, the elastic response of the atomic nucleus to rapidly varying external fields and controlled by $\hbar\omega_0 (\approx 41/A^{1/3})$ MeV, give rise to a variety of low-energy, ω -independent effects, like polarization charges, polarization contributions to effective two-particle interactions (see e.g. [19] p. 515 and 432 respectively) and to two-nucleon transfer amplitudes (see Fig. 1 of ref. [50]). Low-lying modes, the plastic response of nuclei to time varying external probes, lead to retarded, ω -dependent effects, which play an essential role both in the clothing of single-particle motion and in the induced interactions arising from the exchange of these modes between pairs of nucleons (see [19], last lines of Sect. 6.5f, p.432), a subject intimately related to the melting of points 1) and 3) above.

§Among the subjects we do not discuss are the extension of NFT to finite temperature based on

In keeping with the fact that a central issue touched upon both in connection with exotic halo nuclei and with superfluid nuclei is pairing, it is not surprising that subject 4) [18] plays an important role on the examples discussed below.

3 The exotic, halo nucleus ^{11}Li

The weak, but finite stability of light halo dripline exotic nuclei like ^{11}Li , associated with the $s_{1/2}$ and $p_{1/2}$ levels at threshold *, and thus becoming unavailable for the short range bare NN-pairing interaction [61]-[63], so called pairing anti-halo effect, requires a mechanism of Cooper binding mediated by the exchange of long wavelength collective modes. It is the natural scenario for the appearance of extremely low-lying collective dipole modes, that is of giant dipole pygmy resonances (GDPR). This is in keeping with the fact that the neutron halo displays a very large radius, as compared with that of the core nucleons and thus, a small overlap with it (within this context, see App. B and Table B1). This phenomenon has a threefold consequence: i) to screen the bare NN- 1S_0 short range pairing interaction making it subcritical, ii) to screen the (repulsive) symmetry interaction, and (consequently) iii) to bring down at low energies a consistent fraction of the TRK-sum rule associated with the GDR. The two last effects allow for the presence of a dipole mode at very low energies †. Exchanged between the s, p

Matsubara's formalism (see Ch. 9 of [51] and refs. therein; within this context one is reminded of the fact that at room temperature (≈ 25 meV) the atomic nucleus is in the ground state and thus at zero temperature in keeping with the fact that the first excited state of any nucleus is to be found at least at tens of keV), the connections between inhomogeneous damping and motional narrowing both regarding GR and rotations in hot and warm systems (see [51]-[54] and refs. therein), the applications of NFT methods to describe specific aspects of atomic clusters [55]-[58]. Neither the systematic treatment of over completeness and non-orthogonality of the basis states nor the breakdown of symmetries discussed in [59] (in connection with reactions, see [60] (adjoint basis)). Within the above context we refer to the contribution of Daniel Bès to this topical issue.

*Low-energy electric dipole strength is customarily related to a neutron skin [64]. Within this context, one can hardly think of a better example than ^{11}Li , in which case the core (^9Li) radius is ≈ 2.69 fm, while the halo extends to define a radius for ^{11}Li of 3.55 ± 0.1 fm. It is of notice that the interplay between isoscalar and isovector modes in the presence of neutron excess, is a subject with a long tradition (cf. e.g. [19, 65] and refs. therein), and that the search to the answers to questions posed in connection with recent work on exotic nuclei can be facilitated by results to be found in the above mentioned references. Within this context the GDPR plays a central role in determining the value of the dipole effective charge, opposing the contribution of the GDR, in a similar way as the giant quadrupole resonance (GQR) opposes the contribution to the quadrupole effective charge contribution of the isovector GQR (IGQR).

†This is intimately related to the fact that in ^{10}Li , there is a (continuum) single-particle dipole transition of very low energy (≈ 0.5 MeV) between the $s_{1/2}$ and $p_{1/2}$ unbound states lying essentially at threshold. This is a very subtle extension of the statement that single-particle motion is the most collective of all nuclear motions [66], emerging from the same properties of the nuclear interaction (both bare and induced) as collective motion, and in turn at the basis of the detailed properties of each collective mode, acting as scaffolds and filters of the variety of embodiments. One has to add the characterisation of "physical" to "single-particle motion" (i.e. clothed) to englobe in the above statement also the present situation. In other words, while the bare $s_{1/2}$ and $p_{1/2}$ orbitals could never

orbitals heavily dressed by core vibrations (mainly quadrupole) and resulting into parity inversion (^{10}Li) (see Fig. 1(I)), it provides essentially all of the glue needed to bind the neutron halo Cooper pair to the core by ≈ 400 keV (the contribution of the bare pairing interaction being small (≈ 100 keV)) and thus the (weak) stability of the halo field needed to sustain the pygmy resonance (see Fig. 1(II)) [67] Halo and pygmy on top of it are, within this picture, two aspects of the same physics. Namely that associated with the coexistence of two ground states, the normal core- and the halo-based states *. In a very real sense, the monopole halo Cooper pair addition mode of ^9Li , i.e. $|^{11}\text{Li}(\text{gs})\rangle$, and the pygmy resonance of ^{11}Li , i.e. $|^{11}\text{Li}(1^- \otimes p_{3/2}(\pi); 0.4 \text{ MeV})\rangle$, are two states which can only exist in mutual symbiosis. In a nutshell, the pygmy resonance is the quantal reaction the nucleus has at disposition to stabilize dripline species by pulling back into the system barely unbound neutrons which essentially do not feel a centrifugal barrier, generating in the process the halo ground state.

Let us elaborate on this point. In nuclei lying along the stability valley (e.g. ^{120}Sn), one pays a high energetic prize to separate protons from neutrons even in the case of the low-lying GDPR [64], while nucleons outside closed shells can quadrupole polarize the core with ease (see Sect. 4). This is why the induced pairing interaction receives important contributions from low multipole surface modes with the exclusion of $\lambda = 1$. However, in the case of halo nuclei like ^{11}Li , the above arguments do not apply. Better, they are still operative, but if set upside down. In fact the large diffusivity of the halo makes it difficult to e.g. to quadrupole distort it. At the same time, the ground state of the system is poised to acquire a permanent dipole moment. Thus the associated ZPF become quite large. Consequently, the most important intermediate boson being exchanged between the halo neutrons and binding the halo Cooper pair to the ^9Li core, is a dipole, soft E1-, giant pygmy resonance, mode [68, 69]. Thus the halo pair addition mode of $|^{11}\text{Li}(\text{gs})\rangle$ can be viewed as a Van der Waals Cooper pair (dipole pygmy bootstrap mechanism to violate gauge invariance in nuclei, see App. A, Fig. A1).

Halo pair addition modes can be used, in principle, as building blocks of the nuclear spectrum, like standard pairing vibrational modes around closed shell nuclei (e.g. ^{208}Pb) do. Within this context, it is an open question whether, the first excited $(0^+)^*$ (halo) state (2.25 MeV) of ^{12}Be is the analogue of the halo pair addition mode of ^9Li , that is i.e. $|^{11}\text{Li}(\text{gs})\rangle$ and the observed 1^- state [70]-[72] at 0.460 MeV on top of it (that is 2.71 MeV above the ground state) is a member of the associated pygmy resonance, analogue state of the GDPR state of ^{11}Li observed at low energy (≤ 1 MeV).

Summing up, halo Cooper pair or better halo pair addition vibrations and pygmy dipole resonances (soft E1-excitations, vortex-like pair addition mode, App. A) } are

lead to a low-lying GDPR, the corresponding clothed, physical states do so. Consequently, clothed single-particle motion is one of the most collective nuclear motions is the right statement.

*In other words, of the realization of a low-density nuclear system in which neutron skin effects overwhelm in connection with particular states, the role of the “normal” core.

two novel (symbiotic) plastic modes of nuclear excitation. Experimental studies of these excitations, in particular of pygmy resonance based on excited states are within reach of experimental ingenuity and techniques *. They are expected to shed light on a basic issue which has been with us since BCS: the microscopic mechanism, aside from the bare NN-pairing force, to break gauge invariance. Thus, the variety of origins of nuclear pairing.

Furthermore, they are likely to extend (within this context see [19] Sect. 6-6b and refs. therein) the probing of the validity and limitations of the the Axel-Brink hypothesis [74, 75] †. This phenomenon can be instrumental in modulating the transition between warm and hot (equilibrated) excited nuclei, let alone provide a microscopic way to study a new form of inhomogeneous damping. Namely radial isotropic distortion. The importance of this mechanism, which has partially entered the literature under the name of neutron skin, is underscored by the fact that in ^{11}Li this mechanism is able to bring down by tens of MeV a consistent fraction (approximately 8%) of the TRK sum-rule associated with the GDR as a consequence of the fact that changes in density can affect very strongly nuclear properties (saturation phenomena).

3.1 NFT of structure and reactions: the case of the $^1\text{H}(^9\text{Li}, ^{11}\text{Li})^3\text{H}$ two-particle transfer process

The standard setup for direct nuclear reactions involving stable species contemplates a beam of light particles aimed at a (fixed) target of a somewhat heavy nucleus, like e.g. $^{120}\text{Sn}(\text{p}, \text{t})^{118}\text{Sn}$ where the proton is the projectile and ^{120}Sn the target nucleus. The standard set up was maintained with the introduction of (long lived) light projectiles and/or heavy (target) nuclei, like. e.g. in the case of $^{208}\text{Pb}(\text{t}, \text{p})^{210}\text{Pb}$ (unstable projectile, $t_{1/2} = 12.32$ y), $^{210}\text{Pb}(\text{p}, \text{t})^{208}\text{Pb}$ (unstable target, $t_{1/2} = 22.2$ y). Experiments of the first type could be carried out only at selected laboratories, like Harwell (Aldermaston) and LANL (Los Alamos).

The precise meaning of the standard set up became somewhat blurred with the advent of heavy ion accelerators, in which case both target and projectile were heavy nuclei (see e.g. [60] and refs. therein). Nonetheless, the incoming beam was, as a

*In particular, to disentangle whether one has a vortical or an irrotational flow, one can measure the absolute cross section associated with $^9\text{Li}(\text{t}, \text{p})^{11}\text{Li}(1^- \otimes p_{3/2}(\pi))$ and $^{10}\text{Be}(\text{t}, \text{p})^{12}\text{Be}(1^-; 2.71 \text{ MeV})$, as well as the γ -decay to the ground state and to the first excited state, respectively. Making use of the two-neutron spectroscopic amplitudes associated with the vortical picture, one expects to obtain an absolute two-particle transfer cross section larger than by using those associated with the irrotational picture, the situation being inverted for E1-decay. This is in keeping with the fact that in the first case ground state correlations contribute in a constructive (destructive) coherent manner, while in the second case, they do it destructively (constructively) [73].

†According to this hypothesis, on top of each ordinary energy level of the nucleus, there is an identical set of levels displaced upwards by the giant-dipole resonance frequency. If the nucleus is in statistical equilibrium at some high excitation, there is a non-zero probability that it is in one of the dipole states, where it can decay to the base state by emitting a dipole photon (see [51, 76] and refs. therein).

rule, made out of species lighter than that used to make the target. The situation got reversed in connection with the study of exotic nuclei [77], that is the study of species which, like ^{11}Li have very short lifetimes ($t_{1/2} = 9.75$ ms). The probing of pairing phenomenon through two-nucleon transfer processes is then only possible in terms of inverse kinematic, in which an ephemeral ^{11}Li beam is aimed at a proton (hydrogen) gas target, that is, $^1\text{H}(^9\text{Li}, ^{11}\text{Li})^3\text{H}$.

In Figs. 2(a) and (b) a fictitious standard set up to study the two-nucleon pick-up reaction from a gedanken ^{11}Li target is drawn. The detector is assumed to provide, in both cases, information which allows to reconstruct the kinematics of the process (energy, momentum, mass partition). Of course the standard arrangement cannot be operative due to the extremely short lifetime of ^{11}Li , the set up used to carry out the experiment [78] being that schematically shown in Figs. 2(c) and (d) in terms of the initial and final asymptotic states (inverse kinematics). Let us shortly concentrate on the detection of the process populating the first excited state ^9Li ($1/2^-$; 2.69 MeV). In this case the detector array is assumed to provide information concerning the angular distribution of both ^{11}Li and the γ -rays associated with the decay of the quadrupole mode, as well as energy, mass partition, etc. Within this context the recoil mode, represented by a jagged line, is not less “real” than the vibrational (wavy) mode (see App. F).

Concerning the present formulation of NFT, it may look that, while one can calculate structure up to any order of perturbation theory (in e.g. the $\Lambda_\alpha(\alpha = 0)$, or better, the dimensionless parameters f_λ , see [19]), in the reaction case one is not able to do better than second order in v_{np} . One does so, in the structure case, by diagonalizing the particle-vibration coupling Hamiltonian [19, 38], taking of course into account also the effect of four point vertices, and by an orthogonalization procedure in terms of overlaps (dual basis) in the reaction case (see [60, 79], see also [18] and [80]). Now, this picture, as explained in more detail in Sect. 5.2, is misleading. Within the framework of direct reaction theory in general, and of two-nucleon transfer reactions in particular, simultaneous (linear in v_{np}) and successive (bilinear in v_{np}) transfer, properly corrected by non-orthogonality (linear in v_{np}), taking care of the Pauli principle of the active nucleons (see also Fig. 11), provides a complete description of the reaction process. It is to be noted that in all these calculations, global optical potentials to describe elastic scattering in the different channels have been used, with the exception of the analysis of the $^{11}\text{Li}(\text{p,t})^9\text{Li}$ reaction [81] in which case the empirical potential of ref. [78] was employed. This is also in keeping with the non-standard values of the parameters needed to describe the $(^{11}\text{Li}, \text{p})$ elastic channel [82]. Within this context it is of notice that we consider the calculation of the $^{11}\text{Li}(\text{p,p})^{11}\text{Li}$ optical potential among the open problems (see Sect. 5.2).

3.2 Comparison with the data

In Fig.3 the absolute differential cross sections associated with the processes $^1\text{H}(^{11}\text{Li}, ^9\text{Li}(\text{gs}))^3\text{H}$ and $^1\text{H}(^{11}\text{Li}, ^9\text{Li}(1/2^-))^3\text{H}$ and calculated making use of the software

Cooper and of NFT wave functions * displayed in the figure, or better of the associated two-nucleon transfer spectroscopic amplitudes [18, 67, 81] , are compared with the experimental findings [78].

The population of the first excited state of ${}^9\text{Li}$ provides evidence for the presence of a component of the type $|(s_{1/2} \otimes d_{5/2})_{2+} \otimes 2^+; 0^+ > \otimes |p_{3/2}(\pi) >$ in the ${}^{11}\text{Li}(\text{gs})$ wavefunction (see also Fig. 2). The absolute value of the ground state transition depends directly on the $|(s_{1/2}, p_{1/2})_{1-} \otimes \text{GDPR}; 0^+ > \otimes |p_{3/2}(\pi) >$ component of the $|{}^{11}\text{Li}(\text{gs}) >$ wavefunction, through normalization (see Fig. 1(II)b)). This result underscores the importance of having at one's disposal a reliable description of the two-nucleon transfer process (reaction) populating these states, so as to be able to accurately calculate the absolute value of the associated differential cross section and thus test the structure of the wavefunctions describing the states connected in the reaction. In other words, of having at one's disposal a reaction theory of Cooper pair transfer, and associated software implementation, so that discrepancies between predictions and experiment can be associated solely with the structure input.

Summing up, and within the general scenario of the foreword, one can posit that a representative example of the reaction face of the model, is the knowledge concerning how to calculate, at the 10% level uncertainty, absolute two-nucleon transfer reaction cross sections. This in turn has shaped the (structure) reversed face, which provides direct evidence of the central role the induced pairing interaction plays throughout the mass table. In the case of ${}^{11}\text{Li}$, accounting for close to 85% of Cooper pair binding . For about 50% in open shell nuclei lying along the stability valley (see next Section).

4 The chain of superfluid ${}^{118,119,120,121,122}\text{Sn}$ -isotopes lying along the stability valley

An essentially "complete" description of the low-energy structure of the superfluid nucleus ${}^{120}\text{Sn}$ and of its odd- and even-A neighbours ${}^{118,119,121,122}\text{Sn}$ is provided by the observations carried out with the help of Coulomb excitation and subsequent γ -decay and of one- and two-particle transfer reactions, specific probes of particle-hole vibrations, quasiparticle and pairing degrees of freedom respectively, and of their mutual couplings. These experimental findings have been used to stringently test the predictions of a similarly "complete" description of ${}^{118,119,120,121,122}\text{Sn}$ carried out in terms of elementary modes of excitation which, through their interweaving, melt together into effective fields [83], each displaying properties reflecting that of all the others, their individuality resulting from the actual relative importance of each one [84]-[86].

Independent particle and collective vibrations constitute the basis states of the structure calculations. These are implemented in terms of a SLy4 effective interaction [87] and a $v_{14}({}^1S_0)(\equiv v_p^{\text{bare}})$ Argonne pairing potential [88]. HFB provides an

*It is of notice that these wave functions and the associated spectroscopic predictions [67] had to wait short of a decade to become tested and found to be correct [78, 81].

embodiment of the quasiparticle spectrum while QRPA a realization of density ($J^\pi = 2^+, 3^-, 4^+, 5^-$) and spin ($2^\pm, 3^\pm, 4^\pm, 5^\pm$) modes. Taking into account renormalisation processes (self-energy, vertex corrections, phonon renormalization and phonon exchange) in terms of the particle-vibration coupling (PVC) mechanism (Fig. 4), the dressed particles as well as the induced pairing interaction v_p^{ind} were calculated (see [89]; see also [90]-[96]). Adding v_p^{ind} to the bare interaction v_p^{bare} , the total pairing interaction v_p^{eff} was determined. With these elements, the Nambu-Gor'kov (NG) equation (see App. E) was solved selfconsistently using Green's function techniques [97]-[101], the parameters characterizing the renormalized quasiparticle states obtained (Fig. 5).

It is to be noted that in carrying out the above calculations use has been made of *empirically renormalized* collective modes * (see Sect. 4.1). These modes are determined as the QRPA solutions of a separable multipole-multipole interaction with empirical single-particle levels, adjusting the strength to obtain the desired properties (energy and above all, $B(E2)$ -values (β_λ -deformation parameters)). In this way one obtains physical reliable results (see Section 4.2) and also avoids difficulties associated with the zero-range character (ultraviolet divergencies), finite size instabilities and spurious self interactions of most Skyrme forces [103, 104, 105].

The corresponding results provided directly, or were used to work out the following structural quantities in ^{120}Sn and neighbouring nuclei [84]-[86] : **1)** the state dependent pairing gap, **2)** the quasiparticle spectrum, **3)** the $(h_{11/2} \otimes 2^+)$ multiplet splitting, **4)** the $B(E2)$ transition strengths associated with the γ -decay of ^{119}Sn following Coulomb excitation, **5)** the absolute differential cross section associated with the reactions $^{122}\text{Sn}(p,t)^{120}\text{Sn}(\text{gs})$ and $^{120}\text{Sn}(p,t)^{118}\text{Sn}(\text{gs})$, and **6)** the $^{120}\text{Sn}(d,p)^{121}\text{Sn}$ and $^{120}\text{Sn}(p,d)^{119}\text{Sn}$ absolute differential cross sections with which the ^{120}Sn valence orbitals are populated and the associated centroid and splitting of the $d_{5/2}$ clothed orbitals are excited. The relative root mean square standard deviations between theory and experiment are shown in Table 1. These results provide important evidence that choosing as basis states the elementary modes of nuclear excitations, and calculating their couplings following NFT rules, leads to a well funneled landscape of structure and reactions. Namely, a global minimum in the multidimensional space defined by 1)-6), of the difference between theory and experiment as a function of the k -mass, the pairing strength and the collectivity of the vibrational modes (see Fig. 6, see also [84]). In Section 4.2 we elaborate on a particular example of this overall accuracy of NFT predictions for open-shell nuclei, namely on the clothing and breaking of the

*In a similar way in which it has been stated that in describing a many-body system you may choose the degrees of freedom you prefer, although if you choose the wrong ones you will be sorry, one may state that elementary modes of excitation plus renormalization (in some cases empirical renormalization), allows for an economic picture of structure and reactions which converges to the physical observation, in many cases, already in lowest order of perturbation. To the extent of employing the ancient Greek meaning of "find" and "discover" to the word heuristic ($\epsilon\upsilon\rho\iota\sigma\kappa\omega$) and of "serving to discover" of the Oxford dictionary, one may ascribe the connotation of heuristic to the above mentioned protocol (within this context cf. [102])

$d_{5/2}$ valence orbital through the coupling to vibrational states and on the associated $^{120}\text{Sn}(p,d)^{119}\text{Sn}(5/2^+)$ absolute differential cross sections.

We conclude by quoting one of the important results of the work which is at the basis of this section [84]-[86]. The value of the pairing gap $\tilde{\Delta} = \tilde{\Delta}^{\text{bare}} + \tilde{\Delta}^{\text{ind}}$, obtained from the solution of the NFT+NG calculations, and resulting from the contributions of v_p^{bare} and v_p^{ind} are about equal, density modes leading to attractive contributions which are partially cancelled by spin modes (within this context see also [108] and [109]).

4.1 Empirical renormalization

The collectivity of low-lying particle-hole (two-quasiparticle (2qp)) vibrations like e.g. the lowest 2^+ state of the Sn-isotopes ($\hbar\omega_2 \approx 1$ MeV) is specifically measured by the $B(E\lambda)$ transition probability. This quantity is proportional to the density of states which in turn is proportional to the effective mass m^* of nucleons moving in levels close to the Fermi energy. Within an energy interval of approximately ± 5 MeV around ϵ_F , experimental evidence testifies to the fact that $m^* = m$, as well as that the single-particle content of these physical levels is smaller than 1, and consistent with $Z_\omega \approx 0.7$ (see Fig. 5). Because this quantity is equal to $(m_\omega/m)^{-1}$ then $m_\omega = 1.4m$, where m_ω is the so-called ω -effective mass associated with the clothing of single-particle states through the coupling to vibrations ($m_\omega/m = (1 - \partial\Delta E(\omega)/\partial\omega)$, $\Delta E(\omega)$ being the real part of the self-energy). In other words, the ω -mass reflects the retardation and single-particle content of the physical [83] fermions (see [106, 110, 111] and refs. therein)

Nucleon elastic scattering experiments at energies of tens of MeV can be accurately described in terms of an optical potential in which the strength V of the real (Saxon-Woods) potential $V(r)$ is written as $V = V_0 + 0.4E$ where $V_0 \approx -45$ MeV and $E = |\epsilon_k - \epsilon_F|$ ($\epsilon_k = \hbar^2 k^2/2m$) the nucleon energy being measured from ϵ_F . It is possible to obtain essentially the same results by solving the elastic scattering single-particle Schrödinger equation making use of an energy independent potential of strength $V \approx 1.4V_0$ and of an effective mass $0.7m$, the so called k -mass * ($m_k/m = (1 + m/(\hbar^2 k) dV/dk)^{-1}$) (see Fig 2.14 in [106])). This is also valid for deep-hole states.

At the basis of this NFT choice of the parameters characterising the mean field (m_k, V) or alternatively, of a SLy4 effective interaction to calculate the single-particle levels is the fact that, after phonon clothing of the nucleons one obtains $m^* = m_\omega m_k/m \approx m$. It is then not surprising that the collectivity of the low-lying two-quasiparticle vibrational states calculated in QRPA with SLy4 is too weak †. In

*What in nuclear matter is called the k -mass and is a well defined quantity, in finite systems like the atomic nucleus, in which linear momentum is not a conserved quantity, is introduced to provide a measure of the non-locality of the mean field, and is defined for each state as the expectation value of the quantity inside the parenthesis, calculated making use of the corresponding single-particle wavefunction (see e.g. ref. [112], in which m_k is referred to as the non-locality effective mass).

†It is of notice that other parameters of Skyrme interactions enter into play in determining the collectivity of two-quasiparticle vibrations which may overwhelm the effect discussed above concerning

fact, to have the right density of levels one needs to allow the quasiparticles participating in the vibration to excite other vibrations for then reabsorb it (self-energy process) or exchange it with the other quasiparticle (vertex correction). In other words, to couple, through sum rule conserving diagrams, the QRPA vibration with 4qp doorway states [113, 114, 115] made out of a 2qp uncorrelated component and a collective vibrational mode (see Fig. 5, dressed vibrations).

Enter empirical renormalization. Let us choose the experimental vibrational states as the collective modes to use in the doorway states. Let us calculate them by diagonalising in QRPA separable multipole-multipole interactions with $R_0 \partial U(r)/\partial r$ radial form factors [19]. Let us allow nucleons to correlate in the experimental single-particle orbits. Adjust the strength k_λ to reproduce collectivity, namely $B(E\lambda)$ (and thus deformation parameter β_λ) and excitation energy $\hbar\omega_\lambda$. Dress with these empirical modes the SLy4 QRPA vibrations. The fact that already in lowest order of perturbation (see Fig. 7) one obtains essentially the right collectivity, implies that the full iterative process shown in Fig. 7(b) converges to the right, experimental value (within this context the techniques developed in [110] can become important, see also [111], Ch 11, Section on "clothed skeletons"). *Summing up, in this approach the fermions and the vibrational states used in the intermediate states are supposed to be fully dressed, resulting in what is known as a self-consistent perturbation theory. The empirical renormalization we are talking about in the present paper, involves one more step, namely to consider that fully dressed modes coincide with the experimental ones. If using the experimental input one recovers, among other observables, the experiment as output (see Fig. 7), one can conclude that one has a good physical model for the bare quantities.*

Before concluding this section, let us return to the question of the k -mass. The Pauli principle [117] leads, among other things, to the exchange (Fock) potential in nuclei ($U_x(\vec{r}, \vec{r}') = -\sum_{\epsilon_i \leq \epsilon_F} \phi_i^*(\vec{r}') v(|\vec{r} - \vec{r}'|) \phi_i(\vec{r})$), and thus to the k -mass (all of it in the case in which velocity independent forces are used to determine the mean field, a consistent fraction of it otherwise). Thus, an essential nuclear structure element arises from a symmetry-like condition (see also [118, 119]) without any possibility of fine tuning. Be as it may, a way out is that few of the energies of the bare single-particle valence orbitals are slightly modified *empirically*, and thus to be considered among the physical parameters (the $\epsilon_{d_{5/2}}$ case discussed in Sect. 4.2) to be adjusted * to account for the set of experimental findings which provide a complete characterisation of the low-energy structure of atomic nuclei. Now, because single-particle motion can be considered the most collective of all nuclear motions [66], adjusting simultaneously k_2, k_3 and $\epsilon_{d_{5/2}}$, one is forcing that the self consistent relations between single-particle density (wave functions), mean field ($U(r) = \int d^3r' \rho(r') v(|\vec{r} - \vec{r}'|)$, $U_x(\vec{r}, \vec{r}')$) and its fluctuations ($\delta U = \int d^3r' \delta \rho v$) are physically (empirically) respected.

the k -mass [107].

*In fact, to think otherwise will be equivalent to assume that nature was not able, in synthesizing the elements, to do better than Woods and Saxon.

4.2 The $^{120}\text{Sn}(p,d)^{119}\text{Sn}(5/2^+)$ reaction

Within the framework of NFT and of Nambu-Gor'kov (NFT+NG) equations (see App. E) we want to ask the following question: is it possible to find an orbital which belongs to the valence states but for which pairing effects are weak so as to be able to study the effects of the PVC at the level of Hartree-Fock mean field? In other words, to find an orbital a few MeV away from the Fermi energy, but still belonging to the group of valence orbitals and carrying a sizeable *single-particle* strength, so as to be able to test the m_k, m_ω dependence of the results without the quasiparticle dressing? To be able to give a positive answer to the above question, two conditions have to be fulfilled by the orbital parameters: a) be sufficiently away from ϵ_F , so that $u_j v_j \ll 1$ and v_j^2 is close to 1; b) be sufficiently close to ϵ_F so that the single-particle doorway damping mechanism (coupling to three quasiparticle doorway states containing a collective vibration and responsible for the single-particle damping width $\Gamma^\downarrow \approx 0.5|\epsilon_j - \epsilon_F|$ [114, 115], see also [51] p.74) has not become fully operative. The fulfilment of these two apparently contradictory requirements is trying to achieve, and depends delicately on the unperturbed single-particle energy spectrum.

This is one of the reasons why, arguably, the end point of a NFT+NG study of a "complete" set of experimental data "fully" characterising the structure of a nucleus, is to carry out one more iteration, in which the only parameters to be varied are the single-particle HF energies of the valence orbitals *. This is also at the basis of why, again arguably, in studying nuclear structure with theoretical tools, one has to deal with nuclear zones where all bare valence orbital energies are rather homogeneous and their eventual clothing, transferable (e.g. those associated with a group of spherical superfluid nuclei like the Sn-isotopes and, likely, separated from the rest by phase transition regions). Within this context is that Fig 2.30 of [22], where the single-particle levels throughout the mass table are displayed with continuity as a function of A , similar to the way one draws, in a completely different context, a regular crystal as a function of the spatial coordinate (displaying no dislocation), in spite of its attractive simplicity, can be misleading. In fact, according to the above parlance, a plot like that shown in Fig. 2.30, and more recent ones worked out with the help of Density Functional Theory, should look more like a fractal than like a regular crystal. Or like magnetic domains, separated by domain walls.

Let us now return to the discussion of the $d_{5/2}$ strength function in ^{120}Sn . The breaking and concentration of the strength of the single-particle levels lying close to the Fermi energy (valence $d_{5/2}, g_{7/2}, s_{1/2}, d_{3/2}$ and $h_{11/2}$ orbitals) depends, to a large extent, on few, selected, on-the-energy shell renormalization processes. It is then not surprising that the d states, due to their ability to couple to $s_{1/2} \otimes 2^+, d_{5/2} \otimes 2^+, g_{7/2} \otimes 2^+$ doorway states, may display the largest fragmentation ($^{120}\text{Sn}(p,d)^{119}\text{Sn}$ and $^{120}\text{Sn}(d,p)^{121}\text{Sn}$ data)

*Within this context, see last column of Table 1, which provides an implementation of this protocol in the case of tin isotopes.

and within the framework of the theoretical description, are the ones more sensitive to the associated unperturbed HF single-particles energies. This is particularly so for the $d_{5/2}$ orbital, being the one lying further away from ϵ_F and thus most likely to be surrounded by the $2p - 1h$ (3qp containing a collective mode (doorway)) states with similar energy mentioned above to which one has to add the $h_{11/2} \otimes 3^-$ states, and thus more prone to accidental degeneracy.

In keeping with the above discussion, it has been found necessary to shift the (SLy4) bare energy of the $d_{5/2}$ orbital $\epsilon_{d_{5/2}}$ by 600 keV towards the Fermi energy allowing, after the full NFT+NG calculation has been repeated, to obtain a pole at low energy carrying most of the $5/2^+$ strength as experimentally observed. The resulting single-particle spectroscopic amplitudes were then used together with global optical potentials and DWBA, to calculate the absolute cross section of the different fragments of the $d_{5/2}$ valence orbital. The results for the levels predicted at energies below 2 MeV, are shown in Fig. 8. With the $\epsilon_{d_{5/2}}$ shift, theory now provides an overall account of the experimental findings. In other words, renormalizing empirically and on equal footing bare single-particle and collective motion of open-shell nuclei in terms of self-energy and vertex corrections, as well as particle-hole and pairing interactions through particle-vibration coupling, leads to a detailed, quantitative account of the data, constraining the possible values of the k -mass, of the 1S_0 bare NN interaction, and of the particle-vibration coupling strength within a rather narrow window. The natural scenario of a well funnelled nuclear structure landscape (see Fig. 6).

Summing up, and as indicated by the relative root mean square deviation between theory and experiment displayed in Table 1, implementing NFT in terms of empirically renormalised collective modes, and allowing for a moderate variation (slight increase in the present case) in the bare (HF) density of levels, theory becomes accurate, in average, at the 10% level. In other words, with just three parameters, namely the strengths k_2 and k_3 of the quadrupole and octupole separable multipole-multipole interactions (empirical renormalization) and the small relative shift $\delta\epsilon_{d_{5/2}}/|\epsilon_{d_{5/2}} - \epsilon_F| = 0.17$ of the energy of the $d_{5/2}$ valence orbital, one can reproduce the observables 1)-6) listed at the beginning of this section, and completely characterizing the properties of the open shell nucleus ^{120}Sn , within a 10% accuracy (for more details see [84]-[86]). It is of notice that k_2 and k_3 are strongly constrained by the experimental value of $\hbar\omega_\lambda$ and of β_λ ($\lambda = 2, 3$).

4.3 Technical details: bubble subtraction

In the dressing of the single-particles through the coupling with phonons, one has to remember that, in the second order contribution, this procedure implies an independent summation over the intermediate single-particle states for each of the two equivalent fermion lines, i.e. that of the external particle, and that of the particle-hole excitation. Thus, the second-order term is taken into account twice and has thus to be subtracted once. In other words, and according to NFT, whenever there is a fermion line and a boson line which appear and disappear at the same vertices, one must include another diagram in which the phonon line is replaced by a particle-hole pair, and which is

evaluated with an additional minus sign (see [37], Sect. 3, see also [120, 121, 122, 123].

5 Open problems

In what follows we take up one example from structure and one from reactions, namely: **1)** The quantitative role multipole pairing vibrations [29]-[31],[39], [124]-[133],[135] play in clothing elementary modes of excitation, and the systematic and detailed description of the properties of non-conventional modes of vortex-like nature (1^- Cooper pairs); **2)** the implementation in terms of NFT diagrams of a detailed protocol which will eventually allow for the calculation of the optical potential [134]-[138],[139] employing the concepts and elements worked out to describe structure.

5.1 Multipole pairing vibrations

At the basis of renormalization process one finds the coupling of single-particles and vibrations. Aside from angular momentum, parity and eventually spin and isospin quantum numbers, these bosonic modes are characterised by the transfer quantum number α [14]. Particle-hole vibrations have $\alpha = 0$, while pairing vibrations carry $\alpha = +2$ (pair creation modes) and $\alpha = -2$ (pair removal modes) *. As a rule, and with few exceptions [29, 30, 41, 140], renormalization is thought to be associated with the clothing of particles with $\alpha = 0$ vibrations.

Around closed shell nuclei, monopole, but also multipole, pairing vibrations, are very collective. Even more than low-lying surface quadrupole modes as testified by the fact that the ratio of the static $\alpha_0 = | \langle BCS | P^+ | BCS \rangle | (\beta_2)$ to the dynamic $\alpha_{dyn} = \left(\frac{E_{corr}(A+2) + E_{corr}(A-2)}{2} \right) (\beta_2)_{dyn}$ is $\alpha_0/\alpha_{dyn} \approx 0.7$ as compared to $(\beta_2)_0/(\beta_2)_{dyn} \approx 3 - 6$. Consequently, one expects that processes as those shown in Fig. 9 (see also Figs. C3 and C4) lead to important contributions to the ω -dependent (effective) physical mass of the single-particles † (see App. C). Also to the (ω -independent) two-nucleon transfer amplitudes (Fig. 9(d)), similar to the effective charge induced by the coupling of the single-particle to low-lying p-h like vibrations and to giant resonances respectively (Fig. 9(f)).

In Fig. 10 graphs associated with the clothing of the $g_{9/2}$ orbital of ^{209}Pb are shown. In Figs. 10(a) and (b) the lowest order self energy contributions arising from the coupling to the octupole vibration considering only the valence orbitals are given. In Fig. 10(c) and (d) those associated to the coupling with monopole, quadrupole and hexadecapole pairing vibrations. In ref. [140] it was found that the single-particle gap of

*The situation is, of course, more subtle in the case of superfluid nuclei, in keeping with the associated spontaneous breaking of gauge symmetry. In the discussion above we restrict ourselves to situations around closed shell nuclei. Concerning rotations, we refer to the contribution of Daniel Bès to this topical issue.

†To which extent such couplings could partially alter the conclusions of the study presented in e.g. [151] is an open question worth assessing, let alone that associated with (empirical) renormalization of the p-h like modes as done in [84]-[86].

the closed shell system ^{208}Pb decreases, from the bare value ($m_k \approx 0.7m$) by 1.25 MeV due to the coupling to particle-hole modes. Including the pairing vibrational modes this value becomes 1.10 MeV. Their effect seems to be small. This also seems to be in line with the result of ref. [141], which finds that the contribution of the pairing vibrational modes to the imaginary part of the average nuclear field is small. Note however, that in reference [140], only the valence orbitals were considered. Consequently, most of the contributions arise from graphs of the type shown in Fig. 10(d) which lead, as a rule, to a contribution smaller than that associated with e.g. the processes shown in Fig. 10(c) which, in the case of the $g_{9/2}$ valence orbital are the only two PO-like diagrams allowed (note the intermediate hole state in keeping with $\alpha = +2$ nature of the vibration, at variance with graph 10(a) in which the phonon carries transfer quantum number $\alpha = 0$). In fact, within a major shell, the monopole pairing vibration gives no contribution to processes of the type shown in Fig. 10(c), but only to CO diagram (10(d)).

It is to be noted, however, that the situation may be more subtle than just indicated concerning the relative contribution of surface and pairing vibrations to the self energy of valence single-particle states around ^{208}Pb . This is in keeping with the fact that, as seen from Fig D1 (a) and (e), the associated ground state correlations interfere with each other.

Now, among the properties of a physical (dressed) elementary mode of excitation, energy is not the most qualifying property but the response to specific external fields like one- and two-particle transfer reactions for single-particle and pair vibrational modes respectively, as well as inelastic scattering for surface modes. Within this context one can mention $^{207}\text{Pb}(t,p)^{209}\text{Pb}$, $^{210}\text{Pb}(p,d)^{209}\text{Pb}$, as well as $^{209}\text{Bi}(d,d')^{209}\text{Bi}^*$, $^{210}\text{Po}(t,\alpha)^{209}\text{Bi}$ and $^{208}\text{Pb}(^3\text{He},d)^{209}\text{Pb}$. In these cases, the coupling to pairing vibrations is important in the two-nucleon transfer process (effective spectroscopic amplitudes) and in connection with single-particle content in the case of one-particle transfer. Also, indirectly through normalisation in the case of inelastic scattering (see [19, 29, 30, 42, 124] and refs. therein).

The clothing of single-particle motion by pairing vibrations in rapidly rotating nuclei has important effects in the dealignment phenomenon, in particular above the critical Mottelson-Valatin frequency (ω_{cr}), in the difference between the kinematical and dynamical moments of inertia across ω_{cr} , in the cross talk pattern between rotational bands and in band crossing frequencies. As a consequence, particle-pairing vibrational coupling constitutes an essential part of the overall picture developed in nuclei at high rotational frequencies (cf. [132, 133], [142]-[148] and refs. therein; see also e.g. [149] for the coupling to shape vibrations).

5.2 Optical potential: example of the $^{11}\text{Li}(p,p)^{11}\text{Li}$ reaction

Nuclear Field Theory in its graphical implementation, allows for a correct description of nuclear structure and reactions. This is achieved through an orthogonalization prescription based on the renormalization of both single-particle and collective motion in terms of mass (self-energy) and screening (vertex) sum rule

conserving processes at each order of perturbation (also infinite). It respects at the same time Pauli principle by allowing, through particle-vibration vertices linear in particles and vibrations, (quasi) bosonic modes to decay into pairs of fermionic ones and viceversa. Such non-orthogonality corrections carry naturally over to DWBA two-nucleon transfer calculations, including both simultaneous and successive transfer processes *.

The fact that two-nucleon transfer reactions are calculated in second order DWBA may, within the context of NFT, lead to a misunderstanding. In fact, in structure calculations, the small parameter is the inverse effective degeneracy Ω of the space in which nucleons are allowed to correlate. Orthogonalization, Pauli principle, etc., are calculated to different orders in $1/\Omega$. In the case of transfer processes, in particular, Cooper pair transfer, (e.g. a (p,t) reaction) two nucleons may transfer simultaneously or successively. In the first case one neutron is acted upon by the v_{np} interaction while the other follows suit because of (pairing) correlation. In the second case, one neutron at a time is acted upon by v_{np} . Once this is done, there is no more to it. Second order in v_{np} exhausting all the possibilities †. Also because it contains the amplitude describing the process in which a neutron is acted upon by v_{np} in the transfer process, while the other does so because of the non-orthogonality of the single-particle basis associated with target and projectile. Being this a spurious process, the corresponding amplitude has the right phase to subtract such contribution from the sum of simultaneous and successive transfer.

Summing up, physically, second order DBWA transfer fully describes Cooper pair tunnelling, as a result of the fact that correlations, although very weak as compared with mean field effects, lead to Cooper pair transfer cross sections proportional to the density of levels squared, testifying to the fact that Cooper pair is, essentially, successive transfer. This has been duly confirmed in systematic studies [18]. It is of notice that the same picture of Cooper pair tunnelling, is at the basis of the quantitative understanding of the Josephson effect (see Sect. D1) and of the fact that making use of this effect, the most accurate measurements available of the ratio of fundamental constants h/e were obtained, let alone of the validity of BCS to describe superconductivity and to act as paradigm of theories of broken symmetry [5, 7, 12]

Because NFT is based on elementary modes of excitation, modes which carry a large fraction of nuclear correlations, and because its rules apply equally well to both bound and continuum states, it allows for a unified description of both structure and reactions.

*Concerning the question of Pauli principle (also essential in the case of structure NFT) in this case not between e.g. the two halo neutrons, but between the incoming proton and the collective modes of the core (^9Li) we refer to Fig. 11. It is of notice that making use of global optical potentials to describe the elastic channel, or mean field optical potentials to which to add polarization contribution like those displayed in Fig. 12(a), the effect of Pauli principle between a nucleon projectile and the nucleons of the target is considered through the energy (k -dependent strength, so called Perey-Buck potential (intimately connected with the k -mass) (see e.g. [150].))

†Of course, a neutron can go back and forth many times between target and projectile, a fact which would be, as a rule, a rare event.

An example of the above statements is provided by the two NFT-diagrams displayed in Fig. 12, and describing one-particle transfer polarization contributions to the optical potential associated with the elastic reaction $^{11}\text{Li}(p,p)^{11}\text{Li}(\text{gs})$. The elementary modes of excitation, appearing in these diagrams, drawn for simplicity in the language of "traditional" kinematics (^{11}Li target, fixed in the laboratory, on which now shines a proton beam), and not inverse kinematics as the experiment has been actually performed [78], are:

1) single-particles (*structure*, arrowed and solid arrowed lines; *reaction*, relative CM motion (laboratory), curved arrows); 2) vibrations (p-h, wavy lines), 3) pairing vibrations (double arrowed lines), 4) recoil mode associated with a change in mass partition (jagged curve).

In each structure (solid, dot, dotted open circle) and reaction (dashed open square) particle-vibration coupling vertices, symmetries are preserved (angular momentum, parity, gauge (particle-transfer number), etc.), while momentum is not conserved at structure vertices, in keeping with the fact that a nucleus is a finite system. On the other hand, momentum is conserved at the reaction vertices, the relative motion between projectile and target taking place in an "infinite" homogeneous, isotropic space. This is the reason why the recoil modes created by the Galilean transformation which smoothly joins the entrance (eventual also intermediate) and exit relative motion quantal trajectories (and thus lead to the proper scaling between entrance and exit channel for each partial wave in the case of DWBA), propagate together with the asymptotic outgoing particle to the corresponding detector, providing a mnemonic that at transfer reaction vertices matrix elements of the corresponding form factors which also involve recoil phases are to be calculated (cf. App. F).

Summing up, the above NFT polarization contribution to the mean field optical potential awaits to be carried out, and constitutes one of the important challenges in the unification program of structure and reactions.

6 Conclusions

From the results presented above, representative examples of the implementation of the NFT program, it is concluded that this effective field theory provides the rules for designing, and calculating, the graphs describing the variety of physical phenomena associated with nuclear structure as probed by direct reactions, and to work out the different observables.

The fact that they reproduce the corresponding data which completely characterize the spectroscopic properties of open shell nuclei lying along the stability valley as well as exotic nuclei around novel closed shells ($N = 6$) within experimental errors, is intimately related to the fact that NFT- Feynman diagrams can be viewed as graphical solutions, through the interweaving of single-particle and collective modes of nuclear excitation, of the problems of over completeness (non-orthogonality) of the associated basis, and those arising from the identity of the particles appearing explicitly and those participating in

the collective modes (Pauli principle), thus providing the theoretical framework to obtain an accurate solution to the many-body nuclear problem.

Because of the operativity of these solutions concerning both bound as well as continuum states, the NFT rules allow for a unified treatment of both structure and reactions. This last being a program which is lively under way, the calculation of the polarisation contribution to the optical potential constituting one of the important challenges. Summing up, NFT rules in its graphical implementation, allow for a correct description of nuclear structure and reactions through an orthogonalization process based on the renormalization of both single-particle and collective motion in terms of mass (self-energy) and screening (vertex) sum rule conserving processes, respecting at the same time Pauli principle.

This is what unarguably, NFT can do as testified by the documentation presented here or referred to. What it cannot do, is to solve problems regarding ill behaved bare forces, or the consequences of associated particle-vibration coupling vertices which eventually lead to divergences. Within this context, empirical renormalization has proven to be a powerful and physically consistent prescription to implement the NFT program and make connection with experimental data.

7 Hindsight

As a result of the ground breaking contributions of Bohr and Mottelson which we celebrate in the present volume, our understanding of the nuclear structure is based on the observation of independent particle and collective elementary modes of excitations and of their couplings. The Nuclear Field Theory program uses these modes and couplings to consistently build a many-body effective field theory (see e.g. Fig. 7), removing spurious Pauli principle violating terms and non-orthogonality contributions (see e.g. Fig. 4). It is possible then to utilize the resulting many-body correlated wavefunctions for the description of the nuclear structure observables (see e.g. Fig. 1) and nuclear reaction cross sections (cf. e.g. Figs. 2 and 8). The program, although rather well implemented, is not yet fully operative (in particular concerning its reaction part). Not only for the intrinsic difficulties in developing such a complete description of the many-body nuclear structure and reactions phenomena in itself, but also due to inconsistencies in mean field generators leading to uncontrollable spuriousities which only now are being addressed.

To overcome such and others, external, present-day limitations to the validity of the Nuclear Field Theory treatment of the nuclear many-body problem, we implemented an empirical renormalization procedure: tune the particle-vibration coupling vertex to reproduce the experimental properties of low-lying collective states with separable interactions making use of experimental single-particle levels, and treat this procedure as an ansatz which has to consistently recover itself in the RPA calculation of the collective states.

To quote but just two results and one outstanding open problem of the

Observables	SLy4	$d_{5/2}$ shifted	Opt. levels
Δ	10 (0.7%)	10 (0.7 %)	50 (3.5 %)
E_{qp}	190 (19%)	160 (16%)	45 (4.5 %)
Mult. splitt.	50 (7%)	70 (10%)	59 (8.4 %)
$d_{5/2}$ strength (centr.)	200 (20%)	40 (4%)	40 (4%)
$d_{5/2}$ strength (width)	160 (20%)	75 (9.3%)	8 (1%)
$B(E2)$	1.4 (14%)	1.34 (13%)	1.43 (14%)
$\sigma_{2n}(p, t)$	0.6 (3%)	0.6 (3%)	0.6 (3%)

Table 1: Root mean square deviation σ between the experimental data and the theoretical values expressed in keV for the pairing gap, quasiparticle energies, multiplet splitting, centroid and width of the $5/2^+$ low-lying single-particle strength distribution. In single-particle units B_{sp} for the γ -decay (B(E2) transition probabilities) and in mb for $\sigma_{2n}(p, t)$. In brackets the ratio $\sigma_{rel} = \sigma/L$ between σ and the experimental range L of the corresponding quantities: 1.4 MeV (Δ), 1 MeV (E_{qp}), 700 keV (mult. splitting), 1 MeV ($d_{5/2}$ centroid), 809 keV (=1730- 921) keV ($d_{5/2}$ width), 10 B_{sp} (B(E2)), 2250 mb ($\sigma_{2n}(p, t)$), is given (for details see [86]).

implementation of the Nuclear Field Theory program:

- a) The pairing gap of spherical open-shell nuclei is made of essentially *equal contributions* arising from the bare $NN^{-1}S_0$ and from the induced pairing interactions.
- b) Making use of NFT wavefunctions and associated spectroscopic amplitudes, *one can calculate* two-nucleon transfer absolute differential cross sections which provide an overall account of the observations within experimental errors.
- c) Making use of NFT wavefunctions and associated spectroscopic amplitudes, *calculate* the polarization contribution to the nucleon-nucleus optical potential in general, and to that describing the elastic scattering of a proton off ^{11}Li in particular.

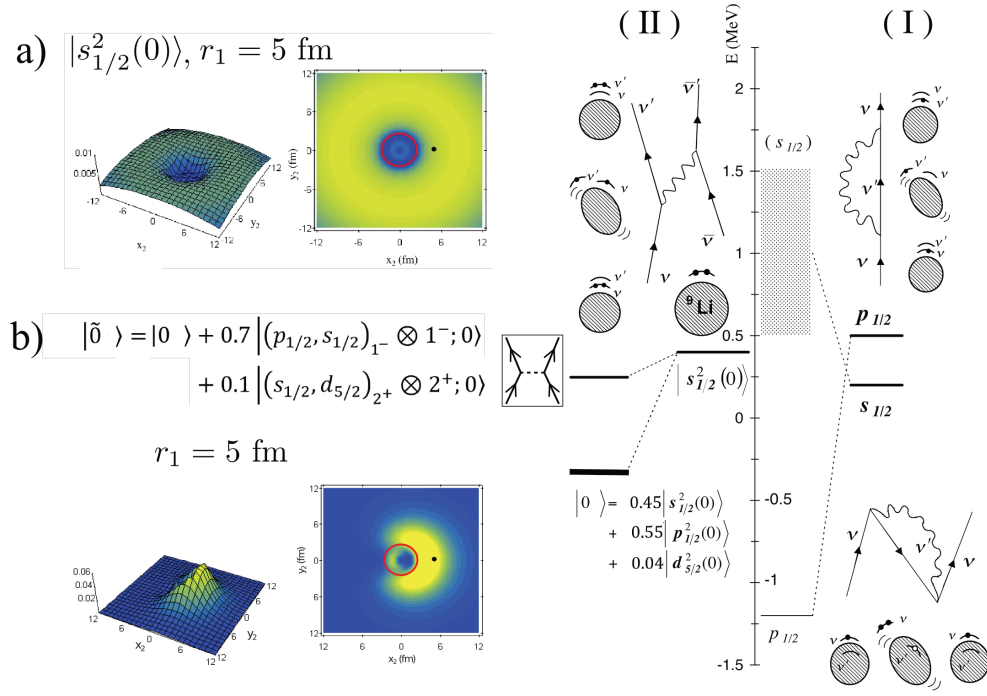


Figure 1: Parity inversion and Cooper pair binding in the N=6 closed shell isotone ^9Li . (I): schematic representation of the clothing of single-particle motion in ^{10}Li . (II) of induced pairing interaction in ^{11}Li . The first process is mainly associated with quadrupole vibrations of the core. The second, with the exchange of the GDPR between the halo neutrons of ^{11}Li (After [67]).

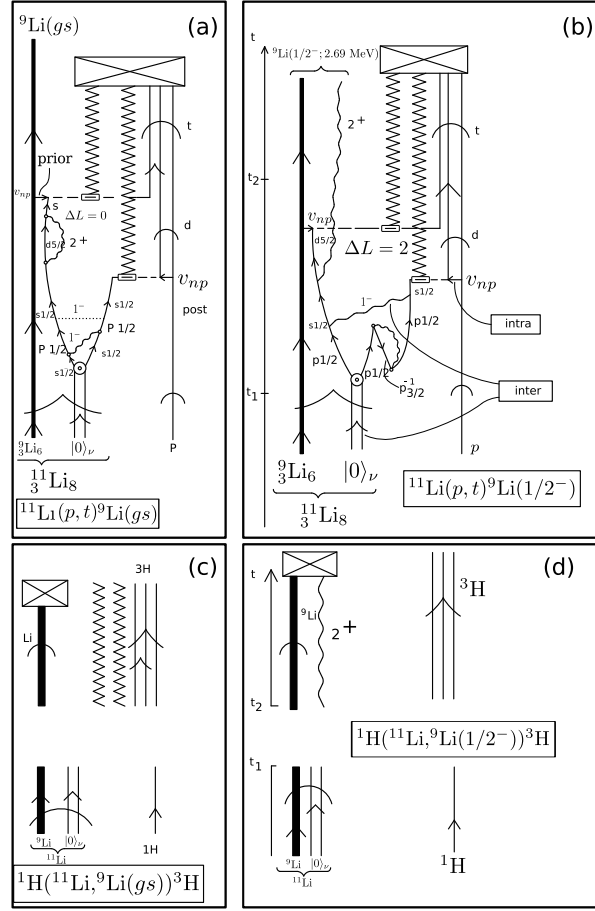
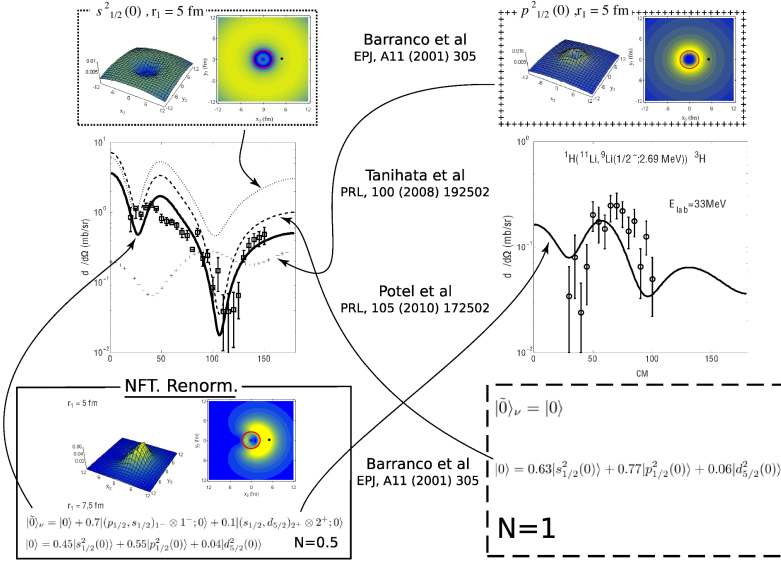


Figure 2: Representation of the reaction $^{11}\text{Li}(p,t)^9\text{Li}$, making use of NFT-Feynman diagrams. Time is assumed to run upwards. A single arrowed line represents a fermion (proton) (p) or neutron (n). A double arrowed line two correlated nucleons. In the present case two correlated (halo) neutrons (halo-neutron pair addition mode $|0\rangle_\nu$). A heavy arrowed line represents the core system $|^9\text{Li}(gs)\rangle$. A standard pointed arrow refers to structure, while "round" arrows refer to reaction. A wavy line represents (particle-hole) collective vibrations, like the low-lying quadrupole mode of ^9Li , or the (more involved) dipole pygmy resonant state which, together with the bare pairing interaction (horizontal dotted line) binds the neutron halo Cooper pair to the core. A short horizontal arrow labels the proton-neutron interaction v_{np} responsible for the single-particle transfer processes, represented by an horizontal dashed line. A dashed open square indicates the particle-recoil coupling vertex (for more details see caption to Fig. 12). The jagged line represents the recoil normal mode (see App. F, discussion connected with Fig. F1) resulting from the mismatch between the relative centre of mass coordinates associated with the mass partitions $^{11}\text{Li}+p$, $^{10}\text{Li}+d$ (virtual) and $^9\text{Li}+t$. It is explicitly drawn as discussed in the text and in App. F as a mnemonic connected with the particle-recoil coupling vertex. The detector array is represented by a crossed squared box.



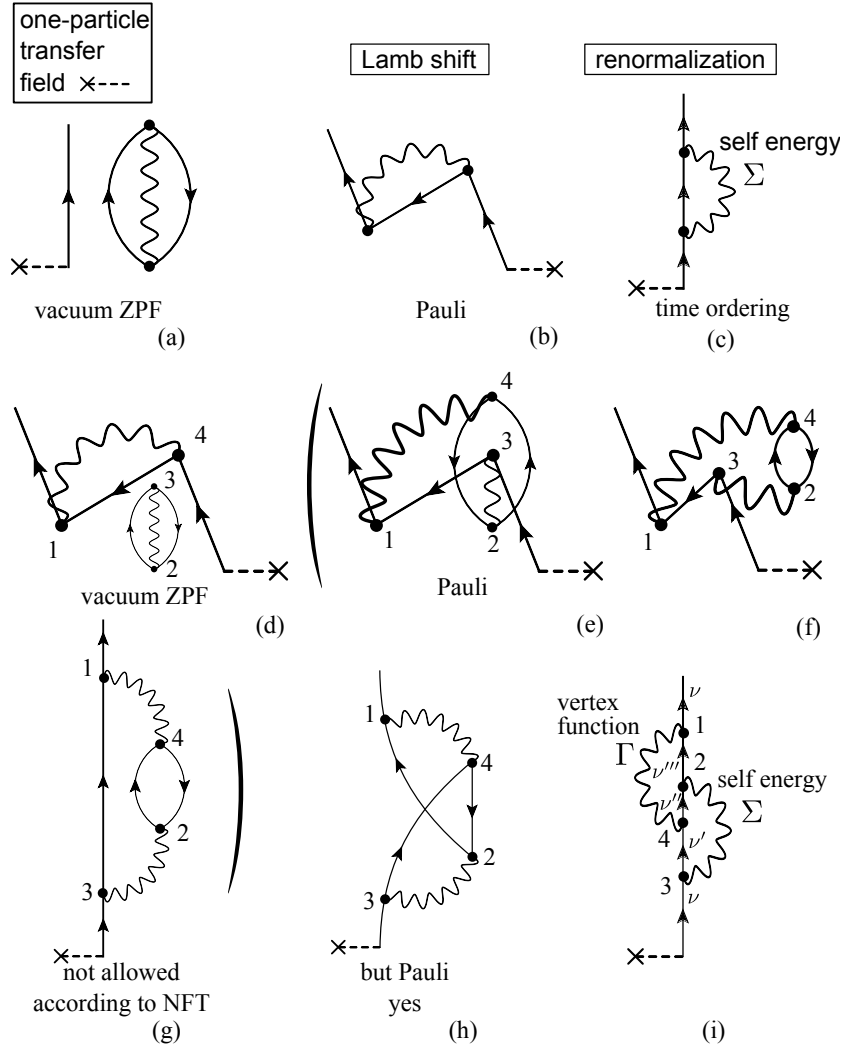


Figure 4: Implementing renormalization. The "physical" (clothed), renormalized [83, 106] properties of a quantal system can be studied by forcing the vacuum to become real, through the action of an external field. A textbook example is provided by single-particle renormalization. That is, by studying how a particle dresses itself in interaction. Here we consider the particle-vibration coupling, the processes involving the bare interaction not being discussed. Renormalization affects both NFT-Feynman diagrams and propagators, the dressing process being implemented in terms of two Green's function.

(a,b,c): Self-energy Σ ; the associated Green's function results from the single-particle interacting with the vacuum as it propagates. The self-energy Σ describes the changes to the particle's mass caused by the coupling to vibrations.

(i): vertex corrections. The corresponding Green's function results from the virtual fluctuations screening interaction between fermions. It is described by the vertex function Γ . This screening changes the coupling constant. It is of notice that the processes **(e),(f)** and **(g)** within brackets are all equal but for time ordering, and arise from process **(d)** from Pauli exchange. Such a process is not allowed because it contains a bubble, as is evident from the time ordering displayed in **(g)**. **(h)** Pauli of **(g)** leading to an allowed process, which by time ordering leads to **(i)**.

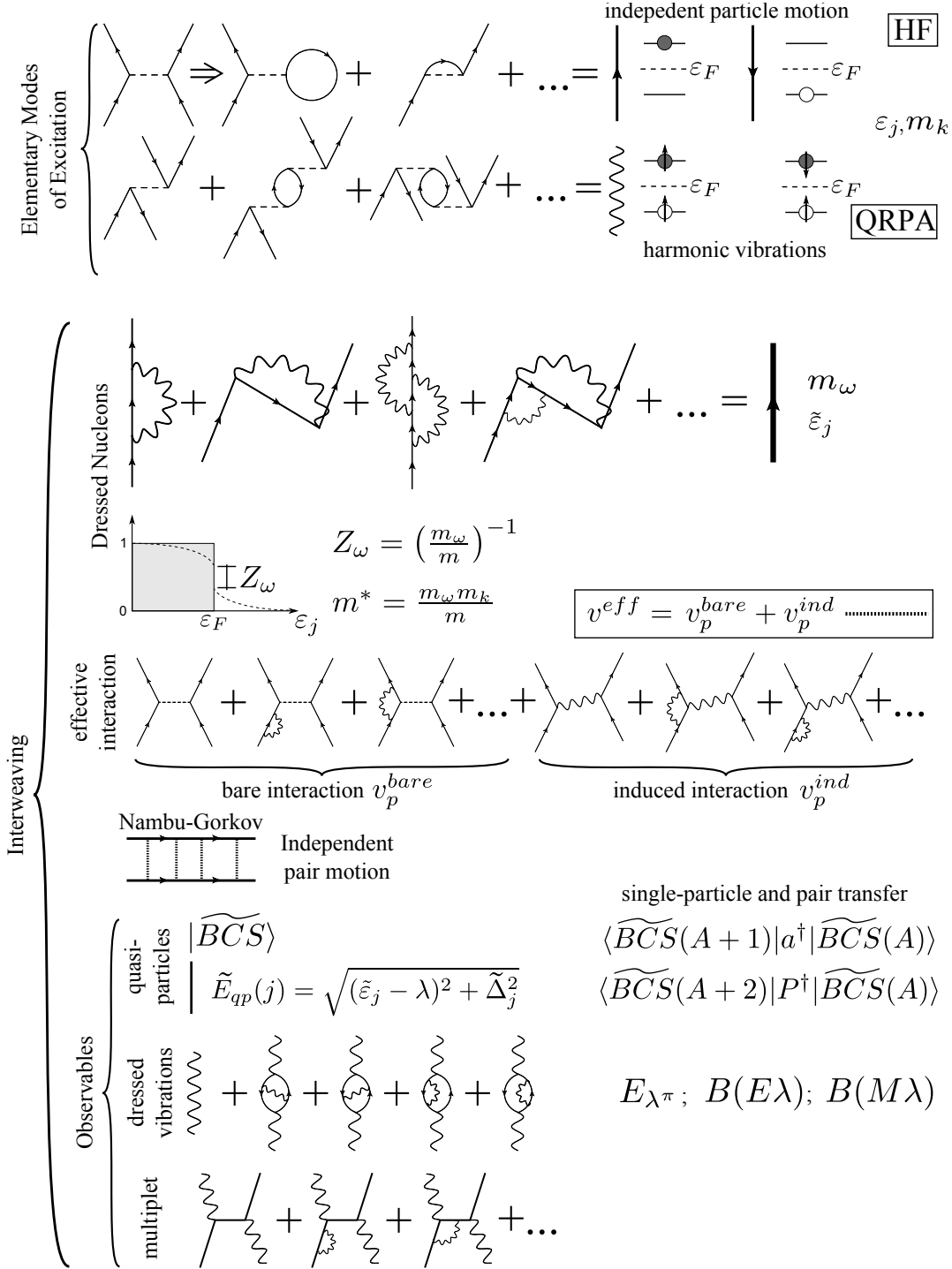


Figure 5: Resumé of the strategy followed to calculate dressed elementary modes of excitation and induced pairing interaction in terms of NFT diagrams of different order propagated by Nambu-Gor'kov equations (see App. E).

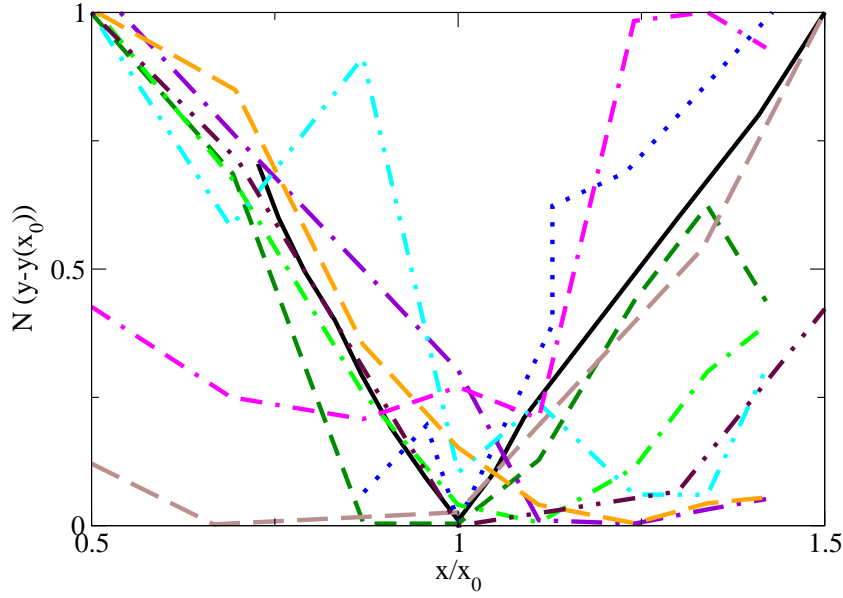


Figure 6: (color online) The root mean square deviations between theory and experiment of different structural properties in ^{120}Sn and neighboring nuclei are shown as a function of the value of one of the parameters (generically denoted by x) used in the NFT+NG calculation, namely the pairing constant G (referred to the value $G_0 = 0.22$ MeV), the effective mass m_k (referred to the value $(m_k)_0 = 0.7m$) and the quadrupole deformation parameter β_2 (referred to the value $(\beta_2)_0 = 0.13$). The different functions $y(x)$ are normalized and shifted so that they vanish for $x = x_0$. The curves represent: the deviation of the pairing gap associated with the $h_{11/2}$ orbital ($\Delta_{h_{11/2}}(G/G_0)$ (solid black curve); $\Delta_{h_{11/2}}(m_k/(m_k)_0)$ (dotted blue curve); $\Delta_{h_{11/2}}(\beta_\lambda/(\beta_\lambda)_0)$ (dashed green curve)); the deviation of the quasiparticle spectrum ($E_{qp}(G/G_0)$ (dashed brown curve); $E_{qp}(\beta_\lambda/(\beta_\lambda)_0)$ (dash-dotted green curve); the deviation of the $h_{11/2} \otimes 2^+$ multiplet splitting $E_{h_{11/2} \otimes 2^+}(\beta_\lambda/(\beta_\lambda)_0)$ (dash-dotted purple curve); the deviation of the centroid position of the $d_{5/2}$ strength function $S_{d_{5/2}}(\beta_\lambda/(\beta_\lambda)_0)$ (dash-dotted cyan curve); the deviation of the width of the $d_{5/2}$ strength function $S_{d_{5/2}}(\beta_\lambda/(\beta_\lambda)_0)$ (dash-dotted pink curve); the deviation of the quadrupole transition strength $B(E2)(\beta_\lambda/(\beta_\lambda)_0)$ (dashed orange curve). For details see [84]-[86].

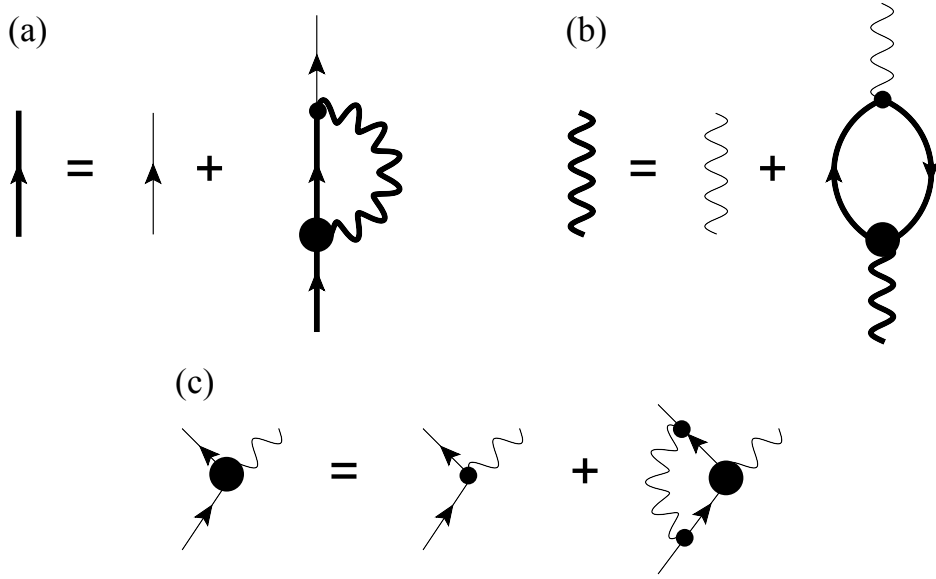


Figure 7: Graphical (NFT-Feynman) representation of the Hedin equations ([152], see also [111]) associated with the renormalization of independent particle and collective nuclear degrees of freedom. These equations are to be solved selfconsistently (note that there are the same dressed components in both sides of the equations), thus implying a full solution of the the quantum many-body problem. At present a viable prescription requires solving the Dyson Equation (a), including vertex corrections (c) perturbatively, making use of phonons empirically renormalized with the help of a properly adjusted separable interaction for the vertex, instead of the full solution of (b) with self-consistent vertex.

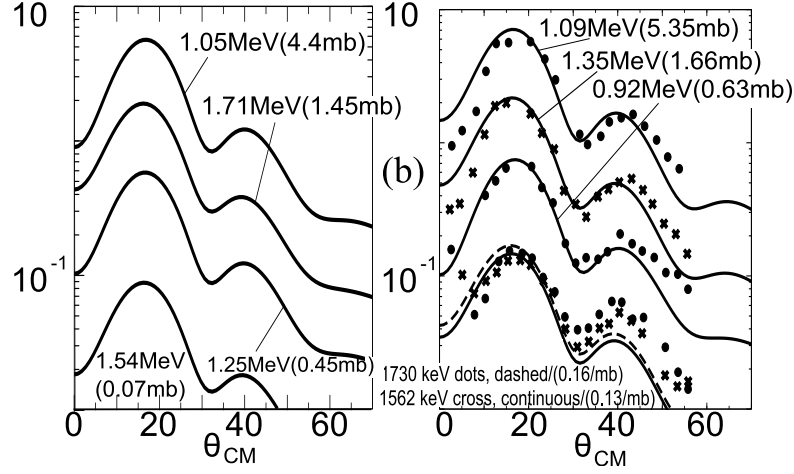


Figure 8: $^{120}\text{Sn}(p,d)^{119}\text{Sn}(5/2^+)$ absolute experimental differential cross sections [116], together with the DWBA fit used in the analysis of the data (right panel) in comparison with the DWBA calculations (left panel) carried out as explained in the text (see also [86]). The energies of the experimental and theoretical peaks are indicated, and the associated cross sections (integrated in the range $2^\circ < \theta_{c.m.} < 55^\circ$) are given in parenthesis.

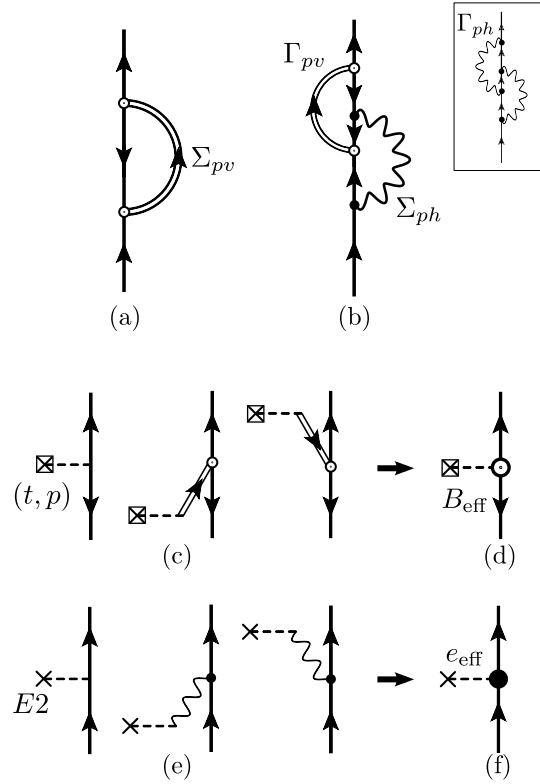


Figure 9: **(a)** Self energy associated with the coupling of pair addition mode (pairing vibration (pv) of any multipolarity and parity). The admixture between particles and holes is apparent. **(b)** vertex correction associated with a multipole pair addition mode (pairing vibration (pv)) in a self-energy process (Σ_{ph}) induced by the coupling of the single particle to a particle-hole (ph) collective mode. The presence of a hole state in the Γ_{pv} process instead of a particle state as in the case of Γ_{ph} (see inset) can lead to important effects, e.g. cancellations. This is in keeping with the fact that a hole state has the same absolute value of e.g. the quadrupole moment of a particle state, but opposite sign, a consequence of the fact that the closed shell has zero quadrupole moment [153]. **(c)** The pairing renormalization processes of the type shown in (a) have important consequences on the absolute value of the two-nucleon transfer process $(N_0-1)(t,p)(N_0+1)$ (e.g. $N_0=126$), in keeping with the fact that the coupling of the external (t,p) field with the pair addition mode leads to an effective two-nucleon spectroscopic amplitude which is strongly renormalized [50] (for a recent experimental study in the quest to observe the giant pairing vibration (GPV) see [154]). **(d)** Effective two-nucleon transfer amplitude. **(e)** This is similar to what happens in the case of e.g. the quadrupole excitation of a single-particle state renormalised by a quadrupole (p-h)-like vibration, processes which lead to **(f)**: effective charge. It is of notice that, as a rule, the ω -dependent contributions to the effective (t,p) or $E2$ values have to be calculated explicitly. Only in the case of high lying modes, like e.g. the GPV and GQR (both isoscalar and isovector), the ω -independent effective two-nucleon transfer amplitudes and e_{eff} can provide an accurate estimate of the renormalization processes.

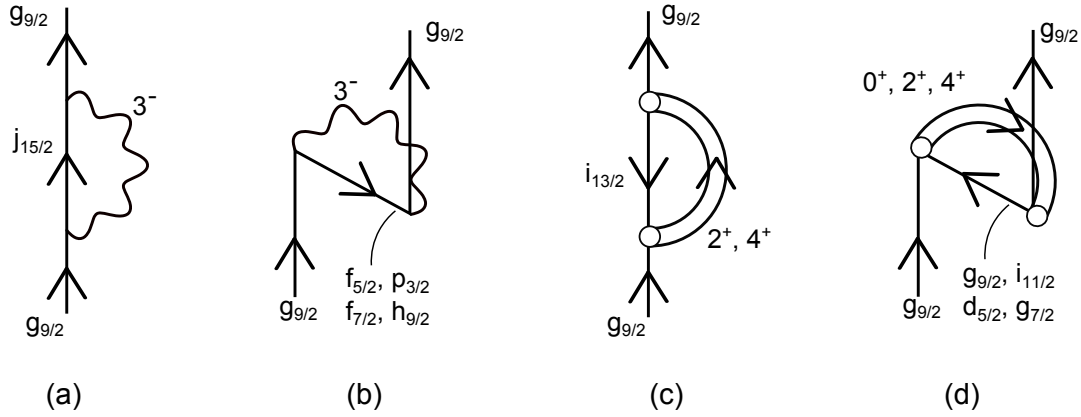


Figure 10: Self-energy diagrams associated with the $g_{9/2}$ neutron single-particle state of ^{209}Pb . The wavy curve in (a) and (b) represents the octupole vibration of ^{208}Pb , the most collective of all low-lying modes of ^{208}Pb ($\hbar\omega_{3-} = 2.62$ MeV, $B(E3) = 32 B_{sp}$). The doubled arrowed curves in (c) represent the quadrupole and hexadecapole pair addition and pair subtraction modes of ^{208}Pb , while in (d) also the monopole one. Single arrowed lines pointing upwards (downwards) stand for single-particle (-hole) states.

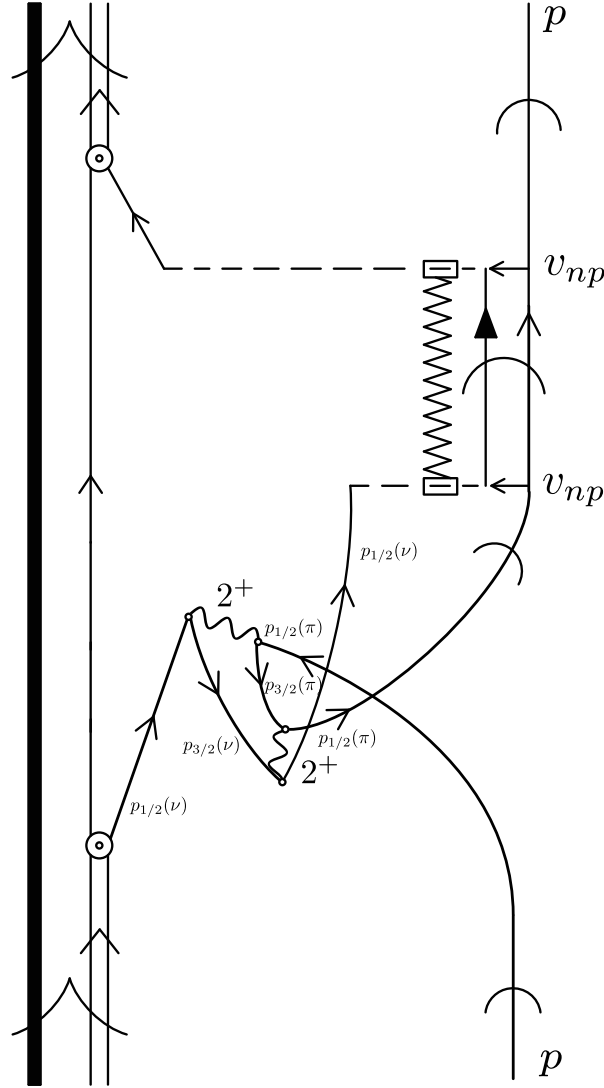


Figure 11: In keeping with standard direct reaction praxis, neither in Fig. 2 nor in Fig.12 antisymmetrization is carried out between the impinging proton and the protons of ^{11}Li . At energies of few MeV per nucleon such processes are expected to contribute in a negligible way to the differential cross section. Within the present discussion ($^{11}\text{Li}(p,p)^{11}\text{Li}$) (see Fig. 12), an example of such processes corresponds to the exchange of a proton participation in the quadrupole vibration of the core, with the projectile, as shown in the figure. Such a process will not only be two orders higher in perturbation in the particle-vibration coupling vertex. It will be strongly reduced by the square of the overlap between a proton moving in the continuum, and a $p_{1/2}$ proton of the ^9Li core bound by about 10 MeV.

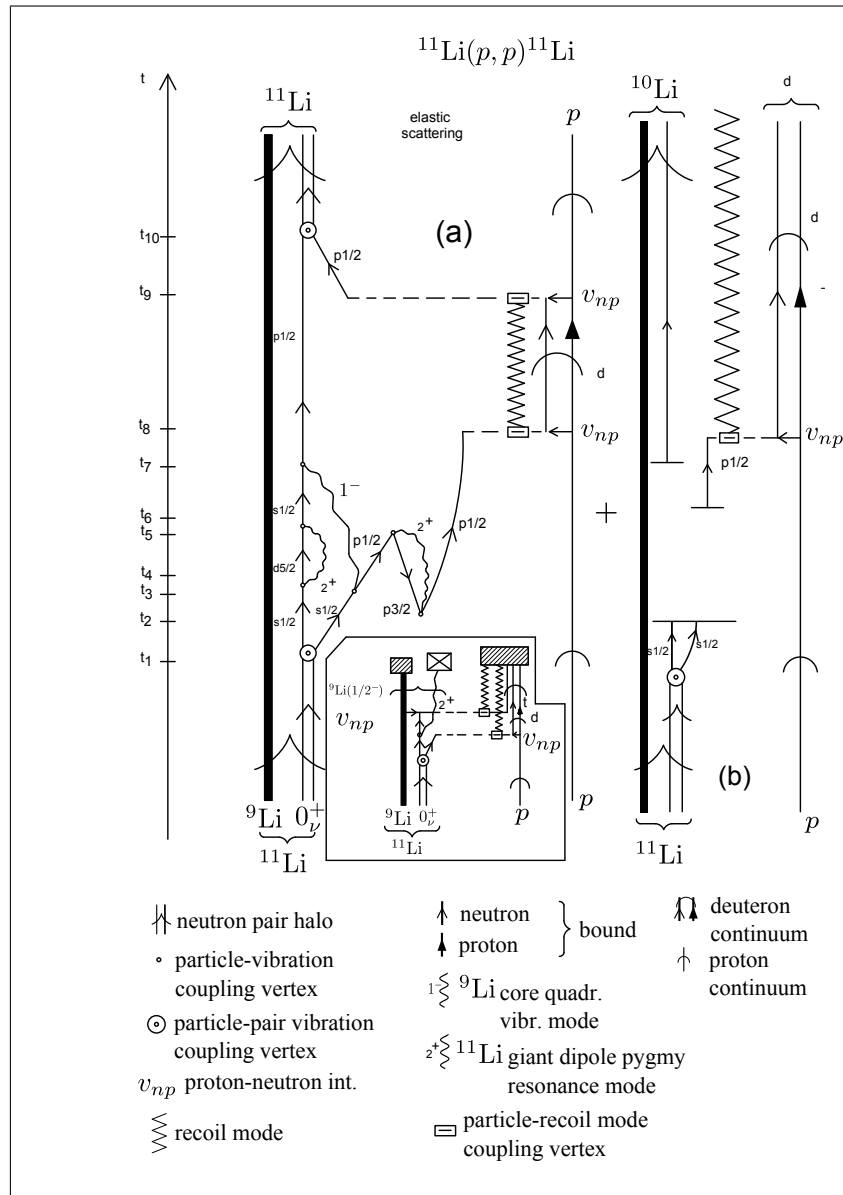


Figure 12: **(a)** NFT-diagram describing one of the processes contributing to the elastic reaction $^{11}\text{Li}(p,p)^{11}\text{Li}$ as the system propagates in time (polarization contribution to the global (mean field) optical potential). Processes taking place between $t_1 - t_7$: The halo pair addition mode $|0_\nu^+\rangle$ decays at time t_1 into a pure bare configuration and its binding to the ^9Li core results from parity inversion where the $s_{1/2}$ continuum orbital is lowered to threshold through clothing with mainly quadrupole vibrational modes and the $p_{1/2}$ bound state suffers a strong repulsion into a resonant state by Pauli principle with particles participating in the quadrupole mode. The resulting dressed neutron states get bound mainly through the exchange of the 1^- giant dipole pygmy resonance (GDPR), represented for simplicity, as a correlated particle hole excitation. At time t_8 , one of the neutrons of the halo Cooper pair is transferred, with the emission of a recoil mode, to the incoming proton projectile through the proton-neutron interaction v_{np} (prior representation), leading to a deuteron. This neutron is, at time t_9 transferred back (to virtual ^{10}Li) through v_{np} acting a second time (post representation), with the simultaneous absorption of the recoil mode. Eventually, at time t_{10} the two neutrons merge, through the particle-pair vibrational coupling, into the halo pair addition mode $|0_\nu^+\rangle$. The real part of the diagram contributes to U_{opt} while the imaginary one to W_{opt} , corresponding to the real and imaginary (absorptive) component of the polarization contribution to the optical potential, arguably to be added to the experimental determined (global) $^9\text{Li}+p$ elastic scattering optical potential. It is of notice that this diagram provides all the elements to extend and formalize NFT rules of structure so as to be able to deal also with reactions. Within this context see [60], pp. 410,412 (figures 28 and 29). **(b)** Same as in (a) up to time t_8 (reason for which no details are repeated between t_2 and t_8). From there on the deuteron continues to propagate to the detector (together with the recoil mode). Likely, the neutron in ^{10}Li will break up before this event. Summing up, in the center of mass reference frame both p and ^{11}Li display asymptotic states in entrance as well as in exit channels in case (a), and only in the entrance channel in case (b), while in the exit channel only ^{10}Li ($^9\text{Li}+n$) and the deuteron do so. *In a very real sense this (diagrams (a) and (b), together with Fig. 2 and eventually that describing anelastic scattering) is a nucleus. Namely, the summed information, through asymptotic states, of the outcome of probing the system with a complete array of experiments (elastic, anelastic and one- and two-nucleon transfer).*

A. Neutron halo pair addition mode and giant dipole pygmy resonance (GDPR): symbiotic elementary mode of nuclear excitation

Halo states like $|^{11}\text{Li}(\text{gs})\rangle$, in which a consistent fraction of the two weakly bound neutrons form an extended low density misty cloud, imply the presence of a low-lying dipole state, resulting from the sloshing back and forth of the cloud with respect to the protons of the core. Microscopically, to form a halo, the two neutrons have to move in weakly bound or virtual single-particle states, with no or little centrifugal barrier. That is, s - and p -states strongly renormalized, and as a result, both lying essentially at threshold. Thus the presence of low-energy $(s, p)_{1-}$ configurations which, coupling to the Giant Dipole Resonance can bring down a fraction of the dipole (TRK) sum rule.

Because of the small overlap existing between halo neutrons and core nucleons both the 1S_0 , NN- and the symmetry-potential become strongly screened, resulting in a subcritical value of pairing and in a weak repulsion to separate protons from neutrons in the dipole channel. As a result, neither the $J^\pi = 0^+$ correlated neutron state (Cooper pair), nor the $J = 1^-$ one (vortex-like) are bound, although both qualify unstintingly to become bound to the core $^9\text{Li}^*$.

Having essentially exhausted the bare NN-interaction channels, the two neutrons can correlate their motion by exchanging vibrations of the medium in which they propagate, namely the halo and the core. Concerning the first one, these modes could hardly be the $\lambda = 2^+, 3^-$ or 5^- surface vibrations found in nuclei lying along the stability valley. This is because the diffusivity of the halo is so large that it blurs the very definition of surface. Those associated with the core ($2^+, 3^-, 5^-$ etc.) provide some glue, but insufficient to bind any of the two dineutron states in question.

The next alternative is that of bootstrapping. Namely, that in which the two partners of the (monopole) Cooper pair exchange pairs of vortices (dipole Cooper pair), as well as one dipole Cooper pair and a quadrupole pair removal mode, while those of the vortex exchange pairs of Coopers pairs (monopole pairing vibrations), but also pairs of dipole pairs, as shown in Figs. A1 and A2(a) and A2(b) respectively. In other words, by liaising with each other, the two dineutrons contenders at the role of ^{11}Li ground state settle the issue. As a result the Cooper pair becomes weakly bound ($S_{2n} = 389$ keV), the vortex state remaining barely unbound, by about 0.5-1 MeV [68, 69]. There is no physical reason why things could not have gone the other way, at least none that we know. Within this context we refer to ^3He superfluidity, where condensation involve $S = 1$ pairs (it is of notice that we are not considering spin degrees of freedom in the present case, at least not dynamic ones).

For practical purposes, one can describe the 1^- as a two quasiparticle state and

*Within this context note the detailed dependence on quantal size effects of these "exotic nuclei" excitations as compared to those discussed in ref. [155]

calculate it within the framework of QRPA adjusting the strength of the dipole-dipole separable interaction to reproduce the experimental findings [67]. In this basis it is referred to as a Giant Dipole Pygmy Resonance (GDPR). Exchanged between the two partners of the Cooper pair (Fig. A1(d)) leads to essentially the right value of dineutron binding to the ${}^9\text{Li}$ core. Within this context one can view the ${}^{11}\text{Li}$ neutron halo as a van der Waals Cooper pair (Fig. A.1(f)). The transformation between this picture and that discussed in connection with (a) and (b) as well as with Fig. A2 can be obtained expressing the GDPR, QRPA wavefunction, in terms of particle creation and destruction operators (Bogoliubov-Valatin transformation) as seen from Fig. A1(a) and (b). A vortex-vortex stabilised Cooper pair emerges.

Which picture is more adequate to describe the dipole mediated condensation is an open question, each of them reflecting important physics characterising the GDPR. In any case, both indicate the symbiotic character of the halo Cooper pair addition mode and of the pygmy resonance built on top of, and almost degenerate with it. Insight into this question can be obtained by shedding light on the question of whether the velocity field of each of the symbiotic states is more similar to that associated with irrotational or vortex-like flow * (within this context see [156]). Some insight into this question could be shed through electron scattering experiments, likely not an easy task when dealing with unstable nuclei. On the other hand, two-nucleon transfer reactions, specific probe of (multiple) pairing vibrational modes, contain many of the answers to the above question (Figs. A3). In fact, ground state correlations will play a very different role in the absolute value of the ${}^9\text{Li}(t,p){}^{11}\text{Li} (1^-)$ cross section, depending on which picture is correct. In the case in which it can be viewed as a vortex (pair addition dipole mode) it will increase it (positive coherence), producing the opposite effect if the correct interpretation is that of a (p-h)-like excitation [73]. Insight in the above question may also be obtained by studying the properties of a quantal vortex in a Wigner cell with parameters which approximately reproduce the halo of ${}^{11}\text{Li}$, and in analogy with what is done in the study of vortices in the environment of neutron stars [157, 158].

A further test of the soundness of the physics discussed above, concerns the question of whether the first excited, 0^+ halo state ($E_x = 2.24$ MeV) of ${}^{12}\text{Be}$ can be viewed as the $|\text{gs}({}^{11}\text{Li}) >$ in a new environment, and thus considered as a novel mode of elementary

*Within this context, one can mention that a consistent description of the GQR and of the GIQR is obtained assuming that the average eccentricity of neutron orbits is equal to the average eccentricity of the proton orbits [65] , the scenario of neutron skin . The fact that the isoscalar quadrupole-quadrupole interaction is attractive and that the valence orbitals of nuclei have, as a rule and aside from intruder states, homogeneous parity, precludes the GQR to play the role of the GQPR as there will always be a low-lying quadrupole vibration closely connected with the aligned coupling scheme and thus nuclear plasticity. Within this context one can nonetheless posit that the GQR, related to neutron skin, is closely associated with the aligned coupling scheme. Making a parallel, one can posit that the GDPR is closely connected with vortical motion. Arguably, support for this picture is provided by the low-lying E1 strength of ${}^{11}\text{Li}$, resulting from the presence of $s_{1/2}$ and $p_{1/2}$ orbitals almost degenerate and at threshold, resulting in a low-lying Cooper pair coupled to angular momentum 1^- . The scenario of vortical motion.

excitation: neutron halo pair addition mode of which the $|1^-(^{12}\text{Be}) ; 2.71 \text{ MeV}\rangle$ is its symbiotic GDPR partner. Studying the electromagnetic decay and eventually identifying the E1-branching ratio $|1^-(2.71 \text{ MeV})\rangle \rightarrow |0^{+*}(2.24 \text{ MeV})\rangle$, and possibly others, insight into the above questions can be deepened through two-nucleon stripping and knockout reactions (see Fig. A4). In particular study the role ground state correlations play in predicting the absolute value of the corresponding reactions.

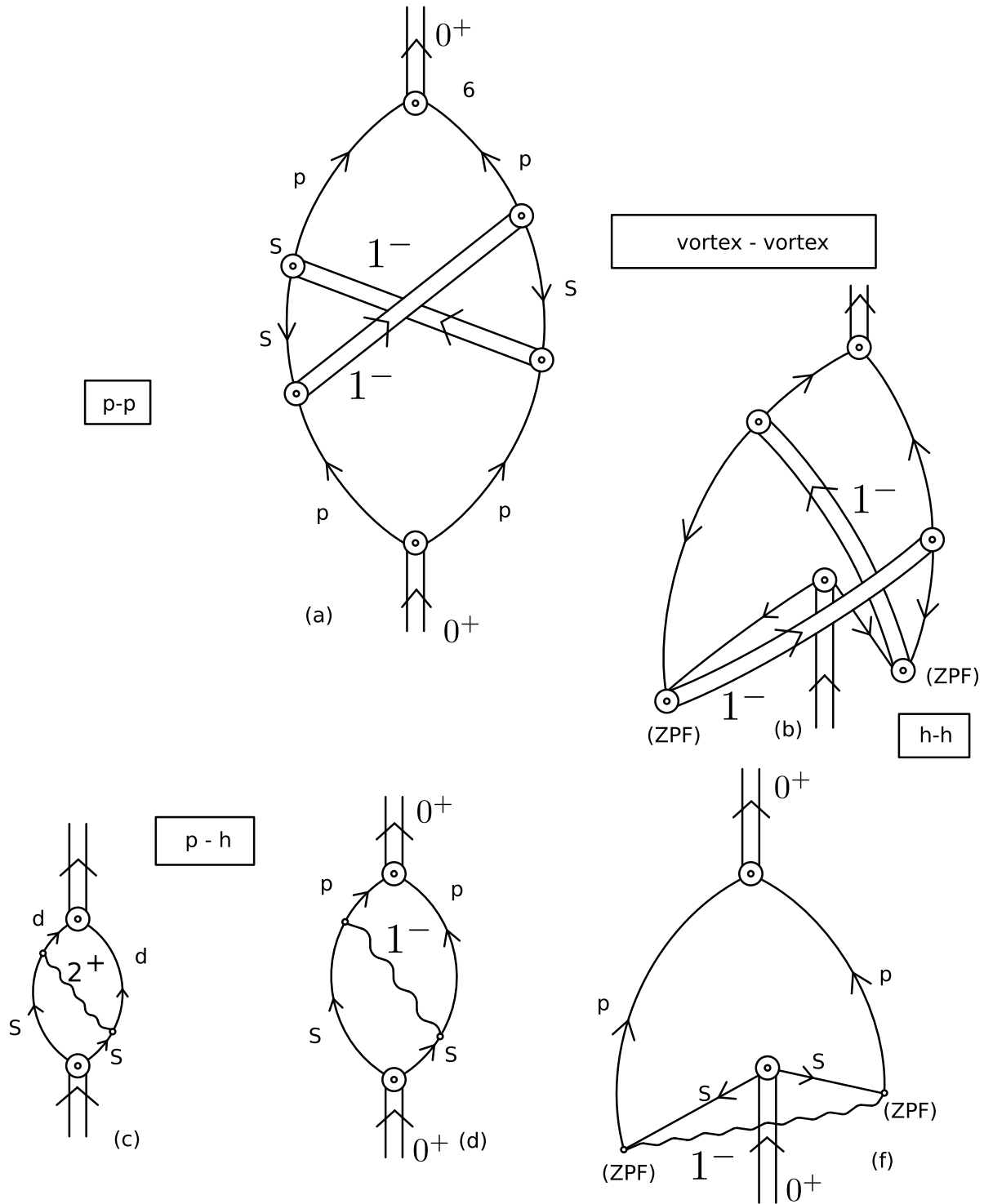


Figure A1: NFT-Feynman diagrams describing the interweaving between the neutron halo pair addition monopole and dipole modes (double arrowed lines labeled 0^+ and 1^- respectively). Above, the exchange of dipole modes binding the 0^+ pair addition mode through forwards going particle-particle p-p (h-h) components. Below, the assumption is made that the GDPR of ^{11}Li can be viewed as a p-h (two quasiparticle), QRPA mode.

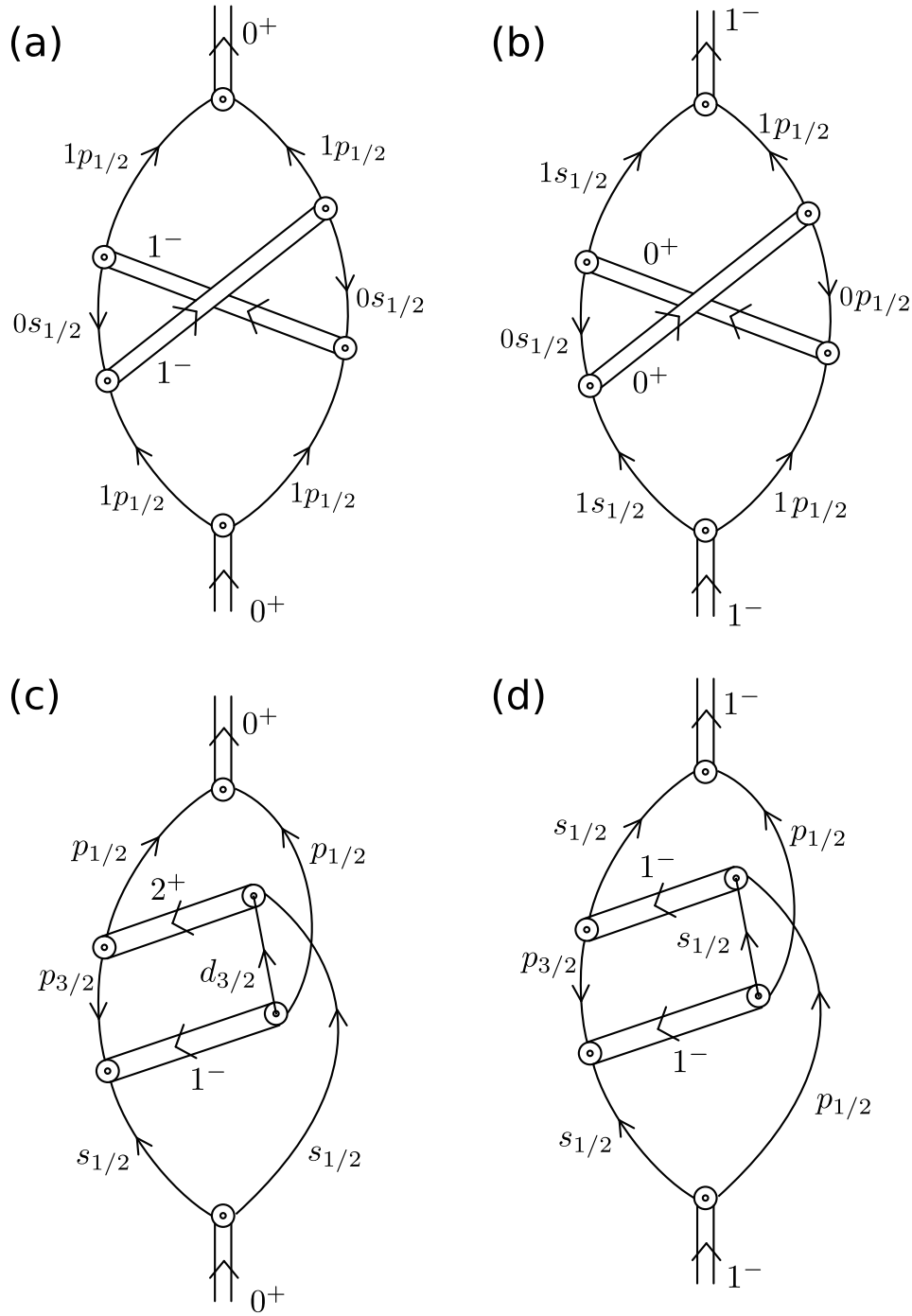


Figure A2: NFT-Feynman diagrams describing, (a,c) some of the particle-particle (pp),hh and ph processes binding the Cooper pair neutron halo and stabilizing ^{11}Li , as well as (b,d) giving rise to the GDPR.

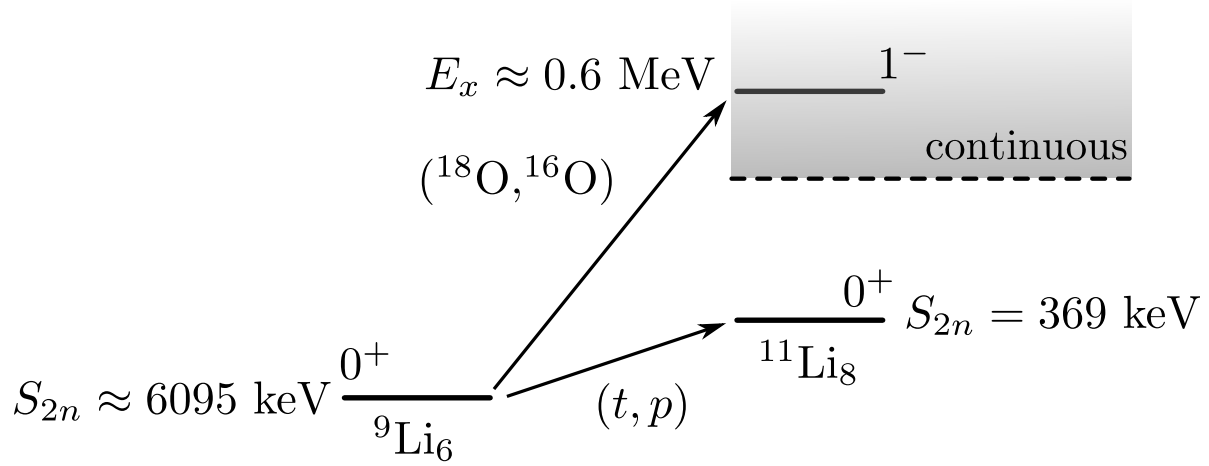


Figure A3: Schematic representation of levels of ^{11}Li populated in two-nucleon transfer reactions. Indicated in keV are the two-neutron separation energies S_{2n} . In labelling the different states, one has not considered the quantum numbers of the $p_{3/2}$ odd proton.

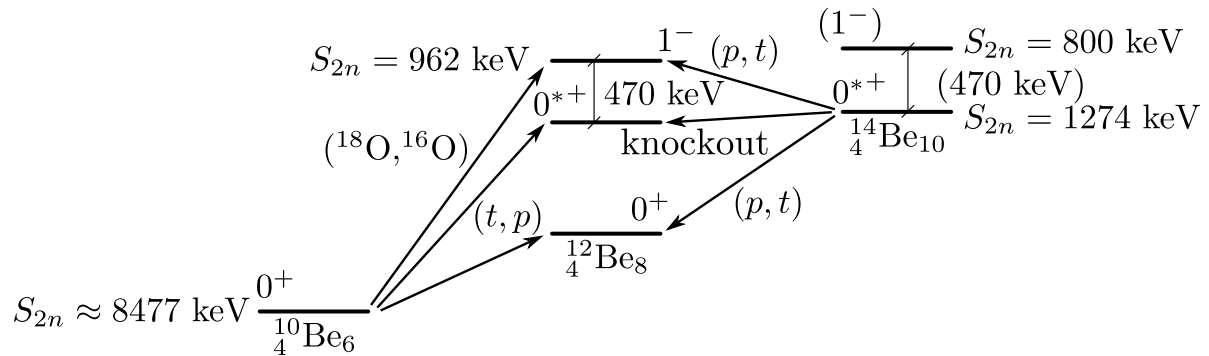


Figure A4: Levels of ^{12}Be expected to be populated in two-nucleon transfer and knockout processes. S_{2n} are the two-neutron separation energies.

B. The pairing vibrational spectrum of ^{10}Be

Calculations similar to the ones discussed in previous sections have been carried out in connection with the expected $N = 6$ shell closure in ^{10}Be (cf. e.g. [159]). In Fig. B1 we display the associated pairing vibrational spectrum in the harmonic approximation. Also given are the absolute two-nucleon transfer differential cross sections associated with the excitation of the one-phonon pair addition and pair subtraction modes excited in the reactions $^{12}\text{Be}(p,t)^{10}\text{Be}(\text{gs})$ and $^{10}\text{Be}(p,t)^8\text{Be}(\text{gs})$ respectively, calculated for a bombarding energy appropriate for planned studies making use of inverse kinematic techniques [162].

The ((2p-2h)-like) two-phonon pairing vibration state of ^{10}Be is expected, in this approximation, to lie at 4.8 MeV, equal to the sum of the energies of the pair removal $W_1(\beta = -2) = 0.5$ MeV and of the pair addition $W_1(\beta = 2) = 4.3$ MeV modes. In keeping with the fact that the lowest known 0^+ excited state of ^{10}Be appears at about 6 MeV [163], we have used this excitation energy in the calculation of the Q -value associated with the $^{12}\text{Be}(p,t)^{10}\text{Be}(\text{pv})$ cross section. The associated shift in energy from the harmonic value of 4.8 MeV can, arguably, be connected with anharmonicities of the ^{10}Be pairing vibrational spectrum, (see Figs. B2 and B3) [43]. Medium polarization effects (see e.g. Fig. B2) may also lead to conspicuous anharmonicities in the pairing vibrational spectrum.

The two-nucleon spectroscopic amplitudes corresponding to the reaction $^{10}\text{Be}(p,t)^8\text{Be}(\text{gs})$ and displayed in Table B1, were obtained solving the RPA coupled equations (determinant) associated with the $^{10}\text{Be}(\text{gs})$ pair-removal mode, making use of two pairing coupling constants, to properly deal with the difference in matrix elements (overlaps) between core-core, core-halo and halo-halo two-particle configurations (for details see [164]). In other words with a "selfconsistent" treatment of the halo particle states ($\varepsilon_k > \varepsilon_F$), in particular of the $d_{5/2}^2(0)$ halo state. The absolute differential cross sections displayed in the figure were calculated making use of the optical parameters of refs. [160, 161] and of COOPER [80].

The two-nucleon spectroscopic amplitudes associated with the reaction $^{12}\text{Be}(p,t)^{10}\text{Be}(\text{gs})$ correspond to the numerical coefficients appearing in Eq. (B3) below, and associated with the wavefunction describing the neutron component of the ^{12}Be ground state (see ref. [159]),

$$\begin{aligned} |\tilde{0}\rangle = & |0\rangle + \alpha|(p_{1/2}, s_{1/2})_{1-} \otimes 1^-; 0\rangle + \beta|(s_{1/2}, d_{5/2})_{2+} \otimes 2^+; 0\rangle \\ & + \gamma|(p_{1/2}, d_{5/2})_{3-} \otimes 3^-; 0\rangle, \end{aligned} \quad (\text{B1})$$

with

$$\alpha = 0.10, \quad \beta = 0.35, \quad \text{and} \quad \gamma = 0.33, \quad (\text{B2})$$

and

$$|0\rangle = 0.37|s_{1/2}^2(0)\rangle + 0.50|p_{1/2}^2(0)\rangle + 0.60|d_{5/2}^2(0)\rangle. \quad (\text{B3})$$

The states $|1^- \rangle$, $|2^+ \rangle$, $|3^- \rangle$ are the lowest states of ^{10}Be , calculated with the help of a multipole separable interaction in RPA (see e.g. Table B2). It is of notice that a rather similar absolute differential cross section to the one displayed in Fig. B1 for the $^{12}\text{Be}(p, t)^{10}\text{Be}(\text{gs})$ reaction is obtained making use of the spectroscopic amplitudes provided by the RPA wavefunction describing the ^{10}Be pair addition mode (see Table B1), provided use of two pairing coupling constants is made. This can be seen from the results displayed in Fig. B4

To assess the correctness of the structure description of $|^{12}\text{Be}(\text{gs})\rangle$ provided by the wavefunction (B1-B3) and of second order DWBA-reaction mechanism (successive, simultaneous plus non-orthogonality) employed to calculate the absolute value of the $^{12}\text{Be}(p, t)^{10}\text{Be}(\text{gs})$ differential cross section [80], we compare in Fig. B5 the predictions of the model for the reaction $^{10}\text{Be}(p, t)^{12}\text{Be}(\text{gs})$ at 17 MeV triton bombarding energy with the experimental data. Theory provides an overall account of observation within experimental errors.

It is of notice that the components proportional to α, β and γ of the state (B1) can lead, in a $^{12}\text{Be}(p, t)$ reaction, to the direct excitation of the $1^-, 2^+$ and 3^- states of ^{10}Be . Such results will add to the evidence obtained in the reaction $^1\text{H} (^{11}\text{Li}(\text{gs}), ^9\text{Li}(1/2^-; 2.69 \text{ MeV}))^3\text{H}$ [78] of phonon mediated pairing [81]. The role of these components is assessed by the fact that (wrongly) normalizing the state (B3) to 1, one obtains a value of $\sigma = 4.5 \text{ mb}$ ($4.4^\circ \leq \theta_{CM} \leq 57.4^\circ$), a factor 2 larger than the experimental value [161] (see Fig. B5).

Let us now return to Fig. B1 * The ratio of the integrated absolute cross section at $E_{CM} = 7 \text{ MeV}$ in the range $10^\circ \leq \theta_{CM} \leq 50^\circ$ appropriate for planned experimental studies making use of inverse kinematic techniques [162] is,

$$R = \frac{\sigma(^{12}\text{Be}(p, t)^{10}\text{Be}(pv; 6\text{MeV}))}{\sigma(^{12}\text{Be}(p, t)^{10}\text{Be}(gs))} = \frac{16.0\text{mb}}{6.9\text{mb}} \approx 2.3, \quad (\text{B4})$$

a result which testifies to the clear distinction between occupied and empty states taking place at $N = 6$, and thus of the *bona fide* nature of this magic number for halo, drip line nuclei. The ratio (B4) reflects the fact that the pairing Zero Point Fluctuations (ZPF in gauge space) displayed by the $|^{10}\text{Be}(gs)\rangle$ as embodied in the pair addition and pair removal modes, and quantified by the absolute values of the associated two-nucleon transfer cross sections, are of the same order of magnitude. This is an intrinsic property of the vibrational modes, in the same way in which e.g. the width (lifetime) of a nuclear state is an intrinsic (nuclear structure) property of such a state. An experiment displaying an energy resolution better than the intrinsic width of the states under study

*In the harmonic approximation, and assuming simultaneous transfer, the cross section $\sigma(r)$ associated with the pair removal mode of a closed shell system ($A_0(p, t)(A_0 - 2)(gs)$) coincides by definition with that of the reaction $(A_0 + 2)(p, t)A_0(pv)$ ($\sigma(pv)$) exciting the two-phonon pairing vibrational mode starting from the ground state of the $(A_0 + 2)$ system, this pair addition mode acting as spectator. However, taking properly into account the contribution of successive transfer, $\sigma(r)$ and $\sigma(pv)$ are expected to differ because of the difference in Q-values associated with the corresponding intermediate, virtual, one-particle transfer states.

will provide structure information. Otherwise, eventually an upper limit. Within this scenario and in keeping with the fact that the successive transfer induced by the single-particle potential is the intrinsically (structure) dominant contribution to the absolute two-particle transfer cross section, Q-value (kinematic) effects can strongly distort the picture. In particular in the case in which single-particle transfer channels are closed at the studied bombarding energies.

ϵ_k [MeV]	$1s_{1/2}$	$1p_{3/2}$	ϵ_i [MeV]	$2s_{1/2}$	$1p_{1/2}$	$1d_{5/2}$
X^r	0.128	1.076	Y^r	0.232	0.214	0.272
Y^a	0.080	0.402	X^a	0.727	0.588	0.543

Table B1: RPA wavefunctions of pair removal and addition 0^+ modes of ^{10}Be , that is, of the ground state of ^8Be and ^{12}Be . The single-particle energies were deduced from experimental binding and excitation energies, and making use of the coupling constants $G_{cc} = 2$ MeV and $G_{hc} = G_{hh} = 0.68$ MeV.

	ϵ_i [MeV]	ϵ_k [MeV]	E [MeV]	X	Y
n	$p_{3/2}$ -8.6	$p_{1/2}$ -3.6	5.0	0.90	0.31
p	$p_{3/2}$ -14.9	$p_{3/2}$ -14.9	7.6	-0.56	-0.29
p	$p_{3/2}$ -14.9	$p_{1/2}$ -7.8	12.2	0.24	0.16
n	$p_{3/2}$ -8.6	$f_{7/2}$ 16.5	25.1	-0.12	-0.10
p	$s_{1/2}$ -29.0	$d_{5/2}$ -1.6	28.4	-0.10	-0.08
n	$p_{3/2}$ -8.6	$f_{7/2}$ 8.8	17.5	-0.10	-0.07
n	$s_{1/2}$ -21.1	$d_{5/2}$ 2.2	28.4	-0.09	-0.07

Table B2: Wavefunction of the lowest 2^+ vibrational state (phonon) of ^{10}Be (obtained from a QRPA calculation, making use of a quadrupole separable interaction and a value of the proton pairing gap of $\Delta_p = 3.8$ MeV while setting $\Delta_n = 0$). The calculated energy and the $B(E2)$ transition strength of the low lying 2^+ are 2.5 MeV and $49.6 e^2\text{fm}^4$ respectively. These results are to be compared with the experimental values of 3.3 MeV and $52 e^2\text{fm}^4$. The quantities ϵ_i and ϵ_k indicate the energy of the hole and of the particle states respectively for either protons (p) or neutrons (n). E denotes the associated two-quasiparticle energies, while X and Y are the QRPA amplitudes of the mode.

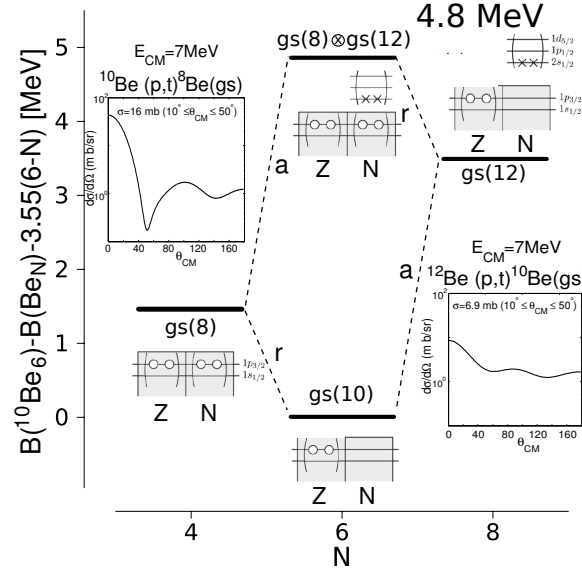


Figure B1: Pairing vibrational spectrum around ^{10}Be and associated absolute two-nucleon transfer differential cross section calculated as explained in the text.

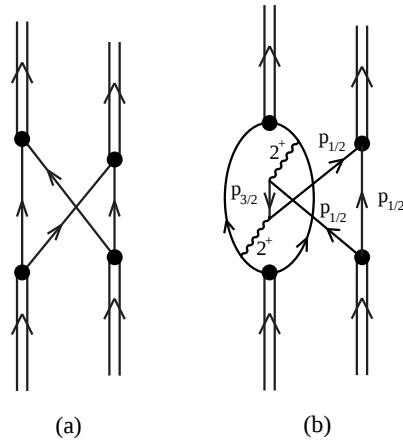


Figure B2: Pairing modes phonon-phonon interaction arising from: (a) Pauli principle processes between pairing modes, and (b) between single-particle and phonon-mediated induced pairing interaction (so called CO diagrams, see e.g. [106]).

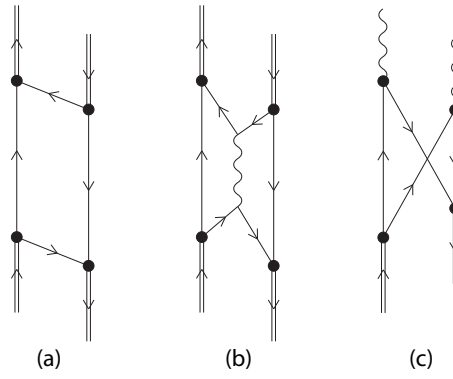


Figure B3: (a),(b) Examples of pair addition and pair removal modes interactions. (c) Interaction between the two-phonon pairing vibration state and the two-phonon particle-hole state.

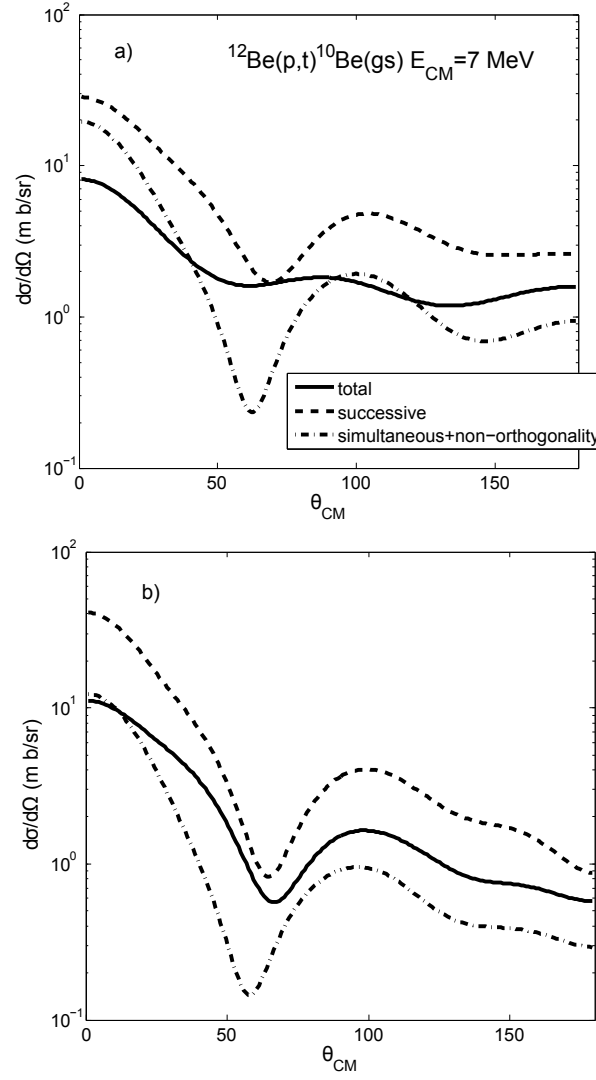


Figure B4: Absolute differential cross section associated with the reaction $^{12}\text{Be}(p,t)^{10}\text{Be}(gs)$ at $E_{CM} = 7$ MeV, calculated making use of : (a) the wavefunction (B1) and (b) the RPA wavefunction describing the ^{10}Be pair addition mode (see Table B1).

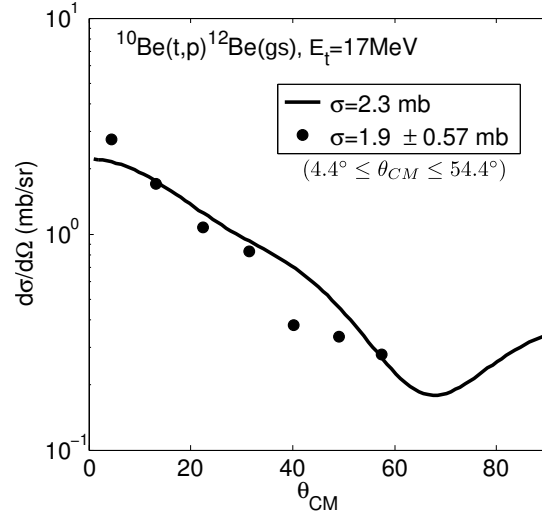


Figure B5: Absolute differential cross section measured [161] in the reaction $^{10}\text{Be}(t,p)^{12}\text{Be}(gs)$ at 17 MeV triton bombarding energy (solid dots). The theoretical calculations (continuous solid curve) were obtained making use of the spectroscopic amplitudes associated with the wavefunction in Eqs. (B1)-(B3), and the optical parameters of refs. [160] and [161] taking into account successive, simultaneous and non-orthogonality processes [18, 80]

Appendix C. Renormalization and pairing vibrations

Renormalization processes associated with the clothing of nucleons moving in valence orbitals around closed shell nuclei through the coupling to surface (particle-hole like) vibrational modes has become fairly customary (see e.g. [151, 120] for two recent examples). The same cannot be said, with rare exceptions (e.g. [140, 165]) regarding clothing through the coupling to pairing vibrations. As mentioned in the text, this state of affairs can hardly be justified in terms of their numerical importance ($\alpha_0/\alpha_{dyn} \approx 0.7$ while $(\beta_2)_0/(\beta_2)_{dyn} \approx 3 - 6$), let alone the lack of experimental information (see e.g. [18, 166, 167] and refs. therein). Nor because pairing vibrations do not smoothly join the particle-hole like vibrations and the single-particle motion, to generate a unified description of the nuclear structure (and reaction) based on the $\alpha = 0, \pm 1, \pm 2$ elementary modes of excitation (α , transfer quantum number) and their interweaving, as emerges from Figs. C1, C2 and C3.

The processes summarised in graph (e) of Fig. C1 lead to the real part of the mean field (both direct and exchange, i.e. Saxon-Woods potential strength $V_0 = U_0 + 0.4E$, and thus $m_k \approx 0.7m$). Processes displayed in Fig. C2(a),(b) give rise to the real and imaginary state-dependent contributions to the particle self-energy. That is, to the polarisation part of the optical potential in the case in which the motion of the nucleon takes place in the continuum (e.g. projectile). In connection with transfer reactions that populate weakly bound or unbound (resonant/virtual state) the information carried out by the above mentioned polarization potential is particularly important. Similar considerations can be made regarding the self-energy processes implying pairing vibrations (pairing resonances in the case of the continuum). Detailed nuclear structure as probed by transfer to the continuum is finally becoming integrated with more standard nuclear structure as a consequence, among other things, of the studies of halo exotic nuclei, and of the associated physics of low-density, highly extended nuclear systems.

Within this context, it is of notice the detailed treatment of a number of the points mentioned above carried out in [165] in connection with a paradigmatic nuclear structure study of transfer to continuum states provided by the reaction ${}^9\text{Li}(d,p){}^{10}\text{Li}$. In particular, the treatment of pairing correlations in the continuum with the help of the Nambu-Gor'kov equation, calculating the radial dependence of the occupation factors and the associated pairing gap (in this connection see [168]). Aside from the simple question of whether a treatment in terms of pair addition and removal modes (cf. Fig. C3, graphs (e) and (f)) was already adequate in the present case considering that ${}^9\text{Li}$ is a closed shell system, in [165] only the monopole component of the pairing interaction was taken into account.

As seen from Fig. C4, multipole pairing modes can renormalise in an important way also the continuum states, let alone the fact that parity inversion is hardly related to particular properties of the spin-orbit term in exotic nuclei, but a standard Pauli principle (Lamb shift-like) process.

Summing up, not considering single-particle renormalization processes is like ignoring the dielectric constant (function) in trying to describe the motion of electrons and photons in vacuum or in water *. Similarly, considering only the effect associated with the coupling to particle-hole modes and neglecting those arising from the coupling to pairing vibrations, is like ignoring protonation of water due to acidic conditions (pH), and its overall consequences for the phenomena under study.

*Or to be more mundane, to ignore the role of the solvent in trying to describe the folding of a protein

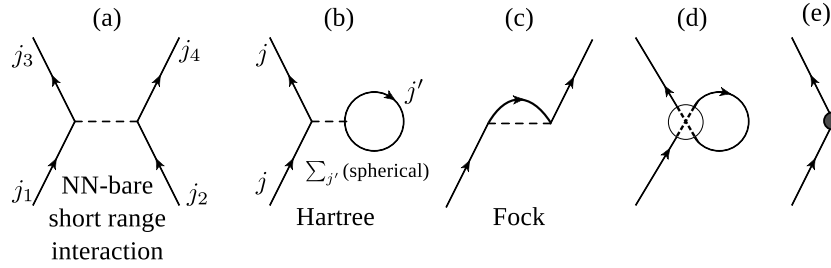


Figure C1: (a) Schematic representation of free NN-scattering. (b) Hartree mean field. (c) Fock potential. (d) Schematic representation of the scattering of one nucleon from all others. (e) Compact notation of above.

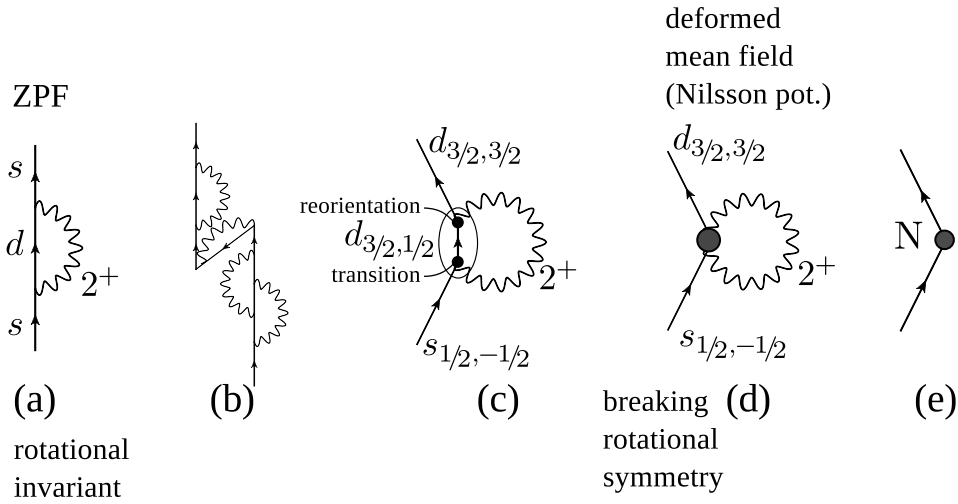


Figure C2: (a) Self-energy (effective mass-like) and (b) vertex corrections processes, renormalizing the properties of single-particle states. A nucleon bouncing inelastically off the nuclear surface sets it into e.g. a quadrupole vibration (phonon), which reabsorbs at a later time. (c) As the collectivity of the 2^+ increases, eventually the system deforms acquiring a static quadrupole moment, which can lead to reorientation effects. (d,e) Compact representation of the above processes. The dot represents the deformed mean field Nilsson potential.

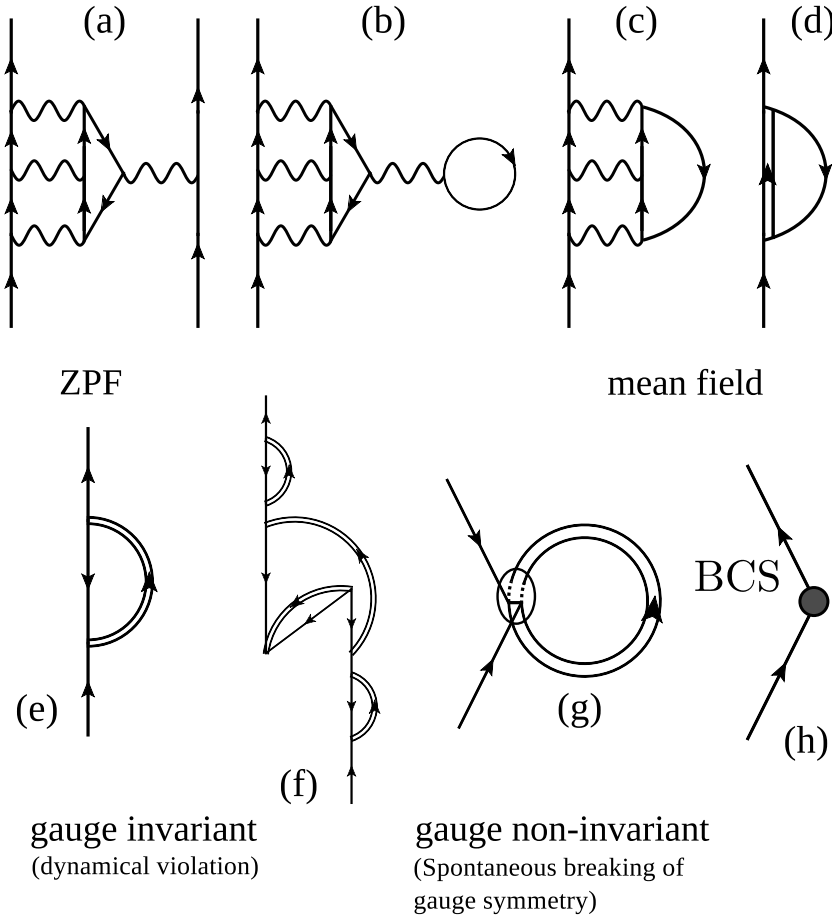


Figure C3: (a) At the basis of superconductivity one finds a class of ladder graphs which contribute to the electron-phonon vertex function Γ and leads to a generalised Cooper pair instability (see [97], p. 166). (b,c). To understand how the above graph enters single-particle self-energy, one needs to close one of the electron lines. (d) We redraw (c) to make connection with the nuclear case. In (e) and (f) the dynamical violation of gauge invariance (mixing of particles and holes) is explicitly expressed in terms of self-energy and of vertex correction diagrams. (g,h) As the collectivity of the pairing mode increases, and eventually the frequencies W_a and W_r of the pair addition and pair removal modes coincide and become equal to zero ($W_a = W_r = 0$, situation encountered for the value of $1/G$ where the corresponding horizontal line encounters the RPA dispersion relation parabola at the minimum), the system undergoes a transition to the superfluid phase (critical value of G).

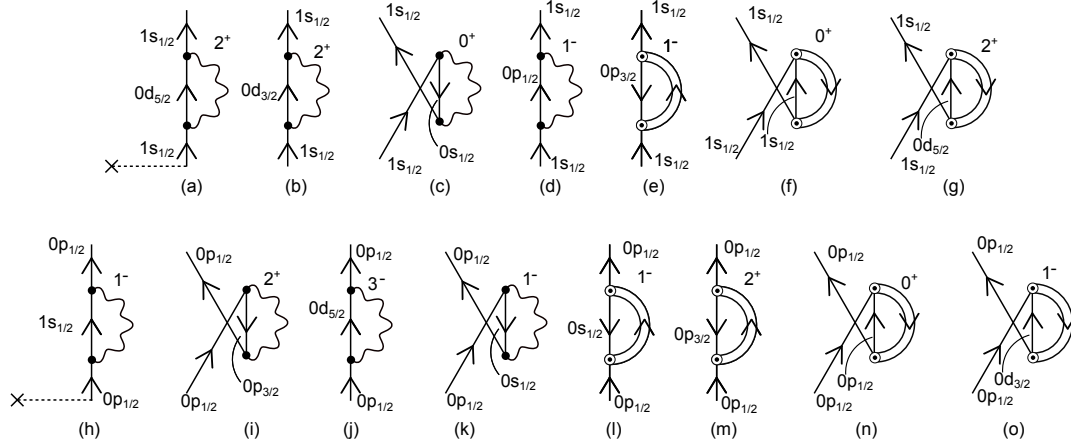


Figure C4: Single-particle self-energy diagrams clothing the $1/2^+$ (a-g), $1/2^-$ (h-o) levels at threshold of ^{10}Li . Wavy lines are associated with particle-hole vibrations of the core ^9Li . Double arrowed lines describe pair addition modes (pointing upwards) i.e. states of ^{11}Li , and pair removal modes (pointing downwards) i.e. states of ^7Li . An arrowed line describes the motion of particle state (pointing upwards) or of a hole state (pointing downwards). A solid dot refers to the particle-vibration (particle-hole-like) coupling. A dotted open circle the vertex representing the coupling of particle (holes) and the pairing modes.

Appendix D. Elementary modes of nuclear excitation

In what follows we comment on specific aspects associated with the "parallels" one can make between collective modes in 3D-space (essentially surface vibrations and quadrupole rotations) and in gauge space (pairing vibrations and pairing rotations).

D.1 Conserving and non-conserving approximation

Let us consider for concreteness a closed shell system and only surface and pairing vibrational modes. To become even more concrete, let us choose ^{208}Pb as the closed shell system, and the low-lying octupole vibration ($\alpha = 0, J^\pi = 3^-, E_x = 2.62 \text{ MeV}$), and monopole and quadrupole pair addition ($\alpha = +2, J^\pi = 0^+, |gs(^{210}\text{Pb}) >, S_{2n} = 9.122,5 \text{ keV}; J^\pi = 2^+, |2_1^+(^{210}\text{Pb}) >, E_x = 795 \text{ keV}$) and pair removal ($\alpha = -2, J^\pi = 0^+, |gs(^{206}\text{Pb}) >, S_{2n} = 14.813,3 \text{ keV}; J^\pi = 2^+, |2_1^+(^{206}\text{Pb}) >, E_x = 803 \text{ keV}$) modes. In the above α, J and π are the transfer (baryon [14]), angular momentum and parity quantum numbers. To lowest order of perturbation NFT of structure (4th order in the particle-pairing vibrational coupling vertex, see [31]) and reactions (embodied in 2nd order in v_{np} DWBA taking into account non-orthogonality corrections, [18]) provides a quantitative account of the experimental findings (see also [166]). One can choose to neglect α and J^π as labels of the variety of states and concentrate on $\alpha = 2 - 2 = 0$ modes and $J^\pi \otimes J^\pi = 0^+$, 2p-2h excitations of the closed shell system [169].

We prefer to base our discussion in terms of elementary modes of excitation (structure), which connect us directly through specific probes (reactions) with experiment. Taking care of the couplings of these modes in terms of NFT rules leads to the clothing of both fermionic and bosonic degrees of freedom. The results are the physical elementary modes of excitation. Their properties provide the spectroscopic input to reaction theories, which properly corrected for non-orthogonality effects, provide the *absolute* differential cross sections (Coulomb excitation, inelastic scattering, γ -decay, one-, two- etc, transfer reactions), to be directly compared with the experimental findings. To close the circle and emphasising the property of *absolute cross section values*, one should be able to work out these quantities with the help of microscopically determined optical potentials calculated making use of the same elements, employed in working out the spectroscopic input the absolute cross sections.

Summing up, the protocol reads: use a basis of elementary modes of excitation and associated specific probes (reaction channels). Treat their interweaving in terms of a unified implementation of NFT of structure and reactions. The resulting *physical* modes and channels together with the microscopically determined optical potential provide a physically consistent theoretical description of nuclear measurements. It connects with experiment through absolute values of the variety of differential cross sections *.

Let us now return to the main subject, namely that of the $\alpha = +2$ and $\alpha = -2$ modes in general and of those of $|gs(^{208}\text{Pb}) >$ in particular. Simplifying, one can say

*Physics is experimental science; it is concerned only with those statements which in some sense can be verified by an experiment... Therefore, what is fundamental to any theory of a specific department of nature is the theory of measurement within that domain [83].

that pairing in nuclei was introduced two times. At first, in terms of the odd-even mass difference in the first (see [170] and refs. therein). Then in terms of the excitation spectrum in the second [13], closely following the BCS theory of superconductivity [3, 4]. The fact that all these works had introduced pairing because of important physical reasons, but not the specific ones, came clearly forward with the work of Josephson [5] and the ensuing arguments with Bardeen [171, 172], resolved in favour of the first one [7, 173, 174]; see also [175]), underscoring the difficulty of the task people were confronted with. It is thus not surprising that similar problems were encountered in nuclear physics regarding the description of Cooper pair transfer, and the question of whether successive transfer breaks pairing or not. That of specifically probing the structure of superconductors, that is, systems whose internal long-range order parameter was assumed to be a phase, the gauge phase ϕ . In such a case quantal fluctuations of the order parameter lead, in the absence of unsymmetrical external forces, to rotations in gauge space ($\omega = \dot{\phi} = \lambda/\hbar$) and thus to a restoration of the original symmetry. *

The external fields (experiment) necessary to "pin down" these quantal fluctuations can only come from systems which themselves violate gauge symmetry. The importance of the Josephson effect, the superconducting tunnelling of electron Cooper pairs across a thin barrier (oxide layer) separating two superconductors, and leading to a DC current $J = J_1 \sin(\phi_1 - \phi_2)$ (AC current $J \sim \sin(\frac{2e}{\hbar}(\Delta V t + 2\delta))$) if biased) is that it provided for the first time an instrument, a clamp, which can pin down the (difference in) gauge phase existing between two superconducting systems [7, 180]. In fact, a metallic superconductor has a rather perfect internal gauge phase order, but the zero point motion of the order parameter is large and rapid ($\dot{\phi} = \lambda/\hbar$). Placing two such deformed systems (rotors) in weak coupling with each other, through Cooper pair transfer acting as tweezers, allows to pin down the (relative) gauge phase, as testified by the oscillations of the $2e$ current reflecting that of the two coupled rotors. From the above narrative, it clearly emerges that two-particle single Cooper pair transfer processes is the specific probe of pairing correlations in atomic nuclei [14], This is true not only to measure the gauge phase coherence of superfluid nuclei (emergent generalised rigidity † and associated pairing rotational bands [15, 181, 182]), but also the dynamic one, in connection with the excitation of pairing vibration bands ‡. It is to be noted that all what has been said for deformation in gauge space can be repeated verbatim

*It is true that other practitioners, among them Tony Leggett [176], prefer to use conserving approximations to discuss about superconductivity and superfluidity. This reminds of Phil Elliott's [177] rejection to discuss about a 3D-deformed -body defining a privileged direction in space (phase coherence, Euler angles), obtaining rotational bands through SU(3) basis diagonalization (see e.g. [178, 179] and refs. therein). In this way one renounces to a powerful tool for individuating collective coordinates, those associated with the quantal fluctuations associated with the restoration of spontaneously broken symmetries .

†That is pushing one pole of the deformed body in gauge space with an external field like (p,t), the whole body reacts at once (no finite velocity propagation of information).

‡Quoting Bohr: "The gauge space is often felt as a rather abstract construction but, in the (two) particle-transfer process, it is experienced in a very real manner "[183].

for deformation in 3D-space both static (quadrupole rotational bands) or dynamic (like e.g. the 2.61 MeV state of ^{208}Pb . This state does not 0^+ labels but 3^- ones, getting them out of the $|gs(^{208}\text{Pb})\rangle$, $J^\pi = 0^+$ group of states. But this does not bother anybody. This is because while one is accustomed to work with measuring instruments which themselves are not rotational invariant * like, e.g., a proton beam which in the laboratory defines a privileged orientation and can thus set a 3D-deformed nuclei into rotation, one does not usually have around devices displaying gauge space coherence. In other words, objects which are wave packets of states with different number of particles, with which one can set a superfluid nucleus (or a nucleus displaying pair addition and subtraction modes) into rotation (vibration) in gauge space. It is of notice that the fingerprint of deformation of finite many body systems (FMBS) are rotation bands (in 3D- gauge- etc. space).

D.2 A-dependence of the pairing contribution to the mass formula and of the pairing gap

Let us now shortly discuss the self consistent value of the nuclear pairing interaction as well as the A -dependence of the pairing contribution to the mass formula, as well as to the pairing gap ([1, 22], and refs. therein). We assume, for the sake of simplicity,

$$V(r_{12}) = -4\pi V_0 \delta(\vec{r}_1 - \vec{r}_2) \quad (\text{D1})$$

to be a single representation of the nuclear pairing interaction. The relation between V_0 and G (constant matrix element pairing force) can be written as

$$G \approx V_0 I(j) \approx 1.2 \text{ fm}^{-3} V_0 / A \quad (\text{D2})$$

where $I(j)$ is the delta-force radial matrix element corrected for nucleon spillout. From the self consistent relation

$$U(r) = 4\pi V_0 \int d^3 r' \delta(\vec{r} - \vec{r}') = -4\pi V_0 \rho(r) \quad (\text{D3})$$

between single-particle potential and density one obtains

$$V_0 = -\frac{U_0}{4\pi\rho_0} \approx \frac{294}{4\pi} \text{ MeV fm}^3 \quad (\text{D4})$$

and thus

$$G \approx \frac{27}{A} \text{ MeV} \quad (\text{D5})$$

With the help of the single j -shell model, in which case the BCS occupation amplitudes are

$$V = \sqrt{\frac{N}{2\Omega}} \text{ and } U = \sqrt{1 - \frac{N}{2\Omega}}, \quad (\text{D6})$$

*This (...angular momentum L is also a conserved quantity, reflecting the isotropy of space ... But states of different L interfere. Otherwise, we would have no sense of orientations. Anything we observe that is not invariant under rotations... represents a wave packet of components with different L [20, 183].

one obtains

$$\Delta = G \sum_{\nu>0} U_\nu V_\nu = G\Omega \sqrt{\frac{N}{2\Omega}(1 - \frac{N}{2\Omega})} = \frac{18}{A^{1/3}} \sqrt{\frac{N}{2\Omega}(1 - \frac{N}{2\Omega})} \text{ MeV}, \quad (\text{D7})$$

where use was made of $\Omega = 2/3 A^{2/3}$. In the case of ^{126}Sn one obtains

$$\Delta \approx \frac{7}{A^{1/3}} \text{ MeV} \approx \frac{7}{5} \text{ MeV} \approx 1.4 \text{ MeV}, \quad (\text{D8})$$

in overall agreement with the experimental findings.

Now, it is well established that in medium heavy nuclei half of the pairing gap arises from the bare pairing interaction and half from the induced one, resulting from the exchange of low-lying collective modes between Cooper pair partners. Within the framework of the slab model [184]-[187], see also [1]

$$\Delta_{slab} = \frac{9.5}{A^{0.62}} \text{ MeV}, \quad (\text{D9})$$

close to a $2/3$ A -dependence in keeping with the surface character of the modes.

Thus

$$\Delta = \frac{1}{2}(\Delta_{bare} + \Delta_{slab}) \approx \frac{1}{2} \left(\frac{7}{A^{1/3}} + \frac{20}{A^{0.62}} \right) \text{ MeV}. \quad (\text{D10})$$

For $A = 126$ one obtains

$$\Delta \approx \frac{1}{2}(1.4 + 1.0) \text{ MeV} \approx 1.2 \text{ MeV}, \quad (\text{D11})$$

again in overall agreement with the experimental findings.

The situation is of course more involved, in keeping with the fact that the coupling to the variety of low-lying collective modes of the Cooper pair partners is a retarded (ω -dependent) process leading to a state dependent pairing gap which can be hardly accurately parameterised in terms of the slab model. Within this context a similar effect is expected concerning the contribution of the zero-point fluctuations (ZPF) to the nuclear mass (binding energy) associated with the different collective modes in general and the multiple pair addition and pair subtraction modes (see Fig. D1 [135]; see also [1], Sect. 8.4).

D.3 The two-nucleon transfer formfactor

Returning briefly to the fact that two-nucleon transfer is the specific tool to probe pairing and thus, the absolute two-nucleon transfer cross sections the quantities to relate theory with experiment one notes that such quantities do not depend on G , as

$$\frac{d\sigma}{d\Omega} \sim |\alpha_0^2| = \left| \sum_{\nu>0} U_\nu V_\nu \right|^2. \quad (\text{D12})$$

In fact, the order parameter is different from zero also in regions in which $G = 0$, e.g in the barrier of a Josephson junction, a fact that does not prevent pair tunnelling. The same of course applies to the case of pairing vibrational nuclei, where α_0 is replaced by α_{dyn} .

The field that causes a pair transfer in actual nuclei has a rather involved and subtle structure. This is due to the fact that the pair transfer process is mainly induced by the

mean single-particle fields in a second order process. One may, however, introduce an effective pair field which in first order perturbation theory, causes the successive transfer of a nucleon pair.

This can be obtained from the expression of the successive transfer amplitude (see [60], Eq. (V.II.44), p. 423), for the reaction $\alpha = a = (b + 2) + A \rightarrow \gamma = F(b + 1) + F(= A + 1) \rightarrow \beta = b + B(= A + 2)$:

$$\begin{aligned}
(a)_{succ} = & - \sum_{aa'} B^{(A)}(a_1 a_1; 0) B^{(b)}(a'_1 a'_1; 0) \left(\frac{2j'_1 + 1}{2j_1 + 1} \right)^{1/2} \\
& \times 2 \sum_{\gamma\mu\mu'\mu''} \frac{(-1)^{\lambda+\mu}}{2\lambda + 1} D_{-\mu\mu''}^\lambda(0, \pi/2, \pi) D_{\mu\mu'}^\lambda(0, \pi/2, \pi) \\
& \times |C^{(A)}(0a_1; I_f)|^2 |C^{(b)}(0a'_1; I_f)|^2 \int_{-\infty}^{\infty} \frac{dt}{\hbar} \tilde{f}_{\lambda\mu'}^{a_1 a'_1}(r) e^{i((E_\beta - E_\gamma)t + \gamma_\beta \gamma(t))/\hbar + i\mu\phi(t)} \\
& \times \int_{-\infty}^{\infty} \frac{dt'}{\hbar} \tilde{f}_{\lambda\mu''}^{a_1 a'_1}(r) e^{i((E_\beta - E_\alpha)t' + \gamma_\gamma \alpha(t'))/\hbar + i\mu\phi(t')}, \tag{D13}
\end{aligned}$$

making use of a number of approximations (parabolic as well as slow phase changes) to perform summations over the single-particle distribution $|C^{(A)}|^2$ and $|C^{(b)}|^2$, i.e. over $\gamma = f + F$, and (see [60], p.444)

$$\sum_{a_1} B^{(A)}(a_1 a_1; 0) (-1)^{l_j} (j_1 + 1/2)^{1/2} N_{a_1}^2 = 4\pi < B | \rho_{+2}^{(A)}(R_A) | A >. \tag{D14}$$

The above expression provides the matrix element of the pair density in the target. The final result is (see [60], Eq. (V.13.8) p. 444) being,

$$(a)_{succ} = \frac{1}{i\hbar} \sqrt{\frac{\pi}{k\ddot{r}_0}} F(r_0) e^{-q^2}, \tag{D15}$$

where the collision time is $\tau = (2k\ddot{r}_0)^{-1/2}$, e^{-q^2} is an adiabatic cutoff factor (cf. [60], Eq. (V.10.3), p.406) and r_0 the distance of closest approach. The function (see [60], Eq. (V.13.8a), p.445),

$$\begin{aligned}
F(r) = & < B | \rho_{+2}^{(A)}(R_A) | A > < b | \rho_{-2}^{(a)}(R_a) | a > \\
& \times \left(\frac{R_A R_a}{R_a + R_A} \right) 2e^{-2k(r - R_a - R_A)} L(\tau), \tag{D16}
\end{aligned}$$

thus acts as an effective form factor for simultaneous pair transfer. One may identify $F(R)$ with the matrix element of the effective pair interaction in the post representation (see [60], Eq. (V.13.3), p.443. see also [168]),

$$F(r) = < \beta | V | \alpha >, \tag{D17}$$

with

$$V(r) = \delta\rho^{(A)}(r - R_a) \left(\frac{R_a R_A}{R_a + R_A} \right)^2 \delta\rho^{(a)}(R_{Aa}) L(\tau). \tag{D18}$$

Comparing Eq. (A.15) with the expression (III.19) of [60] p.108, one finds that $F(r)$ is proportional to the square of the ion-ion potential. Having made use, in writing (A.17), of the exponential function to extrapolate the pair density in the target to the surface

of the projectile, the effective pair field Δ ($V \sim \int d^3r d^3r' \delta\rho \Delta \frac{d\phi}{2\pi}$, see Eq. (V.13.3), p. 443 [60]) is essentially proportional to U_{1a}^2 , where U_{1a} is the mean single-particle field of the projectile *. In connection with App. F it is of notice that in Eq. (D13) one has taken into account full recoil effects through the single-particle form factors $\tilde{f}_{\lambda\mu}^{a_1 a'_1}(r)$, in terms of a recoil phase $\sigma_{\beta\alpha} = \vec{k}_{\beta\alpha}(t) \cdot (\vec{r}_\alpha - \vec{r}_\beta)$.

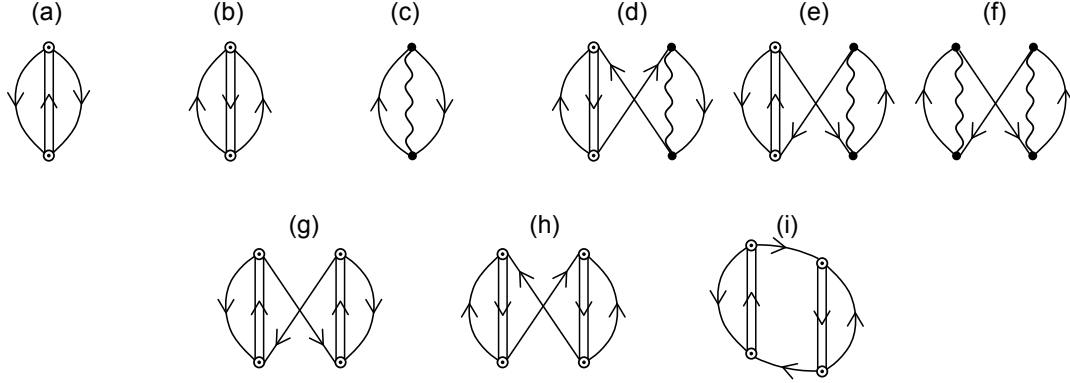


Figure D1: Second order ground state correlations induced by (a) pair addition modes ($\alpha = +2$), (b) pair removal ($\alpha = -2$) and (c) surface ($\alpha = 0$) modes. (d-h) Pauli principle corrections and examples of phonon-phonon interaction, in fourth order perturbation theory [135].

*Within this context, see the difference with the results reported in [188] (see also [139])

Appendix E. The Nambu-Gor'kov equation and particle vibration coupling

The basic vertex associated with the coupling of particles (or holes) to collective surface vibrations reads

$$h(ab\lambda\nu) = -(-1)^{j_a-j_b}\beta_{\lambda\nu} <a|r_1\frac{\partial U}{\partial r_1}|b> <j_b||Y_\lambda||j_a> \left[\frac{1}{(2j_a+1)(2\lambda+1)} \right]^{1/2} \quad (E1)$$

The single-particle states a, b have energy ϵ_a, ϵ_b and occupation amplitudes v_a, v_b ($=1$ for holes and $=0$ for particles). The multipolarity and the energy of the phonon are denoted by λ and $\hbar\omega_{\lambda\nu}$.

This coupling induces the renormalization of the single particle energies and the fragmentation of the associated strength, which can be computed by solving selfconsistently the energy dependent self-energy equations

$$\begin{aligned} \tilde{E}_{a(n)} &= E_a + \Sigma_{a(n)}^{pho} = \\ E_a + \sum_{b,m,\lambda,\nu} \frac{V^2(ab(m)\lambda\nu)}{\tilde{E}_{a(n)} - \tilde{E}_{b(m)} - \hbar\omega_{\lambda\nu}} + \sum_{b,m,\lambda,\nu} \frac{W^2(ab(m)\lambda\nu)}{\tilde{E}_{a(n)} + \tilde{E}_{b(m)} + \hbar\omega_{\lambda\nu}} \end{aligned} \quad (E2)$$

where

$$\begin{aligned} V(ab(m)\lambda\nu) &= h(ab\lambda\nu)(u_a\tilde{u}_{b(m)} - v_a\tilde{v}_{b(m)}) \\ W(ab(m)\lambda\nu) &= h(ab\lambda\nu)(u_a\tilde{v}_{b(m)} + v_a\tilde{u}_{b(m)}). \end{aligned} \quad (E3)$$

The $n - th$ solution (fragment) of the equation is denoted by $a(n)$. Its energy (referred to the Fermi energy ϵ_F) is given by $\tilde{E}_{a(n)} = |\tilde{\epsilon}_{a(n)} - \epsilon_F|$, and the associated occupation amplitude is denoted by $\tilde{v}_{a(n)}$.

In the case of a superfluid system the self-energy equation becomes the 2x2 energy dependent Nambu-Gorkov eigenvalue problem

$$\begin{pmatrix} \tilde{\epsilon}_{a(n)} - \epsilon_F & \tilde{\Delta}_{a(n)} \\ \tilde{\Delta}_{a(n)} & -(\tilde{\epsilon}_{a(n)} - \epsilon_F) \end{pmatrix} \begin{pmatrix} \tilde{u}_{a(n)} \\ \tilde{v}_{a(n)} \end{pmatrix} = \tilde{E}_{a(n)} \begin{pmatrix} \tilde{u}_{a(n)} \\ \tilde{v}_{a(n)} \end{pmatrix} \quad (E4)$$

where the renormalized pairing gap is given by [98]

$$\tilde{\Delta}_{a(n)} = -Z_{a(n)} \sum_{b(m)} \frac{2j_b + 1}{2} V_{eff}(a(n)b(m)) N_{b(m)} \frac{\tilde{\Delta}_{b(m)}}{2\tilde{E}_{b(m)}}. \quad (E5)$$

The matrix elements of the effective pairing interaction $V_{eff}(a(n)b(m)) = V_{bare}(ab) + V_{ind}(a(n)b(m))$ are the sum of the matrix element of the bare interaction $V_{bare}(ab)$ and of the induced interaction:

$$\begin{aligned} V_{ind}(a(n)b(m)) &= \\ \sum_{\lambda,\nu} \frac{2h^2(ab\lambda\nu)}{(2j_b + 1)} \times \left[\frac{1}{\tilde{E}_{a(n)} - \tilde{E}_{b(m)} - \hbar\omega_{\lambda\nu}} - \frac{1}{\tilde{E}_{a(n)} + \tilde{E}_{b(m)} + \hbar\omega_{\lambda\nu}} \right]. \end{aligned} \quad (E6)$$

The eigenvalues of Eq. (E4) are the renormalized quasiparticle energies. They are related to the renormalized pairing gap and to the renormalized single-particle energies $\tilde{\epsilon}_{a(n)}$ by a BCS-like equation:

$$\tilde{E}_{a(n)} = \sqrt{(\tilde{\epsilon}_{a(n)} - e_F)^2 + \tilde{\Delta}_{a(n)}^2}, \quad (\text{E7})$$

where

$$\tilde{\epsilon}_{a(n)} - e_F = Z_{a(n)} \left[(\epsilon_a - e_F) + \tilde{\Sigma}_{a(n)}^{\text{even}} \right]. \quad (\text{E8})$$

In turn, the spectroscopic factor $Z_{a(n)}$ is given by

$$Z_{a(n)} = \left(1 - \frac{\tilde{\Sigma}_{a(n)}^{\text{odd}}}{\tilde{E}_{a(n)}} \right)^{-1}, \quad (\text{E9})$$

where $\tilde{\Sigma}^{\text{even}}$ and $\tilde{\Sigma}^{\text{odd}}$ are the even and odd parts of the self-energy $\tilde{\Sigma}_{a(n)}$.

The eigenstates must satisfy the normalization

$$\begin{aligned} u_{a(n)}^2 + v_{a(n)}^2 - \frac{\partial \Sigma_{a(n)}(E_{a(n)})}{\partial \tilde{E}_{a(n)}} x_{a(n)}^2 \\ + \frac{\partial \Sigma_{a(n)}(-E_{a(n)})}{\partial \tilde{E}_{a(n)}} y_{a(n)}^2 - 2 \frac{\partial (\Delta_{a(n)}/Z_{a(n)})}{\partial \tilde{E}_{a(n)}} u_{a(n)} v_{a(n)} = 1. \end{aligned} \quad (\text{E10})$$

where $x = u(v)$ and $y = v(u)$ for particles (holes).

The single-particle strength

$$N_{a(n)} = u_{a(n)}^2 + v_{a(n)}^2 \quad (\text{E11})$$

is thus smaller than 1 for each fragment, the strongest being the so called quasi particle peak.

Finally the gap may be related to the occupation factors as

$$\tilde{\Delta}_{a(n)} = -Z_{a(n)} \sum_{b(m)} \frac{(2j_b + 1)}{2} V_{eff}(a(n)b(m)) u_{b(m)} v_{b(m)}. \quad (\text{E12})$$

where use has been made of the relation

$$u_{b(m)} v_{b(m)} = N_{b(m)} \frac{\tilde{\Delta}_{b(m)}}{2\tilde{E}_{b(m)}}. \quad (\text{E13})$$

As a simple application of the above formalism we show the consequences that the particle-vibration coupling has on the pairing correlations of particles moving in a single j -shell interacting through a bare nucleon-nucleon pairing potential with constant matrix elements G . For this simple model, the value of the occupation numbers U and V must be the same for all the $2j + 1$ orbitals. In particular, the occupation probability for the case when the system is occupied with N particles,

$$V = \sqrt{N/2\Omega} \quad (\text{E14})$$

$$U = \sqrt{1 - N/2\Omega}, \quad (\text{E15})$$

where $\Omega = (2j + 1)/2$. Consequently, the pairing gap is given by the following relation,

$$\Delta = Z\Omega(G + v_{ind})UV = Z(G + v_{ind})\Omega/2 \quad (\text{E16})$$

The values of G and v_{ind} are about equal and close to $18/A$ MeV and $19/A$ MeV respectively (see [189]).

For the isotopes of Sn ($^{100}_{50}\text{Sn}_{50}$ - $^{132}_{50}\text{Sn}_{82}$) $2\Omega = 32$. Thus, for $^{120}_{50}\text{Sn}_{70}$, $V = \sqrt{20/32} = 0.8$ and $U = \sqrt{1 - 20/32} = 0.61$, leading to $UV \approx 0.5$. Making furthermore use of $Z \approx 0.7$ one obtains $\Delta = 0.9 \times 16 \times (37/120) \times 0.5$ MeV ≈ 1.7 MeV. Taking into account that spin modes, not considered in the estimate of v_{ind} will reduce the above value by $\approx 20\%$, [86], i.e. by ≈ 0.34 MeV, the model prediction becomes $\Delta \approx 1.4$ MeV, which essentially coincides with the experimental value.

Appendix F. NFT and reactions

Nuclear Field Theory was systematically developed to describe nuclear structure processes. This fact did not prevent the translation into this graphical language of expressions which embodied the transition amplitude of a variety of reaction processes, in particular second order (in v_{np}) transition amplitudes associated with two nucleon transfer reactions [190].

The new feature to be considered regarding transfer processes and not encountered neither in structure, nor in inelastic or anelastic processes, is the graphical representation of recoil effects. That is, a physical phenomenon associated with the change in the coordinate of relative motion reflecting the difference in mass partition between entrance, intermediate (if present) and exit channels. In fact, nuclear structure processes, being internal processes, do not affect the center of mass, with a proviso. In fact, the shell model potential violates the translational invariance of the total nuclear Hamiltonian and, thus, single-particle excitations can be produced by a field proportional to the total center-of-mass coordinate. The translational invariance can be restored by including the effects of the collective field generated by a small displacement α of the nucleus. Such a displacement, in the x -direction, gives rise to a coupling (see [19])

$$H_{coupl} = \kappa\alpha F, \quad (\text{F1})$$

where

$$F = -\frac{1}{\kappa} \frac{\partial U}{\partial x}, \quad (\text{F2})$$

and

$$\kappa = \int \frac{\partial U}{\partial x} \frac{\partial \rho_0}{\partial x} d\tau = -A < \frac{\partial^2 U}{\partial x^2} >, \quad (\text{F3})$$

corresponding to a normalization of α such that $< F > = \alpha$.

The spectrum of normal modes generated by the field coupling (F1), namely by a Galilean transformation of amplitude α ($\exp(-i\alpha k_x)$, $\alpha^2 \ll \alpha$), contains an excitation mode with zero energy for which zero point fluctuations diverges in just the right way to restore translational invariance to leading order in α . In fact, while

$$\lim_{\omega_\alpha \rightarrow 0} \frac{\hbar^2}{2D_\alpha \hbar \omega_\alpha}, \quad (\text{F4})$$

diverges, the inertia remains finite and equal to $D_\alpha = AM$, as expected. The additional dipole roots include, in particular, the isoscalar dipole compression modes associated with the operator $\hat{D} = \sum_{i=1}^A r_i^3 Y_{1\mu}(\hat{r}_i)$, which can be viewed as a non-isotropic compression mode (see e.g. [191] and refs. therein)

Naturally, the operators leading to transformations associated with the change in coordinates of relative motion (recoil effects) are Galilean operators ($\sim \exp(-i\vec{k}_{\beta\alpha} \cdot (\vec{r}_\beta - \vec{r}_\alpha))$). Their action (on e.g. the entrance channel), as that of (F1) on the shell model ground state, can be graphically represented in terms of NFT diagrams (or eventual extensions of them). In Figs. 2 and 12 they are drawn in terms of jagged lines. Let us elaborate on this point. When one states that the small displacement α of then nucleus leads to a coupling (F1) one means a coupling between the single-particle and the collective displacement of the system as a whole. When one talks about the spectrum of normal modes associated with such a coupling, one refers to the harmonic approximation (RPA). Thus, to the solutions of the dispersion relation (cf. [19], Eq. (6-244)),

$$-\frac{2\kappa}{\hbar} \sum_i \frac{|F|_i^2 \omega_i}{\omega_i^2 - \omega_a^2} = 1, \quad (\text{F5})$$

where the sum is over single-particle states. This dispersion relation can be represented graphically through the diagrams shown in Fig. F1 (cf. [19], Fig. 6.14). In particular, α acting on the vacuum creates the collective mode. This can also be seen by expressing α in second quantization, namely

$$\alpha = \sqrt{\frac{\hbar\omega_\alpha}{2C_\alpha}} (\Gamma_\alpha^\dagger + \Gamma_\alpha), \quad (\text{F6})$$

where $\sqrt{\hbar\omega_\alpha/2C_\alpha} = \sqrt{\frac{\hbar^2}{2D_\alpha} \frac{1}{\hbar\omega_\alpha}}$ is the zero-point amplitude of the collective (displacement) mode. Now, none of the above arguments loses its meaning in the case in which there is a root with $\omega_\alpha = 0$, in keeping also with the fact the inertia remains finite.

In Figs. 2 and 12 we do something similar to what is done in Fig. F1. The dot, which in this figure represents the particle-vibration coupling, is replaced by a small dashed open square, which we label "particle-recoil coupling vertex". It constitutes a graphical mnemonic to count the degrees of freedom that are at play. In this case the coordinates of relative motion. Also the fact that in connection with the appearance of such vertices one has to calculate matrix elements of precise form factors which involve the recoil phases. However we do not have a simple or, better, universally agreed graphical representation of the particle-rotor coupling * as we have for the particle-vibration coupling (see e.g. graph (c) of Fig. 7). This is also evident from the difficulties in trying to graphically represent such couplings from the vibration ("spherical" or dynamically deformed) to the rotational ("deformed" or statically deformed) schemes

*Something which is certainly not found in [19] (pp. 444-447), neither in connection with the pushing model nor with the rotational model.

(see Figs. C2 and C3). As a result, the representation of these couplings in both 3D- and gauge-space (cf. Fig. C2(e) and C3(h)) are, unimaginatively, equal to the mean field diagram (e) of Fig. C1. The only feature that changes is the label HF,N,BCS. An empirical way out is that of a coarse-grained-like symmetry restoration, in which κ is adjusted in such a way, that the lowest solution of Eq. (F5), although being smaller than the rest of them, remains finite (within this context we refer * to [19], p.446).

Concerning the question of how to measure the recoil phases, one is reminded of the fact that in elastic scattering processes, the phase shifts δ_l , namely the difference in phase between the asymptotic form of the actual radial wavefunction $j_l(kr)$ in the absence of potential, completely determine the absolute differential cross section. This is because the quantities δ_l provide the change in scaling between incoming and outgoing (potential) waves, resulting in the interference between them, so that particle intensity is smaller behind the scattering region ($\theta = 0$), than in front of it. Furthermore, nuclear structure enters only through the reduced mass (aside of course U). Thus, measuring $\sigma(\theta)$ one can determine the values of δ_l and eventually U . In fact, with the exception of the $l = 0$ phase shift (obtained from low energy experiments) the δ_l cannot be measured directly, but can be inferred as empirical quantities from the parameterization of the potential.

In the case of nucleon transfer in general, and of two-nucleon transfer in particular, the situation is similar, albeit more subtle. This is because in this case the nuclear structure input, aside from the potential (v_{np} interaction), encompasses also the pair correlated wavefunctions, aside from Q -value effects. Nonetheless, a detailed measurement of the absolute differential cross sections, arguably allows for a determination of the recoil phases.

Within this context, one can posit that numerical tests of the implementation of NFT of reactions (making use of bona fide NFT structure inputs) have been carried out to the relevant order in v_{np} , namely second order (see end of Sect. 3.1).

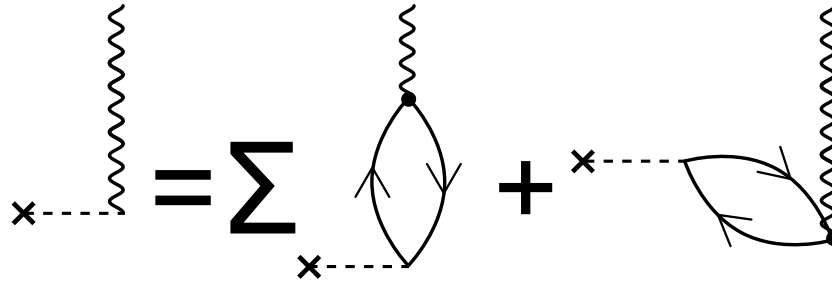


Figure F1: Self-consistent condition for normal modes.

*With no coupling the ZPF $\alpha_0^{(0)}$ of the nuclear CM are small ($\sim A^{-1/3}$). Thus, it is possible to tune κ so as to make the ZPF associated with the lowest root large as compared to $\alpha_0^{(0)}$, but still compatible with the ansatz at the basis of RPA [192].

- [1] D.M. Brink and R.A. Broglia, *Nuclear Superfluidity*, Cambridge University Press (2005)
- [2] L.N. Cooper, *Bound electron pairs in a degenerate Fermi gas*, Phys. Rev. **104**, 1189 (1956)
- [3] J. Bardeen, L. N. Cooper and J.R. Schrieffer, *Microscopic theory of superconductivity*. Phys. Rev. **106** 162 (1957)
- [4] J. Bardeen, L. N. Cooper and J.R. Schrieffer, *Theory of superconductivity*. Phys. Rev. **108** 1175 (1957)
- [5] B.D. Josephson, *Possible new effects in superconductive tunnelling*, Phys. Lett. **1** 251 (1962)
- [6] B.D. Josephson, *The discovery of tunnelling supercurrents*, Rev. Mod. Phys. **46** (1974) 251
- [7] P.W. Anderson, *Special effects in superconductivity*, in The Many-Body Problem, E. R. Caianello ed., vol 2, Academic Press, New York, (1964) p. 113
- [8] I. Giaever, H.R. Hart and K. Megerle, *Tunneling into superconductors at temperatures below 1K*, Phys. Rev. **126** (1962) 941
- [9] I. Giaever, *Electron tunneling and superconductivity*, Rev. Mod. Phys. **46** (1974) 245
- [10] D.J. Scalapino, *The electron-phonon interaction and strong-coupling superconductors*, in Superconductivity, R. Parks ed., Marcel Dekker, New York, (1968) p. 449
- [11] *Superconductivity*, Ed. R. Parks, Marcel Dekker, New York (1986)
- [12] M. Tinkham, *Introduction to superconductivity*, Krieger, Malabar (FL) (1980)
- [13] A. Bohr, B.R. Mottelson and D. Pines, *Possible analogy between the excitation spectra of nuclei and those of the superconducting metallic state*, Phys. Rev. **110** (1958) 936
- [14] A. Bohr, *Elementary modes of nuclear excitation and their coupling*, in Comptes Rendus du Congrès International de Physique Nucléaire, Vol. I, P. Gugenberger ed., Editions du Centre Nationale de la Recherche Scientifique, Paris (1964), p. 487
- [15] D. R. Bes and R.A. Broglia, *Pairing Vibrations*, Nucl. Phys. **80**, 289 (1966)
- [16] J.H. Bjerregaard, O. Hansen, O. Nathan and S. Hinds, *States of ^{208}Pb from double triton stripping*, Nucl. Phys. **89** (1966) 337
- [17] S. Yoshida, *Note on the two-nucleon stripping reaction*, Nucl. Phys. **33** (1962) 685
- [18] G. Potel, A. Idini, F. Barranco, E. Vigezzi and R.A. Broglia, *Cooper pair transfer in nuclei*, Rep. Prog. Phys. **76** (2013) 106301
- [19] A. Bohr and B.R. Mottelson, *Nuclear Structure*, Vol. II, Benjamin, New York (1975)
- [20] A. Bohr, *Rotational motion in nuclei*, Rev. Mod. Phys. **48** (1976) 365
- [21] B.R. Mottelson, *Elementary modes of excitation in nuclei*, Rev. Mod. Phys. **48** (1976) 375
- [22] A. Bohr and B.R. Mottelson, *Nuclear structure*, Vol. I, Benjamin, New York (1969)
- [23] R.P. Feynman, *Quantum electrodynamics*, Benjamin, New York (1962)
- [24] R.P. Feynman, *The theory of fundamental processes*, Benjamin, New York (1962)
- [25] B.R. Mottelson, *Properties of individual levels and nuclear models*, in Proc. Intern. Conf. on nuclear structure, J. Sanada ed., Phys. Soc. Jap. Suppl. **24** (1968) 87
- [26] I. Hamamoto, *Particle-vibration coupling in nuclei ^{209}Bi and ^{209}Pb* , Nucl. Phys. A **126**, 545 (1969)
- [27] I. Hamamoto, *Single-particle components of particle-vibrational states in nuclei ^{209}Pb , ^{209}Bi , ^{207}Pb and ^{207}Tl* , Nucl. Phys. A **141** (1970) 1
- [28] I. Hamamoto, *Nuclear octupole vibrations in isotopes of Pb*, Nucl. Phys. A **155**, 362 (1970)
- [29] D. R. Bès and R.A. Broglia, *Effect of the Multipole Pairing and Particle-Hole Fields in the Particle-Vibration Coupling Problem of ^{209}Pb . (I)*, Phys. Rev. **C3**, 2349 (1971)
- [30] D. R. Bès and R.A. Broglia, *Effective Operators and the Analysis of Single-Nucleon Transfer Reactions on Closed Shell Nuclei*, Phys. Rev. **C3**, 2389 (1971)
- [31] R.A. Broglia, V. Paar and D.R. Bès, *Diagrammatic perturbation treatment of the effective interaction between two-phonon states in closed shell nuclei: the $J^\pi = 0^+$ states in ^{208}Pb* , Phys. Lett. B **37** (1971) 159
- [32] D. R. Bès, G. G. Dussel, R.A. Broglia, R. Liotta and B. R. Mottelson, *Nuclear field theory as a method of treating the problem of overcompleteness in descriptions involving elementary modes of both quasi-particles and collective type*, Phys. Lett. **52B** (1974) 253
- [33] D. R. Bès, R.A. Broglia, G. G. Dussel and R. Liotta, *Simultaneous treatment of surface and pairing*

- nuclear fields*, Phys. Lett. **56B**, 109 (1975)
- [34] D. R. Bès and R.A.Brogia, *Equivalence between Feynman-Goldstone and particle-phonon diagrams for finite many-body systems*, Proc. of the Topical Conference of problems of Vibrational Nuclei, Zagreb, Yugoslavia, Eds. G. Alaga, V. Paar and L. Sips, North-Holland, Amsterdam, p. 1 (1975)
 - [35] D. R. Bès, R.A.Brogia, G. G. Dussel, R. J. Liotta and H. M. Sofia, *The nuclear field treatment of some exactly soluble models*, Nucl. Phys. **A260**, 1 (1976)
 - [36] D. R. Bès, R.A.Brogia, G. G. Dussel, R. J. Liotta and H. M. Sofia, *Application of the nuclear field theory to monopole interactions which includes all the vertices of a general force*, Nucl. Phys. **A260**, 27 (1976)
 - [37] D. R. Bès, R.A.Brogia, G. G. Dussel, R. J. Liotta and R. J. Perazzo, *On the many-body foundation of the nuclear field theory*, Nucl. Phys. **A260**, 77 (1976)
 - [38] D. R. Bes and R.A.Brogia, *Nuclear Superfluidity and Field Theory of Elementary Excitations*, Proc. of the Int. School of Physics Enrico Fermi on Elementary Modes of Excitation in Nuclei, Eds. A. Bohr and R. A. Broglia, North-Holland, Amsterdam, p. 55 (1977)
 - [39] R.A.Brogia, V. Paar and D. Bès, *Effective interaction between the $J = 2^+$ two-phonon states in ^{208}Pb . Evidence of the isovector quadrupole mode*, Phys. Lett. B **37**, 257 (1971)
 - [40] R.A.Brogia, D. R. Bès, R. Liotta, B. R. Mottelson and H. M. Sofia, *Treatment of the spurious states in nuclear field theory*, Phys. Lett. **B 64**, 29 (1976)
 - [41] P. F. Bortignon, R.A. Broglia, D. R. Bès, R. Liotta and V. Paar, *On the role of the pairing modes in the $(h_{9/2} \otimes 3^-)$ Multiplet of ^{209}Bi* , Phys. Lett. **64B**, 24 (1976)
 - [42] P. F. Bortignon, R.A.Brogia, D. R. Bès and R. Liotta, *Nuclear field theory*, Phys. Rep. **30C**, 305 (1977)
 - [43] P. F. Bortignon, R.A.Brogia and D. R. Bes, *On the convergence of the nuclear field theory perturbation expansion for strongly anharmonic systems*, Phys. Lett. **76B**, 153 (1978)
 - [44] P.F. Bortignon, *Nuclear field theory of two-phonon states, Nuclear superfluidity and field theory of elementary excitations*, Proc. of the Int. School of Physics Enrico Fermi on Elementary Modes of Excitation in Nuclei, Eds. A. Bohr and R. A. Broglia, North-Holland, Amsterdam, p. 519 (1977)
 - [45] H. Reinhardt, *Foundation of nuclear field-theory*, Nucl. Phys. A **251** (1975) 317
 - [46] H. Reinhardt, *Functional approach to nuclear field-theory - schematic model with pairing and particle-hole forces*, Nucl. Phys. A **298** (1978) 60
 - [47] H. Reinhardt, *Nuclear field-theory*, Nucl. Phys. A **251** (1978) 77
 - [48] H. Reinhardt, *Application of the nuclear-field theory to superfluid nuclei-quasiparticle-phonon multiplet*, Nucl. Phys. A **251** (1980) 176
 - [49] A. Bohr and R.A. Broglia eds., Proc. of the "Enrico Fermi" Int. School of Physics on Elementary modes of excitation in nuclei, Varenna, Como. Italy, North-Holland, Amsterdam (1977)
 - [50] R.A.Brogia and D. R. Bes, *High-lying pairing resonances*, Phys. Lett. B **69**, 129 (1977)
 - [51] P.F. Bortignon, A. Bracco and R.A. Broglia, *Giant resonances*, Harwood Academic Publishers, Amsterdam (1998)
 - [52] R.A. Broglia, T. Døssing, B. Lauritzen and B.R. Mottelson, *Nuclear rotational damping. Finite-system analogue to motional narrowing in nuclear magnetic resonance*, Phys. Rev. Lett. **58**, 326 (1987)
 - [53] R.A. Broglia, *Theory of relaxation, phase transitions and tunnelling in nuclei*, Proc. of the Int. School of Physics "Enrico Fermi", Course CIV, Frontiers and borderlines in many-particle physics, eds. R.A. Broglia and J.R. Schrieffer, North Holland, Amsterdam, p. 204 (1988)
 - [54] G.F. Bertsch and R.A. Broglia, *Oscillations in finite quantum systems*, Cambridge University Press (1974)
 - [55] R.A. Broglia, P.F. Bortignon and C. Yannouleas, *The electromagnetic response of metal clusters and of nuclei*, in Proc. of the Int. School of Physics "Enrico Fermi", Course CXXI, Perspectives in many-body physics, eds. R.A. Broglia, J.R. Schrieffer and P.F. Bortignon, North Holland,

- Amsterdam, p. 191 (1994)
- [56] R.A. Broglia, *The surfaces of compact systems: from nuclei to stars*, Surf. Sci **500**, 759 (2002)
 - [57] J.M. Pacheco, R.A. Broglia and B.R. Mottelson, *The intrinsic line width of the plasmon resonances in metal microclusters at very low temperature*, Z. Phys. D **21**, 289 (1991)
 - [58] R.A. Broglia, G. Colò, G. Onida and E.H. Roman, *Solid state physics of finite systems*, Springer, Heidelberg (2004)
 - [59] D.R. Bes and J. Kurchan, *The treatment of collective coordinates in many-body systems*, Worlds Scientific, Singapore (1990)
 - [60] R.A. Broglia and A. Winther, *Heavy ion reactions*, Benjamin, Reading, Mass. (1991)
 - [61] K. Bennaceur, J. Dobaczewski and M. Płoszajczak, *Pairing anti-halo effect*, Phys. Lett. B **496** 154 (2000)
 - [62] I. Hamamoto and B.R. Mottelson, *Pair correlation in neutron drip line nuclei*, Phys Rev. C **68** 034312 (2003)
 - [63] I. Hamamoto and B.R. Mottelson, *Weakly bound $s_{1/2}$ neutrons in the many-body pair correlation of neutron drip line nuclei*, Phys Rev. C **69** 064302 (2004)
 - [64] A.M. Krumbholz, P. von Neumann-Cosel, T. Hashimoto, A. Tamii, T. Adachi, C.A. Bertulani, H. Fujita, Y. Fujita, E. Ganioglu, K. Hatanaka, C. Iwamoto, T. Kawabata, N.T. Khai, A. Krugmann, D. Martin, H. Matsubara, R. Neveling, H. Okamura, H.J. Ong, I. Poltoratska, V.Yu. Ponomarev, A. Richter, H. Sakaguchi, Y. Shimbara, Y. Shimizu, J. Simonis, F.D. Smit, G. Susoy, J.H. Thies, T. Suzuki, M. Yosoi and J. Zenihiro, *Low energy electric dipole response in ^{120}Sn* , Phys. Lett. B **744** (2015) 7
 - [65] D.R. Bes, R.A. Broglia and B.S. Nilsson, *Microscopic description of isoscalar and isovector giant quadrupole resonance*, Phys. Rep. C **16**, 1 (1975)
 - [66] B.R. Mottelson, *Selected topics in the theory of collective phenomena in nuclei*, in Proc. of the "Enrico Fermi" Int. school of Physics, Course XV, Nuclear spectroscopy, ed. G. Racah, Academic Press, New York (1962) p. 44
 - [67] F. Barranco, P.F. Bortignon, R.A. Broglia, G. Colò and E. Vigezzi, *The halo of the exotic nucleus ^{11}Li : a single Cooper pair*, Eur. Phys. J. A **11**, 305 (2001)
 - [68] D. Savran, T. Aumann and A. Zilges, *Experimental studies of pygmy dipole resonance*, Prog. Part. Nucl. Phys. **70** (2013) 10
 - [69] R. Kanungo, A. Sanetullaev, J. Tanaka, S. Ishimoto, G. Hagen, T. Myo, T. Suzuki, C. Andreoiu, P. Bender, A. A. Chen, B. Davids, J. Fallis, J. P. Fortin, N. Galinski, A. T. Gallant, P. E. Garrett, G. Hackman, B. Hadinia, G. Jansen, M. Keefe, R. K^oucken, J. Lighthall, E. McNeice, D. Miller, T. Otsuka, J. Purcell, J. S. Randhawa, T. Roger, A. Rojas, H. Savajols, A. Shotter, I. Tanihata, I. J. Thompson, C. Unsworth, P. Voss, and Z. Wang, *Evidence of soft dipole resonance in ^{11}Li with isoscalar character*, Phys. Rev. Lett. **114** (2015) 192502
 - [70] S. Shimoura, A. Saito, T. Minemura, Y. Matsuyama, H. Baba, H. Akiyoshi, N. Aoi, T. Gomi, Y. Higurashi, K. Ieki, N. Imai, N. Iwasa, H. Iwasaki, S. Kanno, S. Kubono, M. Kunibu, S. Michimasa, T. Motobayashi, T. Nakamura, H. Sakurai, M. Serata, E. Takeshita, S. Takeuchi, T. Teranishi, K. Ue, K. Yamada, Y. Yanagisawa, M. Ishihara, and N. Itagaki, *Isomeric 0^+ state in ^{12}Be* , Phys. Lett. B **560** (2003) 31
 - [71] S. Shimoura, S. Ota, K. Demichi, N. Aoi, H. Baba, Z. Elekes, T. Fukuchi, T. Gomi, K. Hasegawa, E. Ideguchi, M. Ishihara, N. Iwasa, H. Iwasaki, S. Kanno, S. Kubono, K. Kurita, M. Kurokawa, Y. Matsuyama, S. Michimasa, K. Miller, T. Minemura, T. Motobayashi, T. Murakami, M. Notani, A. Odahara, A. Saito, H. Sakurai, E. Takeshita, S. Takeuchi, M. Tamaki, T. Teranishi, K. Yamada, Y. Yanagisawa, and I. Hamamoto, *Lifetime of the isomeric state in ^{12}Be* , Phys. Lett. B **654** (2007) 87
 - [72] J. Johansen, V. Bildstein, M. Borge, M. Cubero, J. Diriken, J. Elseviers, L. Fraile, H. Fynbo, L. Gaffney, R. Gernhäuser, B. Jonson, G. Koldste, J. Konki, T. Kröll, R. Krućken, D. Mücher, T. Nilsson, K. Nowak, J. Pakarinen, V. Pesudo, R. Raabe, K. Riisager, M. Seidlitz, O. Tengblad, H. Törnqvist, D. Voulot, N. Warr, F. Wenander, K. Wimmer, and H. De Witte, *Experimental*

- study of bound states in ^{12}Be through low-energy $^{11}\text{Be}(d,p)$ -transfer reactions*, Phys. Rev. C **88** (2013) 044619
- [73] R.A. Broglia, C. Riedel and T. Udagawa, *Coherence properties of two-neutron transfer reactions and their relation to inelastic scattering*, Nucl. Phys. **A169**, 225 (1971)
 - [74] D.M. Brink, Ph.D. thesis, Oxford University (unpublished) (1955)
 - [75] P. Axel, *Electric dipole ground-state transition width strength function and 7-Mev photon interactions*, Phys. Rev. **126**, 671 (1962)
 - [76] G.F. Bertsch and R.A. Broglia, *Giant resonances in hot nuclei*, Phys. Today **39**, 44 (1986)
 - [77] I. Tanihata, H. Hamagaki, O. Hashimoto, Y. Shida, N. Yoshikawa, K. Sugimoto, O. Yamakawa, T. Kobayashi, and N. Takahashi, *Measurements of interaction cross sections and nuclear radii in the light p-shell region*, Phys. Rev. Lett. **55** (1985) 2676
 - [78] I. Tanihata et al, *Measurement of the two-halo neutron transfer reaction $^1\text{H}(^{11}\text{Li}, ^9\text{Li})^3\text{H}$ at 3A MeV*, Phys. Rev. Lett. **100**, 192502 (2008)
 - [79] U. Götz, M. Ichimura, R.A. Broglia and A. Winther, *Reaction mechanism of two-nucleon transfer between heavy ions*, Phys. Rep. **16C** (1975) 115
 - [80] G. Potel, *COOPER*, 2nd order DWBA software to calculate two-nucleon transfer processes, including successive and simultaneous transfer properly corrected by non-orthogonality
 - [81] G. Potel, F. Barranco, E. Vigezzi and R.A. Broglia, *Evidence for phonon mediated pairing interaction in the halo of the nucleus ^{11}Li* , Phys. Rev. Lett. **105** (2010) 172502
 - [82] T. Roger, *Etude des réactions induites par le noyau à halo ^{11}Li avec la cible active MAYA*, Ph.D Thesis, Caen University (2009) (unpublished)
 - [83] J. Schwinger, *Quantum mechanics, symbolism of atomic measurements*, Springer, Heidelberg (2001)
 - [84] A. Idini, G. Potel, F. Barranco, E. Vigezzi and R.A. Broglia, *Well funneled nuclear structure landscape: renormalization*, ArXiv 1504.05335
 - [85] A. Idini, G. Potel, F. Barranco, E. Vigezzi and R.A. Broglia, *Dual origin of pairing in nuclei*, ArXiv 1404.7365
 - [86] A. Idini, G. Potel, F. Barranco, E. Vigezzi and R.A. Broglia, *Interweaving of elementary modes of excitation in superfluid nuclei through particle-vibration coupling: quantitative account of the variety of nuclear excitations*, Phys. Rev C **92** (2015) 014331
 - [87] E. Chabanat, P. Bonche, P. Haensel, J. Meyer and R. Schaeffer, *A Skyrme parametrization from subnuclear to neutron star densities Part II. Nuclei far from stabilities*, Nucl. Phys. A **635** (1998) 231
 - [88] R.B. Wiringa, R.A. Smith and T.L. Ainsworth, *Nucleon-nucleon potentials with and without Δ (1232) degrees of freedom*, Phys. Rev. C **29**, 1207 (1984)
 - [89] F. Barranco, R.A. Broglia, G. Colò, G. Gori, E. Vigezzi and P.F. Bortignon, *Many-body effects in nuclear structure*, Eur. J. Phys. A **21**, 57 (2004)
 - [90] A.V. Avdeenkov and S.P. Kamerdzhiev, *Description of excitations in odd nonmagic nuclei by the Green's function method*, Phys. At. Nucl. **62** (1999) 563
 - [91] E.V. Litvinova and A.V. Afanasjev, *Dynamics of nuclear single-particle structure in covariant theory of particle-vibration coupling: from light to superheavy nuclei*, Phys. Rev. C **84** (2011) 014305
 - [92] E. Litvinova, *Quasiparticle-vibration coupling in a relativistic framework: Shell structure of $Z=120$ isotopes*, Phys. Rev. C **85**, 021303 (2012)
 - [93] P. Ring and E. Litvinova, *Particle-vibrational coupling in covariant density-functional theory*, Phys. At. Nucl. **72** (2009) 1285
 - [94] G. Colò, H. Sagawa and P.F. Bortignon, *Effect of particle-vibration coupling on single-particle states: A consistent study within the Skyrme framework*, Phys. Rev. C **82** (2010) 064307
 - [95] K. Mizuyama, G. Colò and E. Vigezzi, *Effect of particle-vibration coupling on single-particle states: A consistent study within the Skyrme framework*, Phys. Rev. C **86** (2012) 034318
 - [96] N.V. Gnezdilov, N. Borzov, E.E. Saperstein, S.V. Tolokonnikov, *Self-consistent description of*

- single-particle levels of magic nuclei*, Phys. Rev. C **89** (2014) 034304
- [97] J. Schrieffer, *Superconductivity* (Benjamin, New York, 1964)
 - [98] A. Idini, F. Barranco and E. Vigezzi, *Quasiparticle renormalization and pairing correlations in spherical superfluid nuclei*, Phys. Rev. C **85**, 014331 (2012)
 - [99] A. Idini, *Renormalization effects in nuclei*, Ph.D. Thesis, University of Milan (2013), <http://air.unimi.it/2434/216315>
 - [100] V. Somà, C. Barbieri and T. Duguet, *Ab initio self-consistent Gorkov-Greens function calculations of semi-magic nuclei: Numerical implementation at second order with a two-nucleon interaction*, Phys. Rev. C **89** 024323 (2014)
 - [101] V. Van der Sluys, D. Van Neck, M. Waroquier and J. Ryckebusch, *Fragmentation of single-particle strength in spherical open-shell nuclei: Application to the spectral functions in ^{142}Nd* , Nucl. Phys. A **551** (1993) 210
 - [102] A.S. Blum and C. Joas, *From dressed electrons to quasiparticle: the emergence of emergent entities in quantum field theory*, Studies in history and philosophy of science (to be published)
 - [103] V. Hellemans et al, Phys. Rev. C **88**, 064323 (2013)
 - [104] A. Pastore, D. Tarpanov, D. Davesne and J. Navarro, *Spurious finite-size instabilities in nuclear energy density functionals: spin channel*, ArXiv:1505.05043 (2015)
 - [105] D. Tarpanov, J. Dobaczewski, J. Toivanen and B.G. Carlsson, *Polarization corrections to single-particle energies studied within the energy-density-functional and quasiparticle random-phase approximation approaches*, Phys. rev. C **89** (2014) 014307
 - [106] C. Mahaux, P. F. Bortignon, R.A. Broglia, C. H. Dasso, *Dynamics of the Shell Model*, Phys. Reports **120** (1985) 1
 - [107] J. Terasaki and J. Engel, *Self-consistent description of multipole strength: systematic calculations*, Phys. Rev. C **74** (2006) 044301
 - [108] F. Barranco, R.A. Broglia, G. Gori, E. Vigezzi, P.F. Bortignon and J. Terasaki, *Surface vibrations and the pairing interaction in nuclei*, Phys. Rev. Lett. **83** (1999) 2147
 - [109] J. Terasaki, F. Barranco, R.A. Broglia, E. Vigezzi and P.F. Bortignon, *Solution of the Dyson equation for nucleons in the superfluid phase*, Nucl. Phys. A **697** (2002) 127
 - [110] D.R. Bes, G.G. Dussel, R.P.J. Perazzo and H.M. Sofia, *The renormalization of single-particle states in nuclear field theory*, Nucl. Phys. A **293** (1977) 350
 - [111] R.D. Mattuck, *A guide to Feynman diagrams in the many-body problem*, Dover, New York (1976)
 - [112] V. Bernard and N. Van Giai, *Single-particle and collective nuclear states and the Green's function method*, in Proc. of the Int. School of Physics "Enrico Fermi", Course LXXVII, eds. R.A. Broglia, R.A. Ricci, C.H. Dasso, North Holland, Amsterdam, p. 437 (1981)
 - [113] H. Feshbach, *Unified theory of nuclear reactions*, Ann. Phys. **5**, 357 (1958)
 - [114] P. F. Bortignon and R.A. Broglia, *Role of the nuclear surface in a unified description of the damping of single-particle and giant resonances*, Nucl. Phys. A **371**, 405 (1981)
 - [115] G. F. Bertsch, R.A. Broglia and P. F. Bortignon, *Damping of Nuclear Motion*, Rev. of Mod. Phys. **55**, 287 (1983)
 - [116] S. Dickey, J. Kraushaar, R. Ristinen and M. Rumore, *The $^{120}\text{Sn}(p,d)^{119}\text{Sn}$ reaction at 26.3 MeV*, Nucl. Phys. A **377**, 137 (1982)
 - [117] W. Pauli, *Exclusion principle and quantum mechanics*, Edition du Griffon, Neuchâtel, Switzerland (1947)
 - [118] R.F. Streater and A.S. Wightman, *PCT, spin & statistics, and all that*, Benjamin, New York (1964)
 - [119] S. Forte, *Quantum mechanics and field theory with fractional spin statistics*, Rev. Mod. Phys. **64**, 193 (1992)
 - [120] M. Baldo, P.F. Bortignon, G. Colò, D. Rizzo and L. Sciacchitano, *Beyond the mean field in the particle vibration coupling scheme*, J. Phys. G. **42** (2005) 085109
 - [121] N. Vinh Mau, in Theory of nuclear structure, IAEA, (1970), p. 931
 - [122] N. Vinh Mau and A. Bouyssy, *Optical potential for low-energy neutrons: Imaginary potential for*

- neutron- ^{40}Ca elastic scattering, Nucl. Phys. A **257** (1976) 189
- [123] V. Bernard and N. Van Giai, *Effects of collective modes on the single-particle states and the effective mass in ^{208}Pb* , Nucl. Phys. A **348** (1980) 75
 - [124] D. R. Bès, R.A. Broglia and B. Nilsson, *Importance of the quadrupole pairing field in the $J^\pi = 0^+$ vibrations of shape deformed nuclei*, Phys. Lett. B **40**, 338 (1972)
 - [125] E. R. Flynn, G. Igo, P. D. Barnes, D. Kovar, D. Bes and R.A. Broglia, *Effect of multipole pairing particle-hole fields in the particle-vibration coupling of ^{208}Pb (II). The $^{207}\text{Pb}(t,p)^{210}\text{Pb}$ reaction at 20 MeV*, Phys. Rev. C **3**, 2371 (1971)
 - [126] E. R. Flynn, G. J. Igo and R.A. Broglia, *Three-phonon monopole and quadrupole pairing vibrational states in ^{206}Pb* , Phys. Lett. B **41**, 397 (1972)
 - [127] R.A. Broglia, D. R. Bes and B. Nilsson, *Strength of the multipole pairing coupling constant*, Phys. Lett. B **50**, 213 (1974)
 - [128] R.A. Broglia, *Microscopic structure of the intrinsic state of a deformed nucleus*, in Interacting bosons in Nuclear Physics, F. Iachello ed., Plenum Press, New York p. 95 (1981)
 - [129] A. Bohr and B.R. Mottelson, *On the ability of the interacting boson model to describe nuclear-deformation effects*, Phys. Scripta **25** (1982) 915
 - [130] D. Bes and R.A. Broglia, *Nuclear field theory treatment of the interacting boson model*, in Interacting bosons in nuclear physics, ed. F. Iachello, Plenum Press, New York (1978) p.143
 - [131] P.F. Bortignon and R.A. Broglia, *On the interaction of the many-phonon monopole pairing vibrations*, in Interacting bosons in nuclear physics, ed. F. Iachello, Plenum Press, New York (1978) p.151
 - [132] F. Barranco, M. Gallardo and R.A. Broglia, *Nuclear Field Theory of spin dealignment in strongly rotating nuclei and the vacuum polarization induced by pairing vibrations*, Phys. Lett. B **198**, 19 (1987)
 - [133] D.R. Bès, R.A. Broglia, J. Dudek, W. Nazarewicz and Z. Szymanski, *Fluctuation effects in the pairing field of rapidly rotating nuclei*, Ann. Phys. **182**, 237 (1988)
 - [134] C. Barbieri and B.K. Jennings, *Nucleon-nucleus potential in the particle-hole approach*, Phys. Rev. **72**, 014613 (2005)
 - [135] S. Baroni, M. Armati, F. Barranco, R.A. Broglia, G. Colò, G. Gori and E. Vigezzi, *Correlation energy contribution to nuclear masses*, J. Phys. G **30** (2004) 1353
 - [136] W.H. Dickhoff, D. Van Neck, S.J. Waldecker, R.J. Charity and L.G. Sobotka, *Nonlocal extension of the dispersive optical model to describe data below the Fermi energy*, Phys. Rev. C **82**, 054306 (2010)
 - [137] K. Mizuyama and K. Ogata, *Self-consistent microscopic description of neutron scattering by ^{16}O based on the continuum particle-vibration coupling method*, Phys. Rev. C **86**, 041603(R) (2012)
 - [138] A. Bonaccorso and R.J. Charity, *Optical potential for the n - ^9Be reaction*, Phys. Rev. C **89**, 024619 (2014)
 - [139] D. Montanari, L. Corradi, S. Szilner, G. Pollarolo, E. Fioretto, G. Montagnoli, F. Scarlassara, A.M. Stefanini, S. Courtin, A. Goasduff, F. Haas, D. Jelavic Malenica, C. Michelagnoli, T. Mijatovic, N. Soic, C.A. Ur, and M. Varga Pajtler, *Neutron pair transfer in $^{60}\text{Ni}+^{116}\text{Sn}$ far below the Coulomb barrier*, Phys. Rev. Lett. **113**, 052501 (2014)
 - [140] R.P.J. Perazzo, S.L. Reich and H.M. Sofia, *Renormalization of particle and hole state in ^{208}Pb* , Nucl. Phys. A **339** (1980) 23
 - [141] G.F. Bertsch, P.F. Bortignon, R.A. Broglia and C.H. Dasso, *Damping of single-particle states and giant resonances in ^{208}Pb* , Phys. Lett. B **80** (1979) 161
 - [142] S. Frauendorf, *Pairing at high spin*, in Fifty years of nuclear BCS, eds. R.A. Broglia and V. Zelevinsky, World Scientific, Singapore (2013), 536
 - [143] R.A. Broglia, M. Diebel, F. Barranco and S. Frauendorf, *The time response function*, XXIII Int. winter meeting on nuclear physics, ed. I. Iori, Ricerca Scientifica ed Educazione Permanente, Milano (1985), 1
 - [144] Y.R. Shimizu, J.D. Garrett, R.A. Broglia, M. Gallardo and E. Vigezzi, *Pairing fluctuations in*

- rapidly rotating nuclei*, Rev. Mod. Phys. **61** (1989) 131
- [145] Y.R. Shimizu and R.A. Broglia, *A boson expansion approach for including fluctuations in the calculation of the pairing phase transition taking place in strongly rotating nuclei*, Nucl. Phys. A **476** (1988) 228
 - [146] Y.R. Shimizu and R.A. Broglia, *A comparison of the RPA and number projection approaches for calculations of pairing fluctuations in fast rotating nuclei*, Nucl. Phys. A **515** (1990) 38
 - [147] Y.R. Shimizu and R.A. Broglia, *Quantum size effects in rapidly rotating nuclei*, Phys. Rev. C **41** (1990) 1865
 - [148] Y.R. Shimizu, E. Vigezzi and R.A. Broglia, *Effects of pairing correlations on superdeformed bands in the $A \approx 150$ region*, Nucl. Phys. A **519** (1990) 80
 - [149] M. Matsuzaki, Y.R. Shimizu and K. Matsuyanagi, *Quasiparticle-vibration coupling in rotating triaxial odd- A nuclei*, Prog. Theor. Phys. **79** (1988) 836
 - [150] D.J. Rowe, *Nuclear collective motion: models and theory*, Methuen, London (1970)
 - [151] D. Tarpanov, J. Dobaczewski, J. Toivanen and B.G. Carlsson, *Spectroscopic properties of nuclear Skyrme energy density functionals*, Phys. Rev. Lett. **113** 252501 (2014)
 - [152] L. Hedin, *New method for calculating the one-particle Green's function with application to the electron-gas problem*, Phys. Rev. A **139**, 796 (1965)
 - [153] P. F. Bortignon, R.A. Broglia and C. H. Dasso, *Quenching of the mass operator associated with collective states in many-body systems*, Nucl. Phys. A **398**, 221 (1983)
 - [154] F. Cappuzzello, D. Carbone, M. Cavallaro, M. Bondi, C. Agodi, F. Azaiez, A. Bonaccorso, A. Cunsolo, L. Fortunato, A. Foti, S. Franchou, E. Khan, R. Linares, J. Lubian, J.A. Scarpaci and A. Vitturi, *Signatures of the giant pairing vibration in the ^{14}C and ^{15}C atomic nuclei*, Nature Comm. **6** (2015) 6743
 - [155] G.F. Bertsch, R.A. Broglia and J.R. Schrieffer, *Rotating superfluid nuclei*, Nuovo Cim. **100**, 283 (1988)
 - [156] A. Repko, P.G. Reinhard, V.O. Nestrenko and J. Kvasil, *Toroidal nature of the low-energy $E1$ mode*, Phys. Rev. C **87**, 04305 (2013)
 - [157] P. Avogadro, F. Barranco, R.A. Broglia and E. Vigezzi, *Quantum calculation of vortices in the inner crust of neutron stars*, Phys. Rev. C **75**, 022805(R) (2007)
 - [158] P. Avogadro, F. Barranco, R.A. Broglia and E. Vigezzi, *Vortex-nucleus interaction in the inner crust of neutron stars*, Nucl. Phys. A **811** (2008) 378
 - [159] G. Gori, F. Barranco, E. Vigezzi, and R. A. Broglia, *Parity inversion and breakdown of shell closure in Be isotopes*, Phys. Rev. C **69**, 041302 (2004).
 - [160] H. An and C. Cai, *Global deuteron optical model potential for the energy range up to 183 MeV*, Phys. Rev. C **73**, 054605, 2006.
 - [161] H. T. Fortune, G.-B. Liu, and D. E. Alburger, *$(sd)^2$ states in ^{12}Be* , Phys. Rev. C **50**, 1355 (1994).
 - [162] R. Kanungo et. al., *Study of nuclear pairing through $^{12}\text{Be}(p,t)$ reaction*, TRIUMF approved proposal number S1338, 2012.
 - [163] D. E. Alburger, E. K. Warburton, A. Gallmann, and D. H. Wilkinson, *Decay of the 6.18-MeV $J^\pi=0^+$ level of Be^{10}* , Phys. Rev. **185**, 1242, 1969.
 - [164] G. Potel, A. Idini, F. Barranco, E. Vigezzi and R.A. Broglia, *Nuclear field theory predictions for ^{11}Li and ^{12}Be : shedding light on the origin of pairing in nuclei*, Phys. At. Nucl. **77** (2014) 941
 - [165] S.E.A. Orrigo and H. Lenske, *Pairing resonances and continuum spectroscopy of ^{10}Li* , Phys. Lett. B **677**, 294 (2009)
 - [166] R.A. Broglia, O. Hansen and C. Riedel, *Two-neutron transfer reactions and the pairing model*, Adv. Nucl. Phys. **6**, 287 (1973) (see www.mi.infn.it/~vigezzi/BHR/BrogliaHansenRiedel.pdf)
 - [167] R.A. Broglia and V. Zelevinsky eds., *Fifty years of nuclear BCS*, World Scientific, Singapore (2013)
 - [168] R.A. Broglia and A. Winther, *On the pairing field in nuclei*, Phys. Lett. B **124** (1983) 11
 - [169] C.H. Dasso and M. Gallardo, *Macroscopic pairing vibrational model, self-consistent pairing*

- coupling constant and the fifth term of Von Weizsäcker's semiempirical formula*, Phys. Rev. C **74** (2006) 014307
- [170] M.G. Goeppert Mayer and J.H.D. Jensen, *Elementary theory of nuclear shell structure*, John Wiley (New York) (1955)
 - [171] J. Bardeen, *Tunneling from a many-particle point of view*, Phys. Rev. Lett. **6** (1961) 567
 - [172] J. Bardeen, *Tunneling into superconductors*, Phys. Rev. Lett. **9** (1962) 147
 - [173] M.H. Cohen, L.M. Falicov and J.C. Phillips, *Superconductive tunneling*, Phys. Rev. Lett. **8**, 316 (1962)
 - [174] L.P. Gor'kov, *Microscopic derivation of the Ginzburg-Landau equations in the theory of superconductivity*, Sov. Phys. JETP **9**, 1364 (1959)
 - [175] D.G. McDonal, *The Nobel laureate versus the graduate student*, Phys. Today **57** (2001) 46
 - [176] A. Leggett, *Quantum liquids*, Oxford University Press, Oxford (2006)
 - [177] J.P. Elliott, *Collective motion in the nuclear shell model. 1. Classification schemes for states of mixed configuration*, Proc. Roy. Soc. A **254** (1958) 128
 - [178] R.A. Broglia, E. Maqueda and D.R. Bes, *An exact diagonalization of the quadrupole and pairing forces in the nuclear $d-s$ shell*, Rev. de la Union Mateiatica Argentina, Vol XXI, (1965) 107
 - [179] R.A. Broglia and E. Maqueda, *Exact calculation in the $d-s$ nuclear shell*, Nucl. Phys. **86** (1966) 457
 - [180] A. Bohr and O. Ulfbeck, *Quantal structure of superconductivity gauge angle*, in First Topsøe summer school, on superconductivity and workshop on superconductors, Roskilde, Denmark, Riso/M/2756, 1988
 - [181] G. Potel and R.A. Broglia, *Pairing correlations with single Cooper pair transfer to individual quantal states*, in Fifty years of nuclear BCS, eds. R.A. Broglia and V. Zelevinsky, World Scientific, Singapore, p.479 (2013)
 - [182] G. Potel, A. Idini, F. Barranco, E. Viguzzi and R.A. Broglia, *Quantitative study of coherent pairing modes with two-neutron transfer: Sn isotopes*, Phys. Rev. C **87** (2013) 054321
 - [183] A. Bohr, J.M. Leinaas and P. Minhagen *Pairing (or superfluidity) as experienced by the nucleus*, NORDITA preprint, NORDITA- 79/13 (1979)
 - [184] H. Esbensen and G.F. Bertsch, *Surface response of Fermi liquids*, Ann. Phys. **157** (1984) 255
 - [185] H. Esbensen and G.F. Bertsch, *Surface effects on particle self-energies*, Phys. Rev. Lett. **52** (1984) 2257
 - [186] G.F. Bertsch and H. Esbensen, *The classical limit of the surface response in Fermi liquids*, Phys. Lett. B **161** (1985) 248
 - [187] N. Giovanardi, F. Barranco, R.A. Broglia and E. Viguzzi, *Surface effects in nuclear Cooper pair formation*, Phys. Rev. C **65** (2002) 041304
 - [188] C.H. Dasso and G. Pollaro, *Macroscopic formfactors for pair transfer in heavy ion reactions*, Phys. Lett. B **155**, 233 (1985)
 - [189] F. Barranco, P.F. Bortignon, R.A. Broglia, G. Colò, P. Schuck, E. Viguzzi and X. Viñas, *Pairing matrix elements and pairing gaps with bare, effective and induced interactions*, Phys. Rev. C **72**, 0543149 (2005)
 - [190] R.A. Broglia, *Heavy ion reactions*, Lecture notes, Brookhaven Natl. Lab. unpublished (1979)
 - [191] G. Colò, N. Van Giai, P.F. Bortignon and M.R. Quaglia, *On dipole compression modes in nuclei*, Phys. Lett. B **485** (2000) 362
 - [192] B.R. Mottelson, private communication to P.F. Bortignon (1980)